AD-A229 802

WRDC-TR-90-3054

EXTREME TEMPERATURE STRAIN MEASUREMENT SYSTEM

Charles Hulse
Richard Bailey

United Technologies Research Center
East Hartford, Connecticut 06108

August 1990

Final Report for Period Sept 1985 - July 1990

FLIGHT DYNAMICS LABORATORY
WRIGHT RESEARCH AND DEVELOPMENT CENTER
AIR FORCE SYSTEM COMMAND
WRIGHT-PATTERSON AIR FORCE BASE, OHIO 45433-6553

NOTICE
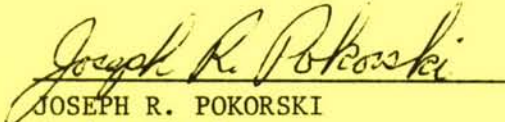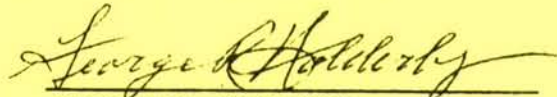
When Government drawings, specifications, or other data are used for any purpose other than in connection with a definitely Government-related procurement, the United States Government incurs no responsibility or any obligation whatsoever. The fact that the government may have formulated or in any way supplied the said drawings, specifications, or other data, is not to be regarded by implication, or otherwise in any manner construed, as licensing the holder, or any other person or corporation; or as conveying any rights or permission to manufacture, use, or sell any patented invention that may in any way be related thereto.

This report is releasable to the National Technical Information Service (NTIS). At NTIS, it will be available to the general public, including foreign nations.

This technical report has been reviewed and is approved for publication.

JOSEPH R. POKORSKI
Project Engineer
Instrumentation Group

GEORGE R. HOLDERBY
Chief, Structures Test Branch
Structures Division

FOR THE COMMANDER

ROBERT M. BADER
Chief, Structures Division

If your address has changed, if you wish to be removed from our mailing list, or if the addressee is no longer employed by your organization please notify WRDC/FIBT , WPAFB, OH 45433-6553 to help us maintain a current mailing list.

Copies of this report should not be returned unless return is required by security considerations, contractual obligations, or notice on a specific document.

REPORT DOCUMENTATION PAGE

Form Approved
OMB No. 0704-0188

1. AGENCY USE ONLY (*Leave blank*)	2. REPORT DATE August 1990	3. REPORT TYPE AND DATES COVERED FINAL 13 Sept 1985 – 31 July 1990

4. TITLE AND SUBTITLE

EXTREME TEMPERATURE STRAIN MEASUREMENT SYSTEM

5. FUNDING NUMBERS

F33615-85-C-3208

6. AUTHOR(S)

Charles Hulse and Richard Bailey

7. PERFORMING ORGANIZATION NAME(S) AND ADDRESS(ES)

United Technologies Research Center
Silver Lane
East Hartford, CT 06108

8. PERFORMING ORGANIZATION REPORT NUMBER

R90-917280-1

9. SPONSORING/MONITORING AGENCY NAME(S) AND ADDRESS(ES)

Flight Dynamics Laboratory (WRDC/FIBT)
Wright Research & Development Center
Wright-Patterson Air Force Base, OH 45433-6553
Joseph R. Pokorski, Project Engineer
(513)255-4213, WRDC/FIBT

10. SPONSORING/MONITORING AGENCY REPORT NUMBER

WRDC-TR-90-3054

11. SUPPLEMENTARY NOTES

12a. DISTRIBUTION/AVAILABILITY STATEMENT

Approved for public release; distribution unlimited

12b. DISTRIBUTION CODE

13. ABSTRACT *(Maximum 200 words)*

A survey and a selection of optimum techniques was made of methods for making strain measurements on aerospace structures from -320°F to 1600°F. Experimental evaluations were made of the two best systems selected, a rod type extensometer and a capacitance device. The rod type extensometer proved experimentally to be the better approach, especially for accurately measuring the strain behavior of an aerospace material under load throughout typical ascent and atmospheric reentry cycles. Some efforts were also devoted to the development of sputtered strain gages on transferable metal foils. These results indicated that strain measuring devices of this type could be developed if appropriate funds for research were available.

14. SUBJECT TERMS

strain measurement
extensometer
strain gages
structural testing
reentry

15. NUMBER OF PAGES
97

16. PRICE CODE

17. SECURITY CLASSIFICATION OF REPORT UNCLASSIFIED	18. SECURITY CLASSIFICATION OF THIS PAGE UNCLASSIFIED	19. SECURITY CLASSIFICATION OF ABSTRACT UNCLASSIFIED	20. LIMITATION OF ABSTRACT Unlimited

FOREWORD

TABLE OF CONTENTS

TABLE OF CONTENTS (CONCLUDED)

LIST OF ILLUSTRATIONS

LIST OF ILLUSTRATIONS (CONCLUDED)

LIST OF TABLES

SUMMARY

A program was conducted to develop a strain measurement system for use in ground based testing of aerospace structures over the temperature range from -320° to 1600° F.

During the first phase of the effort, a general survey was made of various techniques to select those most likely to meet the program goals. A modified commercial rod-type extensometer was selected as the best system to use with a commercially available capacitance device a close second.

The results from measurements of the experimental behavior of these two systems determined in the second phase of the effort are described, together with direct comparisons of their behavior during simulated ascent and atmospheric reentry conditions which were examined in the final phase of the work. The rod-type extensometer appeared to meet all of the goals of the contract provided that it is mounted to minimize relative motions between it and the structure being examined. The capacitive device did not do as well. It was sensitive to even very small disturbances of the leads and showed erratic behavior at low temperatures, probably because of the buildup of frost between the plates.

Preliminary efforts were devoted to the application of sputtered resistance strain gages on transferrable metal foils which could be spot welded to structures under test. The results suggested that this technique offered the potential to be developed as a strain measurement system.

1 - INTRODUCTION

1.1 BACKGROUND

Changes in Air Force operations to include not only missions within our atmosphere but into space require the development of new structures and materials able to operate successfully in the extreme cold as well as at very high temperatures. The importance, the costs, and the risks associated with these new vehicles demand that they be properly tested and evaluated under conditions appropriate to their intended use. The most cost effective method to obtain most of these data is by simulated testing on the ground, typical of that done at the Flight Dynamics Laboratory, Wright-Patterson Air Force Base.

A reliable method to accurately measure the strains in various components of these structures under different amounts of loading is of paramount importance if these evaluations are to provide useful data for analysis. Requirements for accurate measurements of strain at elevated temperatures has become increasingly important to the United Technologies Corporation in order to maintain its leadership in the development of improved gas turbine engines, new high temperature materials, and other space related products. A number of research contracts, IR & D efforts, and publications (Refs. 1 through 9) attest to this interest. The work described in this report is a natural consequence of this mutual interest and the need to make the most effective use of research funds. A preliminary report of the results of these investigations has been presented (Ref. 10).

1.2 PURPOSE/OBJECTIVE

The specific goal of this program was to develop the technology for producing a sensor which could make valid measurements of strain during ground testing of component structual parts from -320°F to 1600°F. The techniques investigated should also have the potential to be improved to extend their range of use from -423°F to 2000°F. This range of temperatures was selected in order to permit the Structural Analysis Group to evaluate the behavior of hypersonic vehicles which will be required in their mission to pass in and out of the atmosphere.

The first phase of this work consisted primarily of an analytical selection process to determine strain measurement techniques which appeared to have the most promise of meeting the environmental requirements. As a minimum, the contractor was to consider resistance (including the use of sputtered thin film strain gages), capacitance and fiber optic

2

strain measuring sensors. A minimum of two strain measurement systems were to be recommended for further evaluation.

The second phase of the effort was to emphasize physical experimentation as a means to further screen candidate systems. For both of these two phases, the temperatures of interest were to vary from liquid nitrogen (-320°F) up to 1600°F. This range was a practical compromise which covered the range of most immediate concern. During the second phase, the contractor was to evaluate and refine the recommended strain measuring systems under elevated temperature and low temperature test conditions in a structural testing laboratory environment using radiant heat lamps and with liquid nitrogen cooling. In the third and final phase, the optimum strain measurement system was to be demonstrated to establish its integrity and reliability. These tests were to include demonstration tests at UTRC in a testing machine under computer control with strain, temperature and time profiles typical of expected atmospheric reentry and ascent conditions. The contractor was finally to conduct a demonstration at the Structures Test Facility at WPAFB to demonstrate the procedures necessary to attach the selected strain measurement system to a structure to be tested.

2 - LITERATURE SEARCH AND SENSOR SELECTION

2.1 TECHNICAL APPROACH

2.1.1 Technical Discussion

Currently commercially available strain gages attached with organic base cements are the most commonly used strain measurement technique for structural testing. Use of these gages to measure static strain is limited to about 700°F. The use of flame sprayed alumina insulation coatings can extend the use of wire strain gages to about 725°F. In these installations, usually 1-mil-diameter wires are held in place by a combination of cement and/or encapsulation in flame sprayed alumina. Encapsulation is accomplished by covering different parts of the gage in different spraying runs until it is completely covered. The following types of strain gage alloy wires have been used: (a) Nichrome, Ni 20Cr, (b) Evanohm, 75Ni 20Cr 2.5Al 2.5Cu, and (c) different FeCrAl alloys, BCL-3, Kanthal A-1 and two new Chinese alloys. These alloys are subject to excessive drifts between about 725° and 1100°F. Wire strain gages with flame sprayed alumina insulation and protective coatings satisfactorily measure dynamic strains up to 1800°F.

The most common method to measure strain in material property evaluations at elevated temperatures is to install two clamps on the sample which support rods that extend down below the furnace. Various kinds of deflection sensors can then be used in this cooler area to measure the relative motions between the two rods. The gage length is defined by the distance between the two clamps. The rods which extend down below the furnace are usually made of the same material so that some of the thermal expansion effects can cancel out, and often a set of rods is used on each side of the sample to compensate for possible sample bending effects. Linear variable differential transformers (LVDT's) are the most commonly used sensors, although super linear variable capacitors (SLVC's) are also used.

In another variation, two clamps or simple contact pressure is used to attach two in-line levers against the side of a sample and then a sensor is used to detect the linear motion between the opposite ends of the levers which are outside of the furnace at ambient temperatures. The rods which contact the sample may also be attached to strain-gage flexures which sense the relative angular motions between the rods.

There are a number of variations and sources of capacitance measurement systems. It was originally thought that there were inherent problems associated with this approach at

very high temperatures because of changes in the electrical properties of air. It was finally realized that the observed effects were really materials effects. As better electrical insulators and precious metal components come into use, this approach becomes more attractive, with the provision that both plates must somehow be directly mounted on the surface of interest.

There are also a considerable number of new and interesting optical approaches for measuring strain. Most of these are not suitable for this application because they do not permit the surface on which the strain is to be measured to simultaneously move in space as parts of the structure deflect upon being loaded. These systems also tend to be very expensive, require a lot of time to set up properly, and need a considerable amount of space for the various optical components.

The development of sputtered thin film resistance strain gages has been worked on for many years, primarily at United Technologies and at the General Electric Company. Gages of this type have the particular advantages of being so thin that they do not cause any aerodynamic disturbances and they can be made with very small gage lengths. The primary problems currently associated with the use of these gages are electrical leakages to ground and slow oxidation attack.

2.1.2 Selection Technique and Results

In order to learn more about the various techniques to measure strain that have been developed or suggested, a search was conducted of the published literature and the information available from commercial vendors. A list of these sources is given in the Bibliography. From the information obtained in the literature survey, our own personal experiences in this general area including the results from a number of contracts, and direct contacts with a variety of vendors and other workers in the field, opinions were formed as to the most suitable strain measurement techniques for this application. The recent series of conferences sponsored by the Society of Experimental Mechanics on the specific subject of strain measurements at elevated temperatures also helped to evaluate the importance of the various problems associated with different techniques.

To select the best approaches for the work in the second phase on a rational basis, a series of parameters or properties were identified on which to base our judgements. Some of these properties were more important than others. For example, accuracy was assigned a higher degree of importance than some of the other properties. Table 1 shows these parameters together with a listing of the factors assigned to them to indicate their relative importance. The formula finally developed to rank the various possible strain measurement techniques was:

Suitability Factor $= 0.9(A) + 0.7(R) + 0.2(C) + 0.5(S) + 0.5(J) + 0.2(TC) + 0.5(SR)$

The final results of this evaluation process are presented in Table 2. The three best approaches in order of rank were (1) a commercial ceramic rod type extensometer, (2) a small commercial capacitive device, and (3) a sputtered foil type thin film strain gage.

6

3 - INDIVIDUAL STUDIES OF DIFFERENT TYPES OF SENSORS

3.1 ROD TYPE EXTENSOMETER

3.1.1 System Description and Operation

A commercial rod type extensometer* was selected as the most likely to satisfy the needs which prompted this work. With this type of sensor, the pointed ends of two ceramic rods are pressed end on against the surface in which strain is to be measured. These points are the only contacts made with the sample which minimizes the potential for thermal stress concentrations caused by shadows on the test surface when radiant lamps are used to heat the structure. Water cooled (or air cooled) flexures are clamped to the opposite ends of both rods so that any angular change between the two rods is detected by the strain-gaged flexures. The gage length is determined by the distance between the pointed ends of the ceramic rods. Any change in gage length is electrically measured by strain gages which are protected from the heat because they are cemented on water cooled flexures.

Figure 1 shows the device used in this work, with the two ceramic rods pressing vertically downward against a flat surface where the strain is to be measured. In the tests at elevated temperatures described in this report, these flexures were located behind an additional water cooled foreplate not shown in Figure 1. The separately water cooled flexures are attached only to the upper ends of the two ceramic rods. Each of these rods is pressed against the sample by separate spring flexures which are shown mounted at the right. The spring loading flexures are mounted on individual pivots so that should only apply loads parallel to the axis of the rods.

The two ceramic rods shown in Figure 1 are made of fused silica glass. The two sets of polycrystalline alumina rods used for our testing were 0.20 in. in diameter and either 4.42 in. or 10.75 in. long.

Experiments using the longer rods were designed to examine the capabilities of this system if the strain gaged flexures were located behind the radiant lamps generally used to heat the structures being tested. Locating the flexures in this position should protect the strain gages from being overheated by the lamps. Experiments using the shorter rods were for applications where lamps would not be used or where an additional water cooled housing would be used around the flexures to prevent them from being overheated.

---

* MTS Systems Corp, Minneapolis, MN, 55424; Model 623.42B-01

7

The manufacturer recommends that the points on each end of the two ceramic rods form a total angle of 90 degrees. A divot forming a total angle of approximately 120 degrees, about 0.006 in. deep is recommended by the manufacturer if a pair of small divots is used to define a specific gage length. In the work reported here, divots were used when the rods were used in a horizontal position, and no divots were used when the rods were vertical.

This type of extensometer has been used extensively at the United Technologies Research Center (UTRC) for measurements of the properties of materials and for closed loop testing machine control at temperatures up to 2200°F. At these temperatures, the use of commercially available single crystal sapphire rods instead of polycrystalline rods is preferred. When fused silica rods are used at too high a temperature, deformation of the points during long term fatigue testing may result in measurement errors (Ref. 11).

The extensometer model used in this program was designed for a gage length of 1 inch. A 1/2-inch gage length model is also available. Either may also be purchased with air cooling rather that water cooling. Experience at UTRC has led to the conclusion that the water cooled model is more stable than the air cooled model.

After the decision was made to examine this specific extensometer in this program, a competitor version came on the market*. This extensometer uses pivot bearings and a capacitive sensor** to measure the angular deflections of the ceramic rods. Elimination of the flexures permits this extensometer to operate with smaller loads against the sample (10 gm/rod versus 400 gm/rod). A version of this extensometer modified at UTRC to use silicon carbide rods (SiC) with chisel ends has been used to 2750° F in air.

3.1.2 Testing Approach

The use of the rod type extensometer in two nonstandard circumstances dominated our considerations of problems that might arise. The first concern that needed to be examined experimentally was how well the extensometer would operate when much longer ceramic rods were used. Use of much longer ceramic rods would permit the strain gaged sensors to be located behind the radiant heating lamps to protect them from the heat.

The second consideration was how sensitive the extensometer would be to relative motions between the sensor and the surface being examined. For example, loading a wing section could result in appreciable motions in space, especially near the end of the wing.

---

*   Instron Corp., Canton, MA.

** Capacitec Corp., Ayer, MA.

8

In the general case, we would expect the sensor to be mounted on studs directly attached to the structure. In this event, the sensor would move with the structure as it was loaded and only small relative motions between the extensometer and the test structure would be expected. In other circumstances, it might be necessary to mount the extensometer to a rigid support that might not move with the structure as it was loaded. What are the correction factors that might be necessary to take into account for these relative motions and how serious would these effects be?

The device used to examine these questions is shown in Figure 2. The extensometer is mounted on three mutually perpendicular slides which permit controlled amounts of different motion to be made relative to the two ceramic points. The particular rods shown in Figure 2 are 12.0 in. long rather that the standard 3.14 in. long. One of the pointed alumina rods presses against a fixed surface while the second rod presses against a coplanar surface mounted on an adjustable machinist's table which permits known amounts of separations between the points (strain) to be introduced.

A Linear Variable Differential Voltage Transformer (LVDT)* with an integral micrometer for calibration is mounted alongside the two ceramic points. The micrometer and transformer core are mounted in a fixed position, and the transformer coils are mounted on the same surface as the second ceramic point. The LVDT and the output of the extensometer through an amplifier** were fed to an XY recorder where the two measurements of identical displacements could be plotted and compared. The changes in the output of the LVDT as the machinists table was adjusted to represent various values of strain could thus be compared with the outputs of the extensometer as it was moved by various amounts in space relative to the surface on which measurements of strain were being made.

3.1.3 Test Results and Conclusions

The effect on the output of the extensometer due to changes in the lengths of the extensometer mounting springs are presented in Figure 3. A balanced set of two of these springs, each mounted at an angle of about 45° to the axis of the rod, provided the force which pressed the pointed end of each alumina rod against the test surface. If the test surface moved away or towards the extensometer, it would result in changes in the lengths of these springs. Because the data shown in Figure 3 indicated that the extensometer was sensitive to relative motions in this direction, additional experiments were made to examine

---

*   Trans-Tek Inc., Ellington, CT.

** BAM-1 Amplifier, Vishay Intertechnology Inc., Malvern, PA

the effect when the alumina rods were loaded using the individually pivoted spring flexures shown in Figure 1 instead of the springs.

The results obtained when the flexures were used are compared with the results with the springs in Figure 4. The flexures are clearly the superior approach. A relative movement of the extensometer system perpendicular to the test surface of 0.4 in. resulted in an apparent extensometer output change of approximately 80 μin. which, for a 1-inch gage length, corresponds to a total strain of only 0.000080 in/in.

The effects on its output of independent motions of the extensometer and its support system transverse to the gage length are shown in Figure 5. Again the use of the flexures instead of the springs is shown to be more desirable. The maximum effects observed during a total relative movement of 0.7 in. was +30 and -10 μin. For a gage length of 1 in., these correspond to strains of +0.000030 and -0.000010 in/in.

Figure 6 presents the effects of relative motions of the extensometer and its support system relative to the gage length, i.e. movement parallel to the direction in which strain is being measured. Again mounting the extensometer with the flexures dramatically reduced the sensitivity of the extensometer to relative motions in this direction compared with the springs. A motion of 0.30 in. resulted in a total offset of about 400 μin, or about 0.000400 in/in for the 1-in. gage length. The effect appeared to be linear with strain suggesting that a single correction factor might be used to compensate for most of this effect.

3.2   CAPACITIVE SENSOR DEVICE

3.2.1   System Description and Operation

The technique that was judged to be the second most likely to meet the contract goals in the preliminary evaluation was a capacitive sensor device*. With this device, the strain is sensed by the unbalance in a capacitance bridge as distances change between two small capacitor plates. Figure 7 shows diagrammatic side and top views of how this device would be installed on a structure for testing. The reference plate, shown at the right, was actually the end of a tube 0.25 in. in diameter which had a circular foil spot welded to the end adjacent to the active plate. The side of the tube was attached to a 0.004-in.-thick foil of Inconel or Hastelloy-X by a row of spot welds parallel to its axis. A second perpendicular row of spot welds, shown as "x's" in Figure 7, attached this tube to the structure and

_____

* Originally purchased from Hitec Inc., now sold by Capacitec Inc., Ayer, MA, (508 772-6033)

10

defined one end of the gage length. The other active or driven component of the system is shown to the left in Figure 7. It is similarly attached to the structure and a second row of spot welds, also noted by "x's" in Figure 7, defined the other end of the gage length.

Two sensors, Model HPC-40-H-5507-1990, were originally purchased. These had stiff metal-sheathed leads with an active element diameter of 0.39 in. and an overall O.D. of 0.18 in. One sensor, S/N 40-2553, operated successfully to 1600°F but the other failed during elevated temperature testing. It was replaced by a larger, more durable sensor, Model HPC-75A-V-T-3M, S/N 75-2834, which had an active sensor diameter of 0.075 inch and an overall O.D. of 0.250 inch. This larger sensor had a much more flexible lead although there was a long rigid section that extended about 2 in. from the sensor body before the flexible lead began.

3.2.2 Testing Approach

The initial experimental concerns about the use of this type of sensor focused on the ease of installation and how sensitive it might be to alignment and changes in alignment. The sensor was installed on the fixture shown previously in Figure 2 where its behavior could be directly compared with the output of a sensitive LVDT that only saw motions parallel to its axis. The capacitive device was mounted on the machinist's table so that its sensitivity could be determined as a function of the initial gap between the plates, so that the active capacitive plate could be rotated by controlled amounts around the axis of strain measurement in the plane of the plate, and so that the effects of the translation of one plate versus the other, parallel to the planes of the plates and perpendicular to the axis of strain measurement, could be determined.

Another device, shown in Figure 8, was also constructed to examine the effects of temperature on the sensor. A passive plate of Hastelloy-X, 1.0 in. in diameter and 0.062 in. thick was placed on top of a fused quartz tube inside a furnace. The sensor body was spring loaded by another quartz tube so that the active plate of the sensor protruded through a hole in the end of another quartz tube as shown in Figure 8. Fused quartz has a very low coefficient of thermal expansion (0.9×10^{-6}/°F), and the tubes were arranged so that their thermal expansions tended to cancel each other. The center quartz tubes were mounted on the actuator of a servo hydraulic closed loop testing machine which had a sensitive LVDT mounted on the actuator outside of the furnace. Controlled motions of the actuator and the outputs of the LVDT were used to measure the sensitivities of the sensor to motion at various temperatures.

11

3.2.3   Test Results and Conclusions

Measurements of the effects of the initial gap between the plates on the deviations from the linear calibration of capacitive strain sensor, S/N 75-2834, are presented in Figure 9. The results show that there were some changes in the calibration depending upon the initial gap, but it had only a small effect over the range of gaps from 0.002 to 0.024 inch.

The effects of motions of the sensors parallel to the faces of the targets for two different sensors are shown in Figure 10. Each of these measurements was made with the gap set near the midpoint of the linear range of the sensor. One sensor, S/N 75-2834, was more stable and showed more symmetrical behavior than the other.

Using a plate containing a slot into which both the target and the body of the active sensor could be wedged during attachment was found to be a convenient method to help in obtaining good alignment so that the centerlines of the two components were on the same axis and the faces of the plates were relatively parallel.

The effects on calibration of the faces of the sensor and the target not being parallel to each other are presented in Figure 11. This was a large effect and may need to be accounted for if the device is not aligned very carefully or if it is used on the surface of a structure which will experience bending strains.

The effect on the output of the sensor caused by heating the sensor at 15°F/min to 1600°F is shown in Figure 12. The effect does not appear to be linear and is greater at higher temperatures. Because of how this sensor was supported, shown in Figure 8, these effects would not be expected to be the same as those which might occur if the device were mounted on an actual structure as shown in Figure 7. Data of that type will be presented in Section 4.2.1. The effect of temperature on the calibration of the capacitive strain sensor is given in Table 3.

The drift with time of capacitive sensor S/N 75-28354 at various elevated temperatures is shown in Figure 13. These data show quite small amounts of drift even at 1600°F when the sensor is mounted as shown in Figure 8. These data may also be contrasted with similar direct comparison data in Section 4.2.3.

3.3   SPUTTERED THIN FILM STRAIN GAGE

3.3.1   Review of Previous Work

12

Prior and current contract and IR & D efforts at United Technologies (UTC) have been devoted to the development of both wire and thin film sputtered strain gages. The development of thin film gages has been of particular interest because they provide the only technique that could be used to measure localized strains in blades and vanes inside running gas turbine engine without causing unacceptable aerodynamic effects. One of the precepts of this contract was that some of this emerging technology might be applied to the need for strain measurements in testing aerospace structures at extreme temperatures.

Several prior contract efforts have concentrated on the development of new resistive strain sensor alloys. The Pd-13 weight % Cr alloy and the Fe-10.6Cr-11.9Al (in weight %) Mod#3 alloy were identified. Current NASA supported efforts are concentrated on the development of the Pd-13Cr alloy. Efforts to develop the FeCrAl alloy Mod #3 were dropped primarily because it showed nonlinear behavior with temperature and changes in its apparent strain versus temperature curves after extended exposures in air at about 1800°F, as shown in Figure 14. These changes are apparently due to oxidation and would be more important if the material were prepared as an unprotected thin film only about 6 μm thick. If covered with a suitable protective overcoat film, the stability of this sensor material might satisfy the relatively short time requirements of this contract.

A major problem identified in prior work at UTC on sputtered thin film strain gages was that typically prepared alumina films used to provide electrical insulation between the gage and the substrate and as a protective overcoat on gages to prevent oxidation attack are inadequate for these purposes. A typical sputtered film of aluminum oxide contains absorbed argon (Ref.12). When the alumina film is heated to an elevated temperature:

(1) The argon is exsolved from the film which results in a porous film.
(2) The films tend to sinter and shrink forming cracks.
(3) The alumina transforms into the more stable alpha crystal structure.
(4) The alumina absorbs or desorbs oxygen to adjust for the correct stoichiometry.

A viable solution to these problems is to sputter the alumina onto a substrate heated to about 1100°F or higher. The argon will then be exsolved from the film as fast as it is entrapped and the shrinkage thus avoided. In addition, the alumina forms immediately in the alpha form. Also very important, upon cooling, the film is put into compression rather than tension as before because the coefficient of thermal expansion of the film is lower than that of the substrate. Alumina films prepared by this hot sputtering procedure show significant improvements in electrical resistances at elevated temperatures and are more effective when used as overcoat films to reduce oxidation attack.

3.3.2 Objectives

Because it may not be practical to disassemble and place structures inside a sputtering chamber, a method is needed to prepare groups of thin film strain gages which can then be individually installed at different locations on the structure being tested. To this purpose, we proposed to examine the potential for preparing sputtered thin film gages on metal foils, 4 to 5 mils thick, which could then be attached where needed by spot welding.

It would simplify and reduce the cost of strain gage devices if we could eliminate or provide substitutes for some of the sputtering steps. We proposed to briefly examine the possibility of using glass films prepared using the transfer tape technique for the electrical insulation layers and, perhaps, as protective overcoat films.

The final subject which we wished to examine was the possibility that the electrical resistance behavior of the FeCrAl alloy developed on a prior NASA contract might be improved by preparing it in the form of a thin film. The resistivity of this alloy is nonlinear with temperature in such a way that its net change is relatively insensitive to temperature as shown in Figure 14. In the temperature range 600° to 1000°F, however, alloys of this general type show instabilities with time which make them difficult to use as strain gage sensors. It has been suggested that these changes may be due to ordering or to magnetic domain effects. If these effects are due to changes in the size of magnetic domains, i.e. changes in the concentration of domain walls, these effects might be reduced or eliminated by preparing them as thin films whose thickness dimensions are much smaller than the size of magnetic domains. Our final objective was to examine this possibility with a sputtered thin film strain gage of the FeCrAl Mod #3 alloy deposited on a thick substrate of Hastelloy-X.

3.3.3 Fabrication studies

As mentioned above, two parallel efforts were undertaken to develop transferrable sputtered strain gages for use in structural testing at temperatures to 1600°F. The first effort was to characterize the electrical behavior of the FeCrAl Mod#3 alloy developed on a previous contract (Refs. 2 and 4) when prepared as a sputtered thin film strain gage. Although resistance testing of the cast material had previously been performed (Fig. 14), no data existed on the performance of this material as sputtered thin film. Work on PdCr has shown that even though a material may exhibit good resistance to oxidation in bulk form, additional protection would probably be needed for a film 6.0 μm thick.

A series of four samples was prepared using the same steps as in the preparation of

14

previous sputtered film gages (Ref. 4). Hastelloy-X substrates (3.0 in. x 0.50 in. x 0.040 in.) were polished to a 0.4-μm surface finish, coated with 0.010 in. of electron beam vapor deposited NiCoCrAlY, repolished, removing 2 to 5 mils of the coating, and finally heat treated at 1800°F in vacuum and then in air. The grown aluminum oxide layer formed in this way was continuous and adherent. The substrates were next heated to 1100°F and a 2.0-μm alumina insulation layer applied by R.F. magnitron sputtering. This layer was also continuous and adherent. The FeCrAl gage element was applied next also by R.F. magnitron sputtering.

The masking procedure used for these samples varied from that used in previous work in that the FeCrAl was first sputtered over the entire surface without any mask being present. A photoresist mask was then applied to the surface using standard photolithographic techniques, and the excess FeCrAl layer was removed from around the sensor by ion beam etching. Use of this technique eliminates the possibility of contamination under the FeCrAl due to incomplete removal of the photoresist from the sputtered alumina layer. The use of ion beam etching also leaves each leg of the grid with slightly tapered edges instead of the vertical, ragged edges typical of films sputtered over resist and then torn loose when the resist is removed. The tapered edges also result in a tighter, more uniform overcoat layer in these areas.

Resistance measurements after removing the photoresist mask were as follows:

Sample#	GageR	R to Gnd.
P87-9-1	119.1 Ω	>20 MegΩ
P87-9-2	17.2 Ω	30 Ω
P87-9-3	16.6 Ω	>20 MegΩ
P87-9-4	15.3 Ω	14.8 Ω

Because of the low gage resistance and insulation resistance of three of the samples, only sample P87-9-1 was deemed suitable for overcoating and testing. The low resistances were caused by spot defects in the alumina insulation layer, which resulted in shorts through the substrate.

The final step in sample preparation was applying overcoats for oxidation protection. The lead tab areas were protected by the application of a 1-μm-thick ion beam deposited Pt layer. Ion beam deposition was used instead of R.F. sputtering because of its superior adhesion as shown in previous work. The remainder of the sensor was protected by a 2.0-μm-thick sputtered alumina layer which, like the insulation layer, was sputtered with the substrate at 1100°F. Because the working gas used for the sputtering of alumina is an argon-20% oxygen mixture, sputtering was begun while the substrate was at 650°F with

15

the temperature raised to 1100°F after the first 0.25μm of alumina was deposited. This prevented oxidation of the FeCrAl from occurring at 1100°F before the protective layer was formed.

Because sample P87-9-1 would be tested in UTRC's resistivity testing facility which makes electrical contact with the sample through electrically insulated clamps, no welded leadwire attachments to the sputtered lead tabs were required.

The first work undertaken to develop strain gages on transferrable foils was to develop a technique to prepare satisfactory insulation layers on foils. In addition to providing the required electrical resistance at 1600°F, the insulation material must provide good strain transfer and remain adherent when the foil is heated or strained.

Two approaches were examined. The first approach, chosen for its potential low cost and ease of application, was to use a glass transfer tape. The tape consisted of a glass frit and organic binder which could be pasted down on the foil and fired to form layer of fused glass, typically 1 to 2 mils thick. The two glass compositions which were investigated, a borosilicate and lead-alumina-silica glass, were selected because of their high firing temperatures of 1830°F and 2200°F, respectively. Both glasses were found to react to some extent with the FeCrAl sputtered material at elevated temperatures, as well as being somewhat soft at 1600°F. This approach was deemed unacceptable without additional effort to develop a high temperature glass which would not react with sputtered metallic layers.

The second approach was to use a NiCoCrAlY layer sputtered onto the Hastelloy-X followed by a sputtered alumina layer. This approach was derived from the techniques previously developed for use on turbine blades and vanes. It was decided that the NiCoCrAlY layer should not be deposited on a 5-mil Hastelloy-X foil by electron beam vapor deposition because this would probably result in severe distortion of the foil. A 10-μm to 15-μm-thick layer of sputtered NiCoCrAlY was substituted. Because bulk Hastelloy-X substrates were normally polished to a 0.4 μm surface finish prior to the oxidation heat treatment to form a layer of grown alumina, attempts were made to polish the Hastelloy-X foils prior to sputtering the NiCoCrAlY layer. The surface finish of the material upon which a sputtered layer is being deposited normally has a large effect on the uniformity of the sputter deposited materials. A sputtered layer containing large nodules and crevices is more likely to contain easy paths for oxygen diffusion.

The foils proved to be difficult to polish with consistent results, primarily because of problems associated with holding the foils during polishing. The foils tended to warp due to stresses in the side being polished. A vacuum plate was designed and used to hold a

3.5-in. x 3.5-in. foil with some success. The foils were removed and turned over several times during polishing to work both surfaces equally. The polished foils had highly polished areas (surface roughness < 0.02 μm) interspersed with moderately polished areas (surface roughness > 1.0 μm).

A layer of NiCoCrAlY was sputtered on one side of both polished and as-received foils. The foils were then heat treated at 1800°F, first in a vacuum and then in air to form a grown alumina layer from the NiCoCrAlY. When used with the thicker vapor deposited coatings, this heat treatment forms an alumina layer approximately 1.5-μm-thick. Approximately one quarter of the aluminum present in a 15-μm-thick film of NiCoCrAlY would be needed to form this much alumina.

The films were very warped after heat treatment. The sputtered surface was concave, and the grown oxide layer had spalled or cracked in large areas. In an attempt to overcome this problem, a second batch of foils was prepared with NiCoCrAlY sputtered on both sides of the foil. Two of these foils also had diagonal cuts made at their corners, and their edges were bent at 90 degrees to further restrict warping during heat treatment. Although these modifications resulted in less warping of the foils, they did not completely alleviate it and spalling of the oxide still occurred. In addition to creating a reservoir of aluminum for oxide formation, the NiCoCrAlY layer is also said to provide a relatively ductile stress relief layer between the alumina and the Hastelloy-X. Reducing the thickness of the NiCoCrAlY may have reduced the effectiveness of this layer in providing stress relief during cooling from 1800°F. A decision was made to prepare a series of foils eliminating the grown oxide layer. These foils, which still had NiCoCrAlY applied to both sides, had a 2.0-μm alumina layer sputtered on one surface while the foil was at 1100°F. This series of foils had minimal warping and an adherent oxide insulation layer.

The adherence of the sputtered alumina was better on the as-received foil surface than on the additionally polished surfaces. It was also observed that the nonuniform polish could result in differences in the surface morphology of the sputtered film. Although uniformly well polished foils might be produced with an extended effort, it was decided to use the surface as-received for the preparation of the remainder of our samples.

A final set of foils was fabricated with sputtered NiCoCrAlY on both surfaces and the oxidation heat treatment eliminated. A 6-μm-thick grid of FeCrAl was sputtered on top of the alumina layer. A 1-μm ion beam deposited layer of Pt was next applied to the lead tabs to provide oxidation resistant surfaces for attaching the lead wires. The remainder of the sample was protected from oxidation by the application of a 2.0-μm alumina overcoat. Like the insulation layer, this layer was also sputtered with the foil at 1100°F, which places

the alumina in compression upon cooling. Insulation resistance measurements on the completed samples showed that the majority of the samples had an insulation resistance below 20 megohms because of defects in the alumina insulation layer. The best two of these samples were prepared for attachment to the Mar M-246 test bar (see Section 4.1 and Fig. 20) by ion beam etching away the alumina layers at two locations adjacent to the ends of the strain gage grid. This was done to provide clean areas for spot-welding the foils to the test bar. The best foil was welded to the bar using a 0.20-in.-long row of spot welds at each end of the grid. Platinum wires, 3 mils in diameter, were attached to the lead tabs by parallel gap spot welding. These 3-mil strain relief wires were similarly attached to the three main lead wires, which were 0.010 in. in diameter.

3.3.4 Test Results on a Bulk Substrate

A sputtered FeCrAl gage on a 0.062-in.-thick Hastelloy-X substrate (Sample P87-9-1) was tested to 1600°F to determine the thermal coefficient of resistance (alpha) and stability. All testing was performed in air. A heating rate of 80°F/min was used except where noted. The room temperature resistance of the gage at the start of testing was 119.1 Ω. The resistance was stable throughout the testing below 1600°F, changing only $\pm 0.5 \Omega$ (0.4%) during 8 heating cycles to 1500°F and 100 hours of drift testing at 600°F to 1000°F.

Three initial heating and cooling cycles were performed to 1100°F, 1350°F, and 1550°F. The average thermal coefficient of resistance from 75°F to 1070°F during these cycles was 73.0 $\mu\Omega/\Omega/F$. The third cycle is presented in Fig. 15 which shows that the resistance vs. temperature curve is nonlinear. The thermal coefficient of resistance increases in magnitude to 1100°F at which point there is a break in the curve which then flattens. This break can be seen more clearly in the plots of the thermal coefficient of resistance (alpha) vs. temperature also shown in Fig.15. A curve with this shape was also seen in the cast material previously tested (Ref. 4), although the values of alpha were much lower for the cast material. A microprobe analysis was made to determine the chemical composition of the sputtered FeCrAl. The results shown below revealed that the composition of the sputtered film varied significantly from the composition of the previously tested cast material which provides an explanation why the data in Fig. 15 differs from that shown in Fig. 14.

Composition of FeCrAl Samples:

	Cr (Wt %)	Al (Wt %)
FeCrAl Mod#3 (cast)	10.6	11.9
P87-9-1 (sputtered)	11.7	4.8

Because other strain gage alloys in wire form have shown serious stability

problems in the temperature range 700°F to 1100°F, a series of drift tests were made over this temperature range to measure the drift of the sputtered film. To maintain consistency with previous work on drift testing of similar alloys (Ref.13), the sample was first heated to 1200°F and then rapidly cooled to the drift test temperature at the start of each 16-hour drift test. Drift tests were run at 600°F, 700°F, 800°F, 900°F, and 1000°F. The results of this series of tests are shown in Fig.16. A dramatic change can be seen between the data at 700°F, which shows a slight positive initial drift followed by a gradual return to the starting resistance, and that at 800°F which shows a large initial negative drift which stabilized after four hours. Above 800°F the magnitude of the total drift decreases to $< 300\ \mu\Omega/\Omega$ at 1000°F. A second drift test at 800°F was run after the 1000°F drift to show that the magnitude of the drift does not decrease as a result of exposure to a higher temperature. This second drift is compared to the first 800°F drift test in Fig. 17. During these six drift tests the value of alpha remained stable, changing from 73.0 $\mu\Omega/\Omega/F$ at the start of testing to 74.2 $\mu\Omega/\Omega/F$ at the conclusion of this low temperature drift testing.

The stability of the sputtered FeCrAl was also evaluated by an additional 16-hour drift test at 1600°F. For this test, the sample was heated directly to 1600°F with data taken after allowing the sample temperature to stabilize for 5 min. Problems with the test equipment produced erratic data for the first 2.5 hours of this test. The data is shown in Figs.16 and 17. The steady positive drift after the first six hours is believed to be caused by oxidation of the FeCrAl due to defects in the overcoat. The drift rate did not appear to be decreasing after 16 hours at temperature. Alpha measured after this test had increased from 74.2 $\mu\Omega/\Omega/°F$ to 93.2 $\mu\Omega/\Omega/°F$, which is another indication that the composition of the alloy had changed as a result of oxidation at 1600°F. The R.T. sample resistance had decreased from 118.6Ω to 115.0Ω at the conclusion of the 1600°F drift test.

To check the reproducibility of the sputtered material and to see if extensive cycling through 800°F would have any effect on exhausting the metallurgical transformation, 100 thermal cycles were run from a minimum of 500°F to a maximum of 1100°F at 100°F/min. with 5-min. soaks at 500 and 1100°F. The 2nd, 50th, and 100th cycles are plotted in Fig. 18 which shows no changes due to this cycling. The heating and cooling data do not track precisely on each other due to the thermal inertia of the substrate at this high a rate of temperature change. This cycling also had a minimal effect on the drift at 800°F which is shown as drift #3 in the upper plot in Fig 17. Both alpha and the resistance at room temperature did not change as a result of this testing.

4 - DIRECT COMPARISON TESTING

4.1 TESTING SYSTEMS

The testing facility shown in Figure 19 was used for elevated temperature and cryogenic testing of the rod type extensometer, the capacitance strain sensor, and the thin film strain gage on a transferrable foil. The two major components were a 110 KIP capacity servohydraulic testing machine* and a vertical radiant energy clam shell furnace**. The strain measuring devices were attached near the center of a 20-inch-long bar of a nickel base alloy (MAR M-246) which was 0.75 in. in diameter. The test bar extended out of both ends of the furnace to facilitate the application of tensile loads by the test machine. Flats were milled on opposite sides of the bar to create a reduced cross section of 0.25 x 0.70 in. near the center 6.5 in. of the bar. Liquid nitrogen could be introduced into a cup on the top of the furnace so that it would run down the bar to cool it. A second metal cup, held in place with an "O" ring fitting below the furnace, collected the excess liquid nitrogen until it evaporated. A closer view of the test section of the bar with the capacitive sensor and rod type extensometer in place is shown in Figure 20. The thin film strain gage and a low temperature commercial gage mounted on the opposite side of the bar are not visible in Figure 20.

The capacitive sensor and target were both spot welded to 0.70-in. x 1.00-in. pieces of 0.005-in.-thick Hastelloy-X foil. Using a 0.005 in. shim to set the sensor gap, the sensor and target foils were spot welded to the bar by a single row of spot welds perpendicular to the sensor axis. The 1.00 inch between these two rows of spot welds thus set the gage length at 1.00 in. for this sensor. The sensor lead cable was routed down the bar and out the bottom of the furnace and secured to the bar with three equally spaced spot welded Hastelloy-X straps. Two models of capacitive sensors were tested. These sensors (Model HPC-75A-V-T-3M & HPC-75C-V-N-3B) were described in Section 3.2.1.

The extensometer was mounted on a fixture which stood outside the furnace and was bolted to the bed of the test machine. This fixture incorporated two slides, one of which allowed the extensometer mounting plate to be moved vertically to align the flexures which held the extensometer body with the center of the reduced section in the MAR M-246 test bar. The second slide allowed the mounting plate to be moved toward or away from the test bar to increase or decrease the force holding the extensometer against the test bar. Two

---

* MTS Systems Corp., Model 311.21S, Minneapolis, MN.
** Quad Elliptical Furnace, Model E4-10, Research Inc., Minneapolis, MN.

different length alumina rods were used to simulate testing with and without a bank of radiant heaters in a test on an actual structure. The test setup for the longer rods also required the use of a spring attached to the upper extension rod to support part of the weight of the extensometer body. Two divots for rod contact with the bar were made on the original curved bar surface centered between the machined flats. These divots set the gage length at 1.00 in. for the extensometer.

Prior to installation on the test bar, each sensor was calibrated at room temperature using a mechanical calibration fixture. Both of the capacitive sensors were calibrated over a linear range of ±0.010 inch with a sensitivity of 0.002 in./volt. The extensometer was calibrated over a linear range of ±0.020 inch when using the short rods (4.42 in.), with a sensitivity of 0.0027 in./volt. When the longer rods were used (10.75 in.), the linear range was expanded to ±0.050 inch and the sensitivity decreased to 0.0063 in./volt.

For initial tests at room temperature, a commercial strain gage* was also attached to the test bar to determine the actual strain on the bar. This gage was removed from the bar at the start of elevated temperature testing. It had been planned to use the measured cross-section of the bar and book values for the modulus of Mar M-246 at the test temperature to determine the actual strain on the bar at elevated temperatures. This plan was modified when the modulus of the bar at room temperature did not agree with the book value. Initial room temperature measurements of the elastic modulus of the Mar M-246 bar were 24.6×10^6 and 24.8×10^6 lb/in^2 for the commercial strain gage and the rod type extensometer respectively. The agreement between the different techniques was excellent. Unfortunately, the book value for the elastic modulus of this material is 29.8×10^6 lb/in^2. The calibration of the testing machine load cell, as well as all calculations were checked without finding the reason for this discrepancy. Chemical analysis of a piece from the end of the bar confirmed that it was MAR M-246. Conversations with the fabricator revealed that the bar had been cast transversely. We suspect that, because of the thermal masses associated with the casting gates and risers, the section of the bar we used may have been solidified in a semidirectional manner. This effect may have been accentuated by the fact that most of the material we were testing was fairly close to the center axis of the bar due to the reduced cross section. Our room temperature strain results were used to calculate an adjusted effective cross section for the bar. This area was then used with the book values for the relative change in elastic modulus with temperature to provide an accurate reference strain under stress at elevated temperatures.

Four ISA type K inconel-sheathed thermocouples were spot welded to the bar to measure the temperature of the bar as well as variations in temperature as the test bar was

---

* Micro-measurements Division, Measurements Group, Inc., Raleigh, NC

thermally cycled. These thermocouples were located on the face of the reduced section beside the capacitive sensor, on top of the capacitive sensor, on the opposite face below the sputtered gage, and on the surface of the bar between the points of the extensometer rods.

The outputs of all of the strain sensor systems as well as the thermocouple outputs and the load output of the testing machine were fed to a computerized data acquisition system* for storage and data reduction. The testing machine internal bridge completion was used to complete the extensometer circuit instead of the Bam-1 used in an earlier phase of the work. Bridge completion for the thin film strain gage was through a Wheatstone bridge circuit fabricated at UTRC. The data acquisition system was programmed to collect data from all inputs at a user selected interval. All sensors were re-zeroed at the start of each test. The calibrations for both the capacitance sensors and the extensometer were entered into the computer so that the results were stored and printed as μstrain readings.

4.2 TEST RESULTS

4.2.1 Apparent Strain

For experiments to measure the effects caused by changes in sample temperature, a preload of 100 lbs. (23 μstrain) was applied to the test bar at room temperature. This load was to be maintained throughout the test by placing the test machine in the load control mode. This small load was intended to keep the fixturing tight as the bar expanded or contracted and to prevent any movement of the bar during testing. During the first thermal cycle to 1600°F, however, this load was not maintained as the bar expanded, and the side loading on the bar from the extensometer rods caused the bar to rotate or move sideways. This movement led to slippage of the extensometer rods, which may have contributed to the failure of the thin film strain gage during this test. Because the strain gage failed on the first cycle at 1470°F, these data represent the only elevated temperature data obtained for the sputtered strain gage on a transferrable foil. The sputtered FeCrAl film had completely spalled or been torn away from the sputtered alumina insulation layer when examined at the end of this run. The data from both the sputtered gage and the extensometer are shown in Figure 21. As can be observed in Figure 21, the extensometer began to slip between 1200°F and 1300°F, with the extension rods closing rapidly above 1300°F. The apparent strain data shown in Figure 21 for the sputtered FeCrAl gage on foil is in good agreement with the previous data for this same alloy sputtered on a solid Hastelloy-X substrate. These data are also included in Figure 21. The average thermal coefficient of resistance from 75°F

---

* 3852A Data Acquisition/Control Unit, Hewlett Packard, Cupertino, CA.

22

to 1200°F was 83.1 $\mu\Omega/\Omega/°F$.

A second sputtered gage on Hast-X foil was spot welded to the bar prior to the resumption of testing. This gage had been fabricated using the same procedures as the first, but had low insulation resistance. It was attached to the bar to check gage survivability with no resistance data taken because of its low resistance to ground. The attachment techniques were the same as for the original gage, with the exception that no leadwires were attached. This gage survived all of the testing described in Section 4.2 without any spalling of the FeCrAl. Some small sections of the alumina overcoat did spall, primarily at the edges of the sputtered FeCrAl. An accurate measurement of gage resistance could not be made because of the continued low insulation resistance to the foil. The condition of this gage at the completion of all testing is shown in Figure 22. The external dimensions of the active grid are 0.12 x 0.12 in. The areas where the overcoat had begun to spall can be seen as darker patches on the edge of the right lead film and near the bottom third of the grid legs.

A total of four thermal cycles to 1600°F were run at two different heating rates and the data collected from the two remaining strain sensors. Apparent strain data for the MTS extensometer from three of these cycles is shown in Figure 23. Increasing the heating rate by a factor of 3 from 50°F/min. to 150°F/min. had no effect on the data. The run made with the longer extension rods showed an increased temperature sensitivity of 3.7 percent at 1600°F compared with the shorter rods. The apparent strain recorded by the extensometer should agree with the increase in the gage length due to thermal expansion of the Mar M-246 bar. The book value of the thermal expansion of Mar M-246, also shown in Figure 25, was approximately 11 percent higher than the apparent strain recorded by the extensometer. Since the test bar appeared to have an elastic modulus which differed from the book value, its thermal expansion may also differ from the standard value. Because independent confirmation of the bar's coefficient of expansion would require removing a test piece from the bar, no other investigations of its thermal expansion were made.

Figure 23 also shows data collected from two different capacitive sensors during identical thermal cycles. A significant difference in sensor output can be seen depending on the rate of temperature change and whether the bar is being heated or cooled. The two sensors showed fairly close agreement when heated or cooled at the same rate. The output expected from this type of sensor during heating is more difficult to predict because the thermal expansion of the sensor itself will have a large effect on the size of the sensor gap. The thermal expansion of the sensor should tend to cancel out most of the thermal expansion of the Mar M-246 bar. Temperatures recorded by the thermocouples spot welded to the bar and on top of the capacitance sensor showed that a large temperature difference was established when the lamps were first turned on at the start of a heating cycle. The sensor temperature rose 125°F above the temperature of the test bar surface in the first 2

23

minutes of a 150°F/min. heating cycle. The expansion of the sensor and target during this rapid heating would account for the decrease in sensor gap which resulted in the large negative apparent strain at the start of the thermal cycle at 150°F shown in Figure 23. This temperature difference had dropped to 20°F when the bar reached 1500°F. Upon cooling, the sensor temperature quickly dropped 85°F below the bar temperature. This decrease in sensor temperature relative to the bar would tend to increase the sensor gap resulting in the steep slope of the apparent strain curve at the start of cooling. The break in the cooling curve at 150°F/min. was caused by the introduction of a cooling gas to help maintain the rapid cooling rate. The average apparent strain change from 75°F to 1600°F was -1.8 µstrain/°F for the two capacitive sensors.

Apparent strain data were also collected for both extensometer configurations during cooling cycles to -310°F. Because cooling was accomplished by introducing liquid nitrogen at the top of the furnace which then flowed down over the surface of the bar, a controlled rate of cooling could not be maintained. The cooling rates tended to be slow until a bar temperature of -100°F was reached, at which point the liquid nitrogen wetted the bar resulting in a quick drop to -310°F. Extensometer data for both rod lengths is presented in Figure 24. The data show a higher degree of scatter than the data taken during heating cycles to 1600°F which may have been due to the rapid cooling and thermal gradients generated in the bar. The heating curve with 4.42-in. rods shows less scatter as the liquid nitrogen was turned off and the lamps heated the bar back to room temperature. The average apparent strain change of 6.5 µstrain/°F upon heating from -100°F to 75°F is in good agreement with the average apparent strain of 6.1 µstrain/°F obtained while heating from 100°F to 1600°F .

Apparent strain data from ambient to -310°F for the two capacitance sensors is also shown in Figure 24. The cooling curves from 75°F to -50°F show a gradual increase in apparent strain which is consistent with the elevated temperature data. Below -50°F, however, the apparent strain goes negative indicating a decrease in sensor gap. Since the thermocouple welded to the top of the sensor showed that the sensor reached -310°F at approximately the same time as the surface of the bar, this negative apparent strain cannot be explained by the sensor being warmer than the bar. It is possible that moisture condensing and freezing on the cold face of the sensor may be having an effect on its output.

4.2.2 Strain Sensitivity

In order to evaluate the ability of each sensor type to accurately record changes in strain at temperatures from -310°F to 1600°F, the test bar was loaded to 1000 µstrain at a strain rate of 10 µstrain/sec. at six predetermined temperatures (-310°F, 75°F, 400°F,

24

800°F, 1200°F, and 1600°F). A preload of 23 µstrain was maintained to keep the fixturing tight and the sample aligned in the grips while heating to the test temperatures and during a 2-minute temperature stabilization prior to the load cycle. This 23-µstrain preload was used as the starting point for each loading cycle. Two load cycles were run at each temperature, one after the 2-minute temperature stabilization period, and the second after a 30-minute resistance drift test at temperature. Both sensors were electrically rezeroed before the start of each load cycle.

The results obtained for the second 75°F load cycle for all of the sensors tested are shown in Figure 25. The load strain curve obtained using the commercial strain gage is also shown in these plots. The upper plot in Figure 25 shows the results for both configurations of the extensometer. The results are in close agreement with those measured by the commercial gage (+0 µstrain/-30 µstrain), and show minimal hysteresis between loading and unloading (<10 µstrain). The lower plot in Figure 25 shows the results obtained for the two different capacitive sensors tested. The sensor with the stiff lead cable (S/N 2834) gave a good representation of the actual strain during loading; however, there was a large hysteresis effect upon unloading. The width of the loop changed when the sensor was removed from the bar and reattached, but it could not be eliminated. The method used for securing the lead cable appears to have an effect on the ability of the sensor to record strain. The sensor with the flexible leadcable (S/N 2968) showed less hysteresis, but did not give as accurate a representation of strain. This sensor was removed from the test bar and the calibration rechecked on the calibration fixture. Because the calibration agreed with the original, it was concluded that the attachment of the lead cable has an important effect on sensor performance.

Figures 26 through 29 show the strain vs. load performance of all the sensors tested at elevated temperatures. As described in Section 4.1, a theoretical load vs. strain curve was calculated for each test temperature using the measured modulus of Mar M-246 and the effective cross-sectional area of the bar. All curves shown are from the second load cycle at the test temperature. The initial loading cycles were similar, with the exception that in some instances the capacitive sensors were still showing some drift at the start of the load cycle. This drift was apparently due to the sensor requiring longer than 2 minutes to stabilize after heating to the test temperature. The upper plots show the results for the extensometer which continued to give accurate strain readings to 1600°F. In most cases, the extensometer appeared to read slightly low, but within 5 percent of the theoretical strain. Some increase in scatter is also observed in the data obtained at 1600°F.

The lower plots in Figures 28 through 31 show the results for the capacitive strain sensors which continued to show the same basic characteristics as they had at 75°F. The

sensor with the stiff lead cable (S/N 2834) continued to show a large amount of hysteresis up to temperatures of 800°F. Above 800°F, the hysteresis was reduced, but the curves became nonlinear with deviations of up to 130 μstrain from the theoretical values between 0 to 100 μstrain. At 1200°F this deviation had increased to +250 μstrain at 1600 μstrain. At 1600°F the sensor with the flexible leadcable (S/N 2968) continued to show slightly less hysteresis then sensor S/N 2834 but the indicated strain was only 28 percent of the theoretical 1400 μstrain.

Figure 30 shows the strain vs. load results for all sensors at -310°F. The upper plot shows the results obtained for the extensometer using both the long and short rods. Although the set-up with the short rods gave results similar to those at 75°F, the longer rods indicated strains which were 18 percent greater than the theoretical values. The reason for this apparent increase in strain sensitivity is not clear, especially in light of the continued good performance of the shorter rods. The lower plot in Figure 32 `shows the results for the capacitive sensors. Although the hysteresis previously seen with S/N 2834 has decreased, both sensors indicate strains of only 45 to 55% of the theoretical values using the strain calibration obtained at 75°F. The stress vs load curves of both sensors were reproducible at -310°F, suggesting that although the collection of moisture and frost on the sensor face might be a source of error during apparent strain tests, this may not be a serious problem if the sensor is properly calibrated and kept at subzero temperatures.

4.2.3 Drift

The ability of the extensometer and capacitive sensors to record static strain at temperatures from -310°F to 1600°F was examined by holding the test bar at the test temperature for 30 min. with a constant load of 100 lbs. (23 μstrain). The output of each sensor and thermocouple was recorded every min. during the test. At the beginning of each drift test, the bar had been at the test temperature for approximately 5 min. The radiant furnace was able to hold the bar at the test temperature within ± 1°F for the entire test and therefore no correction to the data for changes in temperature was needed. Drift tests were conducted at intervals of 200°F from 200°F to 1600°F, in addition to tests at 75°F and -310°F. Data from these tests are presented in Figures 31 through 40.

Figure 31 shows the results of the drift tests at 75°F, with the extensometer results presented in the upper plot and the capacitive sensor results in the lower plot. The capacitive sensors showed virtually no change in output during this test. The maximum variation from zero was + 10 μstrain for sensor S/N 2834. The scatter was less than 2 μstrain for each sensor. The extensometer showed a larger degree of scatter than the capacitive sensors, with the long rods showing deviations from zero of ±30 μstrain and the shorter rods deviations of ±10 μstrain.

Figures 32 through 39 show the results of drift tests at elevated temperatures. The capacitive sensors continue to show good stability up to temperatures of 600°F with little scatter in the data and overall drifts of ±20 μstrain. Above 600°F, the total drift of both capacitive sensors increased with S/N 2834 showing large positive drifts at 1400°F and 1600°F. This sensor is an earlier version than S/N 2968 which contained modifications in materials and fabrication techniques for high temperature use. These improvements appeared to be demonstrated in the improved stability of this sensor at 1400°F and 1600°F. The extensometer also performed well at temperatures up to 1200°F with total drifts of ±20 μstrain and scatter of ±40 μstrain for both the long and short rods. Above 1200°F, the scatter and drift increased with the largest drift being -100 μstrain for the shorter rods at 1400°F.

Figure 40 shows the stability of all sensors at -310°F. The capacitive sensors again show a high degree of stability with maximum deviations from zero of ±15 μstrain for S/N 2968. This stable behavior was in sharp contrast to the behavior of these sensors when cycled between 400°F and -310°F during ascent testing described in Section 4.2.4 below. The extensometer also shows stable behavior at -310°F with an overall drift of only ±20 μstrain.

4.2.4 Simulated Ascent and Reentry

In order to properly test an aerospace structure, it is important to be able to measure experimentally the magnitude of the critical strains that it might experience during ascent and reentry through the atmosphere. One of the requirements of this contract was to conduct a demonstration of the ability of the selected strain measurement system to function accurately under these conditions. Ascent conditions were to be approximated by heating with an applied stress of about 570 lbs/in² from -310°F to 400°F at about 150°F/min. followed by a 1.5-minute soak at 400°F. Thereafter, the system would be cooled down to -310°F again at about 30°F/min. Reentry would be simulated by heating at an applied stress of about 570 lbs/in² from room temperature to 1200°F at 150°F/min. (2.5°F/sec) followed by a 10-minute hold at that temperature. The system would then be heated at about 30°F/min to 1600°F, held there for 15 minutes, and then cooled to room temperature at about 30°F/min.

Figure 41 shows measurements of strain produced by the extensometer with 4.42-in. and 10.75-in.-long rods together with the temperature readout from a thermocouple spot welded to the test bar during ascent cycles. The strain measurements are smooth and follow the shapes of the temperature curves. These temperature and strain curves would not be

expected to be identical even if perfectly scaled because (a) there may be some dynamic delay in the center of the test bar reaching temperature as quickly as a thermocouple spot welded to the surface and (b) thermal expansion is not linear with temperature, the temperature coefficient becoming gradually larger as the temperature increases.

The simultaneous outputs from two different capacitive sensors obtained simultaneously with the data shown in Fig. 41 are compared with the same temperature readings in Figure 42. The capacitive systems do not directly measure the thermal expansions of the test bar for reasons discussed earlier, and therefore they do not produce curves which have shapes similar to those produced by the output of the thermocouple. Because the temperatures of these sensors are different from the temperatures of the test bar and because of the magnitude of the strain signals produced, these sensors do not appear to be suitable for use in high rate transient temperature conditions.

Temperature and strain data from the extensometer obtained during simulated reentry conditions are presented in Figure 43 for alumina rod lengths of 4.42 in. and 10.75 in. Again the strain data follow the temperature record, and there is good agreement for different rod lengths and good repeatability between different thermal cycles. Figure 44 shows data from two different capacitive sensors obtained during the same two cycles. The data curves from these sensors are similar but different for the two different sensors. The general shape of the strain data does not correspond to that of the temperature because the thermal expansions of the sensors themselves are involved, and their temperatures are not the same as that of the test bar.

4.3 DISCUSSION

The extensometer performed the best and if properly used should provide reliable strain measurements over the full range of temperatures investigated. The other two strain measuring approaches also appeared capable of providing strain data over this range, but they had significant disadvantages. In the case of sputtered thin films, more development work is needed to fully appreciate their potential.

One advantage of the capacitive sensor over the extensometer is that it could be mounted on internal surfaces which could not be reached by the rods of the extensometer. In this work, the advantage of the capacitive sensor being very small appeared to be offset by the fact that this made the capacitance of the lead wires an important component of the capacitive bridge. Any movement of these leads became an important source of error. This would be an important consideration if the structure being tested moved during loading. The use of a sensor with a much larger diameter probe might reduce the importance of this

problem.

Another problem with the capacitance approach was that the output was sensitive to the thermal expansion of the sensor and its temperature could be appreciably different from that of the surface on which it is attached. This could also be a problem with foil mounted strain gages. Metal cans or shades could be used to reduce these effects, but these may affect the uniformity of heating and result in thermal stress concentrations. This might not be as important a problem if these strain sensors were used on internal surfaces. It should not be a problem with sputtered strain gages deposited directly on a part of the structure that could be removed and would fit inside a sputtering unit.

A particular advantage of the extensometer over the other two approaches is that it is water-cooled and remote from direct heating. As a matter of convenience, therefore, it only needs to be calibrated at room temperatures.

Another advantage of the extensometer not being directly exposed to the temperature of the sample is that it should be capable of use at much higher temperatures. For example, it might be used to measure the strains in carbon/carbon composite structures at extreme temperatures with the sensing unit behind the heaters or enclosed in a water-cooled case. Making use of spring-loaded point contacts with the test structure avoids significant attachment problems that would have to be overcome with other techniques. Reactions between the alumina rods and carbon would be expected at temperatures above about 2800°F. A composite sensing rod consisting of a pointed graphite rod at the hot end that fitted inside a fused silica tube which was melted and ground to a point at the other end might be developed for use at higher temperatures. The presence of the fused silica glass section at the cooler end would significantly reduce the amount of the heat being conducted down the graphite rod that reached the water-cooled flexure. For more severe applications, the possibility of difficulties due to overheating the rods or their being displaced by moving gas streams might be reduced by also enclosing the rods in water-cooled tubes which would not interfere with the ability of the rods to follow strains in the structure under test.

The simplest type of structural testing would be isothermal testing where loads are applied and removed at a fixed temperature and the change in strain measured. During ascent and reentry, however, the temperatures of different parts of the structure will be changing by different amounts and at different times. These conditions can result in thermal strains, and knowledge of these strains and their corresponding stresses may be of primary importance in the structural evaluation. An important advantage of the extensometer demonstrated in this effort was that it can be used so that when the temperature was rapidly changing and then suddenly fixed, no transient strain effects were observed. As a measure of how well these measurements followed the behavior of the test

bar, the strains measured with those that should have occurred in the test bar are compared in Table 4. After making corrections for apparent strains at the 1250°F and 1500°F hold temperatures, the average error in strain using both rod sizes was -0.00014 in/in.

5 - ACCOMPLISHMENTS AND CONCLUSIONS

This work revealed that, although many different techniques to measure strain at extreme temperatures have been developed or suggested, there are few candidates that appear to be accurate or reliable enough for use in testing aerospace structures. Different techniques have different limitations, and an important part of the test plan should include consideration of how to minimize the limitations and/or disadvantages of the particular techniques selected. The major accomplishments and conclusions from this work are as follows:

1. A comparative evaluation was made of different strain measuring techniques for potential use in structures testing from -320° to 1600°F.

2. From the 17 systems considered, a ceramic rod type extensometer was considered as the best approach, followed by the use of a small capacitive device.

3. Experimental evaluations verified that the extensometer was superior to the capacitive sysem used.

4. Mounting of the rod type extensometer could be a problem especially if it is not able to move with a structure that deflects significantly during testing.

5. Use of a flexure system of loading the rods against the structure was superior to the direct use of springs.

6. Numerical data are presented which details the effects of various relative motions on the output of the extensometer.

7. With some decrease in sensitivity, longer rods can be used with the extensometer so that the water-cooled sensor flexure can be located behind radiant heating lamps.

8. The capacitive device was stable with time but very sensitive to changes in the position of the lead wires.

9. The capacitive device tended to show hysteresis effects.

10. The capacitive device became erratic at low temperatures, perhaps because of the

buildup of frost between the plates.

11. Preliminary efforts were made to develop a thin film sputtered strain gage system on a 0.005-in.-thick foil which could be spot welded to a structure.

12. A sputtered strain gage of an FeCrAl alloy was stable to 1600°F when sputtered directly on a test bar.

13. Preparing the FeCrAl alloy as a thin film appeared to reduce the undesirable drift effects usually observed in this class of sensor alloys in the 600° to 1000°F range.

REFERENCES

1. Hulse, C. O., Stetson, K. A., Grant, H. P., Jameikis, S. M., Morey, W. W., Raymondo, P., Grudkowski, T. W., and Bailey, R. S.: Advanced High Temperature Static Strain Sensor Development Program, NASA CR-179520, Contract NAS3-22126, Lewis Research Center, (1987).

2. Hulse, C. O., Bailey, R. S., Grant, H.P., and Przybyszewski, J. S.: High Temperature Static Strain Gage Development Contract, NASA CR-180811, Lewis Research Center, Contract NAS3-23722, (1987).

3. Hulse, C.O., Bailey, R.S., Grant, H.P., and Przybyszewski, J.S.: Development of a High Temperature Thin Film Static Strain Gage, Turbine Engine Hot Section Technology 1987, pp. 43-51, NASA Conf. Pub. 2493.

4. Hulse, C. O., Bailey, R. S., and Lemkey, F. D.: High Temperature Static Strain Gage Alloy Development Program, NASA CR-174833, Lewis Research Center, Contract NAS3-23169, (1985).

5. Stetson, K. A.: Demonstration Tests of Burner Liner Strain Measuring System, NASA CR-174743, Lewis Research Center, (1985).

6. Hulse, C.O., Bailey, R.S., and Grant, H.P.: The Development of a High Temperature Static Strain Sensor, Turbine Engine Hot Section Technology, NASA CP-2444, p. 85-90, (1986).

7. Stetson, K. A.: The Use of Heterodyne Speckle Photogrammetry to Measure High-Temperature Strain Distributions, Proc. SPIE, Vol. 370, p. 46, (1983).

8. Stetson, K. A., Demonstration of Laser Speckle System on Burner Liner Cyclic Fatigue Rig, NASA Rept No. CR-179509, (1986).

9. Hulse, C.O., Bailey, R.S., Grant, H.P., and Przybyszewski, J.S.: Review of Current NASA Thin Film Static Strain Gage Research at United Technologies, Fourth Annual Sensors Exposo. International, (1989).

10. Hulse, C.O. and Bailey, R.S.: Extreme Temperature Strain Measurement System, Phase 1 Report, Contract F33615-85-C-3208, UTRC Report R88-917791-1.

11. Anton, D.L.: A Comment to "Anisotropic Fatigue Hardening of a Ni-Base Single Crystal at Elevated Temperature," Scripta Metallurgica, Vol 16, pp. 479-482, (1982).

12. Gardner, R.A., Peterson, P.J., and Kennedy, T.N.: Stability of Rf-sputtered Aluminum Oxide, J. Vac. Sci. Technol., V 14, No. 5, pp. 1139-45, (1977).

13. Grant, H.P., Anderson, W.L., and Przybyszewski, J.S.: Rotating Tests of Advanced High Temperature Wire and Thin-Film Strain Gages, 24th Joint Propulsion Conference, AIAA/ASME/ASEE, AIAA-88-3146, (1988).

BIBLIOGRAPHY

Phase One Review of Literature and Sources of Elevated
Temperature Strain Measurement Devices and Information

LITERATURE:

1. Walters, D. J., and Hales, R., An Extensometer for Creep-Fatigue Testing at Elevated Temperatures and Low Strain Ranges, Jour. of Strain Analysis, Vol. 16, No. 2, (1981).

2. Findley, W.N., and Mark, R., Multiaxial Creep Behavior of 303 Stainless Steel, Brown Univ., Annual Report for Oak Ridge National Laboratory, ORNL-SUB-3599-4, (1975).

3. Lant, C. T., and Qaqish, Optical Strain Measurement System Development - Phase I, NASA Contractor Report 179619, Lewis Research Center, (1987).

4. Hulse, C. O., Stetson, K. A., Grant, H. P., Jameikis, S. M., Morey, W. W., Raymondo, P., Grudkowski, T. W., and Bailey, R. S., Advanced High Temperature Static Strain Sensor Development Program, NASA CR-179520, Contract NAS3-22126, Lewis Research Center, (1987).

5. Hickson, V. M., Gas Strain Gages and Their Circuitry, Ministry of Defense, Aeronautical Research Council, R. & M. No. 3734, Structures Dept., R.A.E., Farnborough, England, (1973).

6. Harrigill, W. T., and Krsek, A., Method for Measuring Static Young's Modulus of Tungsten to 1900K, NASA TN D-6794, Lewis Research Center, (1972).

7. Ho, E. T. C., and MacEwen, S. R., A Facility for Precise Measurement of Mechanical Properties at Elevated Temperatures, Jour. Metals, p. 25, (1983).

8. Jenkins, J. M., Fields, R. A., and Sefic, W. J., Effect of Elevated Temperatures on the Calibrated Strain Gages of the YF-12A Wing, NASA Dryden Flight Center, SESA Spring Meeting, (1978).

9. Hulse, C. O., Bailey, R. S., Grant, H.P., and Przybyszewski, J. S., High Temperature Static Strain Gage Development Contract, NASA CR-180811, Lewis Research Center, Contract NAS3-23722, (1987).

10. Hulse, C. O., Bailey, R. S., and Lemkey, F. D., High Temperature Static Strain Gage Alloy Development Program, NASA CR-174833, Lewis Research Center, Contract NAS3-23169, (1985).

11. Motoie, K., Sakane, M., and Schmidt, J., An Extensometer for Axial Strain Measurement at High Temperature, Mechanics of Materials, Vol 2, p. 179, (1983).

12. Noltingk, B. E., McLachlan, C. V., and O'Neill, High Stability Capacitance Strain Gages for Use at Extreme Temperatures, Proc. Inst. Elect. Engrg., Vol. 119, p. 879, (1972).

13. Bloss, R.L., Trumbo, J.T., and Melton, C.H., Development of a Strain Measuring Standard for Temperatures up to 1370° C, National Bureau of Stds. Report 9061, AF Flight Dynamics Order 33(615)-66-5008, (1966).

14. Meltz, G., and Snitzer, E., Fiber Optic Sensor, U.S. Patent 4,295,738, United Technologies, (1981).

15. Day, M. F., and Harrison, G. F., Design and Calibration of Extensometers and Transducers, Chapter 14, Symposium on High Temperature Properties of Materials, Teddington, England, p. 225-40, Publ. HMSO, London, England, (1982).

16. Gillette, O. L., Measurement of Static Strain at 2000° F, Experimental Mechanics, p. 316, Vol. 15, (1975).

17. Weise, R.A., and Foster, J. H., High Temperature Strain Gage System for Application to Turbine Engine Components, AFWAL TR-80-2126, Final Report, General Electric Co., (1981).

18. Snitzer, E., and Meltz, G., Wide Band Multicore Optical Fiber, U.S. Patent, 4,300,816, United Technologies, (1981).

19. Stetson, K. A., Demonstration Tests of Burner Liner Strain Measuring System, NASA CR-174743, Lewis Research Center, (1985).

20. Hulse, C.O., Bailey, R.S., and Grant, H.P., The Development of a High Temperature Strain Gage System, Turbine Engine Hot Section Technology, NASA CP-2405, p. 45, (1985).

21. Keusseyan, R. L., and Che-Yu Li, Precision Strain Measurement at Elevated Temperature using a Capacitance Probe, Jour. Testing & Evaluation, Vol. 9, No. 3, p. 214, (1981).

22. Chandler, R. L., and Dent, E. J., Temperature Compensated Strain Gages, Elec. Engrg., p. 414, (1960).

23. Hobart, H. F., Evaluation Results of the 700° C Chinese Strain Gages, NASA Conf. Pub. 2443, p. 77, (1985).

24. Lei, J. F., Scaarbaf, M., and Brittain, J. O., Elevated Temperature Strain Gage, Turbine Engine Hot Section Technology 1987, NASA Conf. Pub. 2493, p.53, (1987).

25. Budhani, R. C., Prakash, S., Doerr, H. J., and Bunshaw, R.F., Summary Abstract: Oxygen Enhanced Adhesion of Platinum Films Deposited on Thermally Grown Alumina Surfaces, J. Vac. Sci. Technol., Vol. 4, p 3023, (1986).

26. Thompson, R.A., Jorgenson, W.E., and Callbresi, Optical Technique for Strain Measurement of Material Specimens at Elevated Temperatures, Sandia Labs., Sand-75-8261, (1975).

27. Babcock, S. G., Hochstein, P. A., and Jacobs, L.J., High Heating Rate Response of Two Materials from 72° to 6000° F, Final Tech. Report SAMSO TR-69-393, (1970).

28. Foster, R. L., Capacitive Non Contact Displacement Sensors Use in High Temperature Environments to 1000° C, Fifth Annual Hostile Environments and High Temperature Measurements Conference, Soc. Exp. Mechanics, (1988).

29. Dunphy, J. R., Meltz, G., and Elkow, R.M., Distributed Strain with a Twin-Core Fiber Optic Sensor, Trans ISA, Vol 26, No.1, p 7, (1987).

30. Dunphy, J. R., and Meltz, G, Fiber Optic Sensor Development for High Speed Diagnostics, Soc. for Exp. Mechanics Conf. on Optical Methods and Composites, Keystone, Colo., (1986).

31. Atkinson, W.H., Cyr, M. A., and Strange, R. R., Survey and Evaluation of Measurement Techniques for Temperature, Strain and Heat Flux for Ceramic Components in Advanced Propulsion Systems, Final Report Contract NAS3-25141, NASA Lewis Research Center, (1988).

32. Stetson, K. A., The Use of Heterodyne Speckle Photogrammetry to Measure High-Temperature Strain Distributions, Proc. SPIE, Vol. 370, p 46, (1983).

33. Sharpe, W. N., Application of the Interferometric Strain/Displacement Gage, Opt. Engrg, Vol. 21, p 483, (1982).

34. Stetson, K. A., Demonstration of Laser Speckle System on Burner Liner Cyclic Fatigue Rig, NASA Rept No. CR-179509, (1986).

35. Wu, Tsen-tai, et al; Development of Temperature-Compensated Resistance Strain Gage for Use to 700° C, Exp. Mech., Vol. 21, No. 3, p 117, (1981).

36. Bertodo, R., Platinum Metal Alloys for the Measurement of Steady Strains at High Temperatures, Proc. Inst. Mech. Engrg., Vol. 178, No. 34, p 907, (1964).

37. Easterling, K., High Temperature Resistance Strain Gages, Brit. Jour. Appl. Physics, Vol. 1, p 1743, (1968).

38. Lemco, M. M., Development of Strain Gages for Use to 1311 K (1900° F), NASA CR-132485, (1974).

39. Zhi-qi, and Pei-quig, H., Development of the Self-Temperature Compensated Resistance Strain Gage Used up to 700° C, ASME Paper 81-GT-118, (1981).

40. Bertodo, R., Precious Metal Alloys for High-Temperature Resistance Strain Gauges, Brit. Jour. Appl. Physics, Ser. 2, Vol. 1, p 1743, (1968).

41. Wnuk, S. P., Capacitive Strain Gages for Measurements to 2000° F, Fifth Annual Hostile Environments and High Temperature Measurements Conference, Soc. for Exp. Mechanics, (1988).

SOURCES:

Optical Techniques

• BLH Electronics, Inc., 42 Fourth Ave., Waltham, Mass. 02154, Phone (617) 890-6700, Laser strain gages, Diffractogage

• Mechanical Technology Incorporated, 968 Albany-Shaker Road, Lantham, New York 12110, Phone (518) 785-2323, noncontacting, "Fotonic" fiber bundle sensor

• Dual Core Fiber Optic Strain Gage with Laser input, United Tech. Research Center, E. Hartford. CT 06108, James R. Dunphy, Phone (203) 727-7006

• Instron Corp., 100 Royall St., Canton, Mass., 02021, Phone (617) 828-2500

• Laser Speckle Interferometry, Stetson & Yamaguchi, See References

• Measurements Group, Inc., P.O. Box 27777, Raleigh, North Carolina, Phone (919) 365-38000, Photoelastic coatings or models using a polariscope

• Mechanical Technology Incorporated, 968 Albany-Shaker Road, Lantham, New York 12110, Phone (518) 456-4131, Reflective Light, Fiber bundles, "Fotonic Sensors", to 600°F

• Moire´ Technique, optical interference between two gratings, See References

• Optron Corp., 28 Hazel Terr., Woodbridge, CT 06526, Phone (203) 389-5384

• "Sharp" Technique, Interference patterns produced by light beams reflected from two diamond pyramid hardness indentations, (See References 33)

• Zygo Corp., Laurel Brook Road, Middlefield, CT 06455, Phone (203) 347-8506, Mfg. Laser Interferometers. High Speed Scanning Laser Beams interrupted by flags attached to test samples.

Electrical Resistance Strain Gages

• Ailtech, Automation Products Division, Eaton Corp., 5340 Alla Road, Los Angeles, CA 90066, Phone (213) 822-3061, Weldable and embedable integral lead strain gages, to 1200°F.

• William T. Bean, Inc., 18915 Grand River Ave., Detroit, Mich, 48223, Rep. Andress-Peskin Corp., P.O. Box 268, Natick, Mass 01760, Phone (617) 653-3919, Strain gages and accessories.

• BLH Electronics, 75 Shawmut Road, Canton, Mass., 02021, Phone (617) 821-2000, Gages and equipment

• Dentronics Inc., 60 Oak Street, Hackensack, New Jersey 07601, Phone (201) 343-9405, Platinum-tungsten gages.

• Electrix Industries, Inc., P.O. Box 306, Lombard, IL 60148, Phone (312) 627-6802

Foil Strain gages.

• HiTEC Corp., Nardone Industrial Park, Westford, Mass 01886, Phone (617) 692-4793, High temperature static and dynamic, flame sprayed and welded.

• Instron Corp., 100 Royall St., Canton, Mass., 02021, Phone (617) 828-2500, A wide variety of extensometers.

• Micro Engineering II, 14 North Benson Ave., Upland, Calif., 91788, Phone: (714) 946-2110, Semi-conductor and foil strain gages.

• Micro-Measurements Division, Measurements Group, Inc., P.O. Box 27777, Raleigh, North Carolina, 27611, Phone (919) 365-3800, Strain gages & instruments

• MTS Systems Corp., P.O. Box 24012, Minneapolis, Minn., 55424, Phone (612) 944-4000, Wide variety of strain-gaged extensometers

• Precision Foil Technology, 28 N. Benson Ave., Upland, CA., 91786, Phone (714) 946-1000, Foil gages

• Precision Measurement Co., P.O. Box, 7676, Ann Arbor, Michigan 48107, Phone (313) 995-0041, Extensometers

• Showa Measuring Instruments Co., Lyd., 423-9, Kamihirose-Kasumigaseki, Sayama-shi, Saitama, 350-13, Japan

• Texas Measurements, Inc., P.O. Box 2618, College Station, Texas 77840, Phone (409) 764-0442, Tokyo Sokki Kenkyujo Co., Ltd.

• Tinius Olsen Testing Machine Co.,Inc., Easton Road, P.O. Box 429, Willow Grove, PA 19090-0429, Phone (215) 675-7100, Wide variety of strain-gaged extensometers

Capacitive Techniques

• Automatic Systems Laboratory, Construction House, Grovebury Road, Leighton Buzzard, Beds. England LU7 8SX, Phone: Leighton Buzzard 4624, Mfg. Super Linear Variable Capacitors (SLVC), power supplies & read-outs; American Rep: Willard L Pierce Assoc., Box 200, Allison Park,PA 15101, Phone (412) 487-4141

• Capacitec, 87 Fitchbury Rd., P.O. Box 790, Ayer, MA 01432, Tel: (508) 772-6033

• GV Planer Ltd., CERL-Planer Capacitive Transducer, Windmill Road, Sunbury -on-Thames, Middx., England, Phone: Sunbury 86262-3-4-5

• HiTEC Corp., Nardone Industrial Park, Westford, MA 01886, the Boeing capacitive gage, Tel: (617) 692-4793

• Mechanical Technology Incorporated, Represents Wayne Kerr Ltd., 968 Albany-Shaker Road, Lantham, New York 12110, Phone (518) 785-2323

Differential Transformers

• Omutec,A Division of Odetics, Inc., 2871 Metropolitan Place, Pomona, Calif., 91767-1893, Phone (714) 596-1461, Mfg. DC-DC Linear LVDT transducers

• Pickering & Company, Inc., Measurement and Controls Div., 101 Sunnyside Boulevard, Plainview, N.Y. 11803, Phone (516) 349-0200, Mfg. DC-DC LVDT's & RVDT's, power supplies & read-outs

• Schaevitz Engineering, U.S. Route 130 & Union Ave., Pennsauken, N. J., Phone (609) 662-8000

• Tinius Olsen Testing Machine Co., Inc., Easton Road, P.O. Box 429, Phone (215) 675-7100, Variety of LVDT extensometers

• Transducer Division, Sanborn Company, A Division of Hewlett-Packard, 175 Wyman St., Waltham, Mass. 02154, Phone (617) 894-6300, Mfg. LVDT's

• Transducers and Systems, Inc., Twin Lakes Road, North Branford, CT, 06471, Phone (203) 481-5721, A Prime Technology Company, AC-AC & DC-DC LVDT, linear and rotary, signal conditioning and out puts

• Trans-Teck Incorp., Route 83, P.O. Box 338, Ellington, CT, Phone (203) 872-8351,Mfg. AC-AC & DC-DC Linear Differential Transformer transducers for linear and angular displacement, power supplies, read-outs

Eddy Currents

• Kaman Sciences Corporation, 1500 Garden of the Gods Rd., P.O. Box 7463, Colorado Springs, Colorado 80933, Mfg. multi-purpose variable impedence transducer based on the eddy current loss principle, power supplies & read outs

Brittle Coatings

• Magnaflux Corporation, 7300 West Lawremce Avenue, Chicago, IL 60656, Peabody International Corp., Materials Testing Laboratories, 230 Murphy Road, Hartford, CT, (203) 522-3253, Vendor Electrix Industries, Inc., P.O. Box 306, Lombard, ILL 60148, Phone (312) 627-6802, usable to 600°F

• Measurements Group, Inc., P.O. Box 27777, Raleigh, North Carolina, 27661 "TENS-LAC", Phone (919) 365-3800

FLEXURE

STRUCTURE

ELECTRICALLY
SHIELDED LEAD
WIRES

STRAIN GAGE SENSOR

WATER COOLING
LINES

FUSED QTZ
RODS
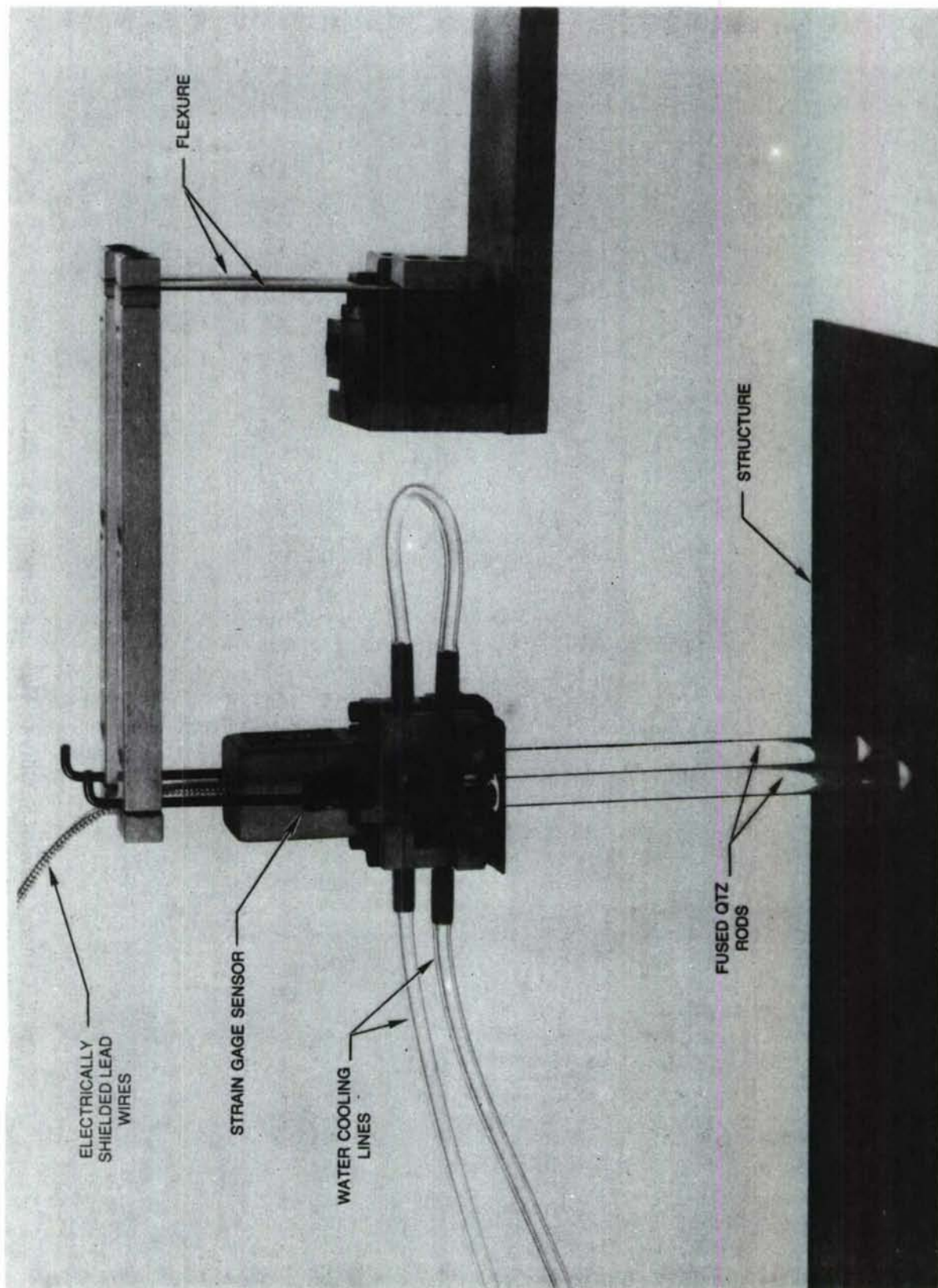
Figure 1 Rod Type Extensometer Mounted for Structure Testing
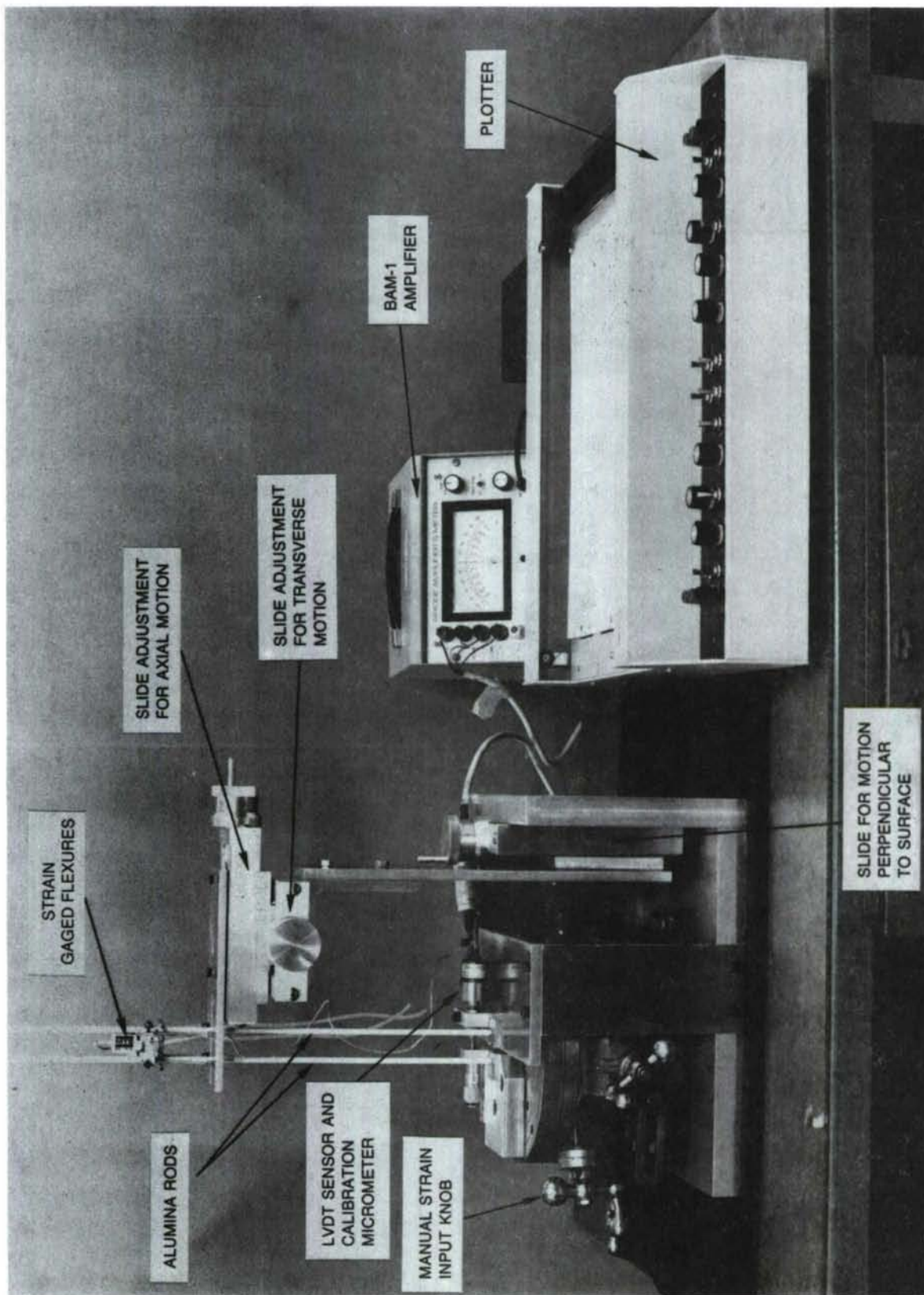
Figure 2 General View of Facility to Measure Sensitivity of Extensometer to Relative Motions
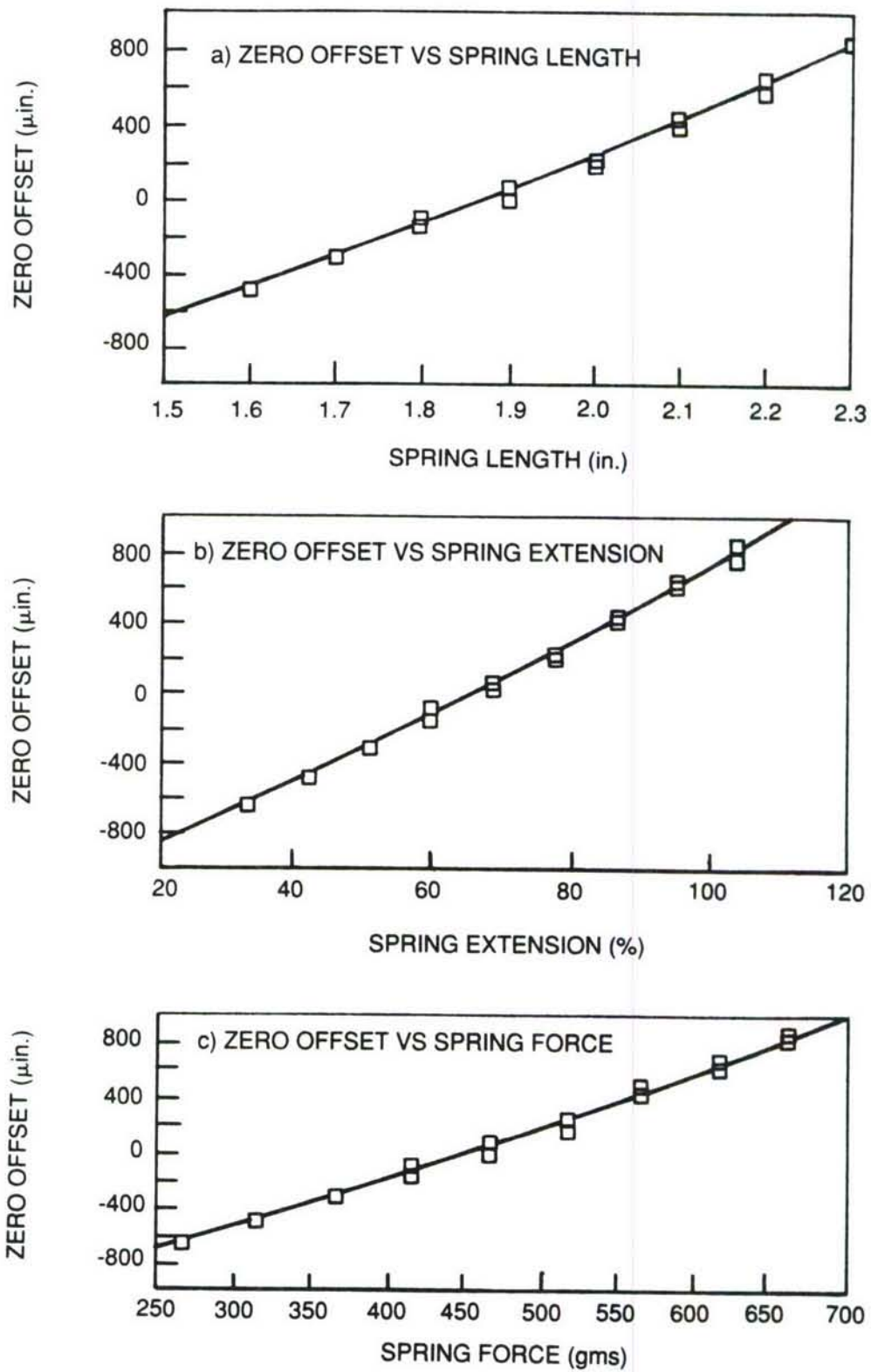
Figure 3 Changes in Zero Offset of Extensometer with Change in Spring Length

90-6-49-1
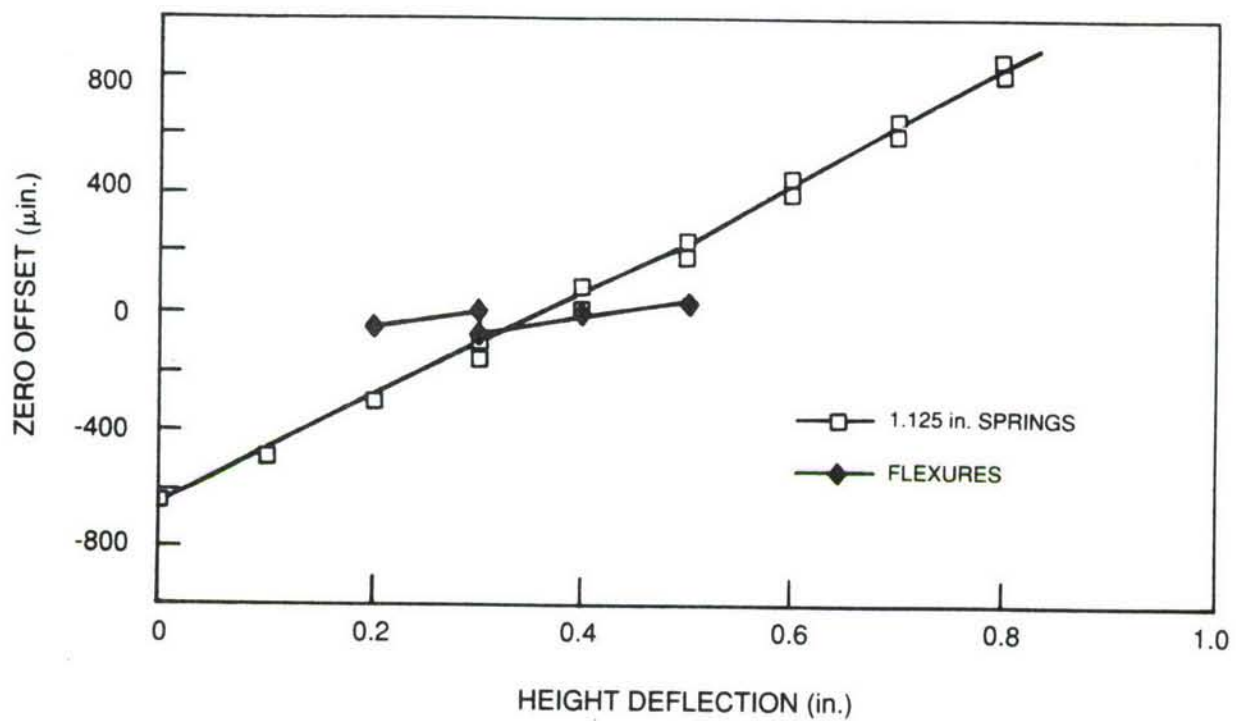
Figure 4 Effect of Changes in Distance Between Extensometer Mounting Plate and Measurement Surface

90-6-49-3

44
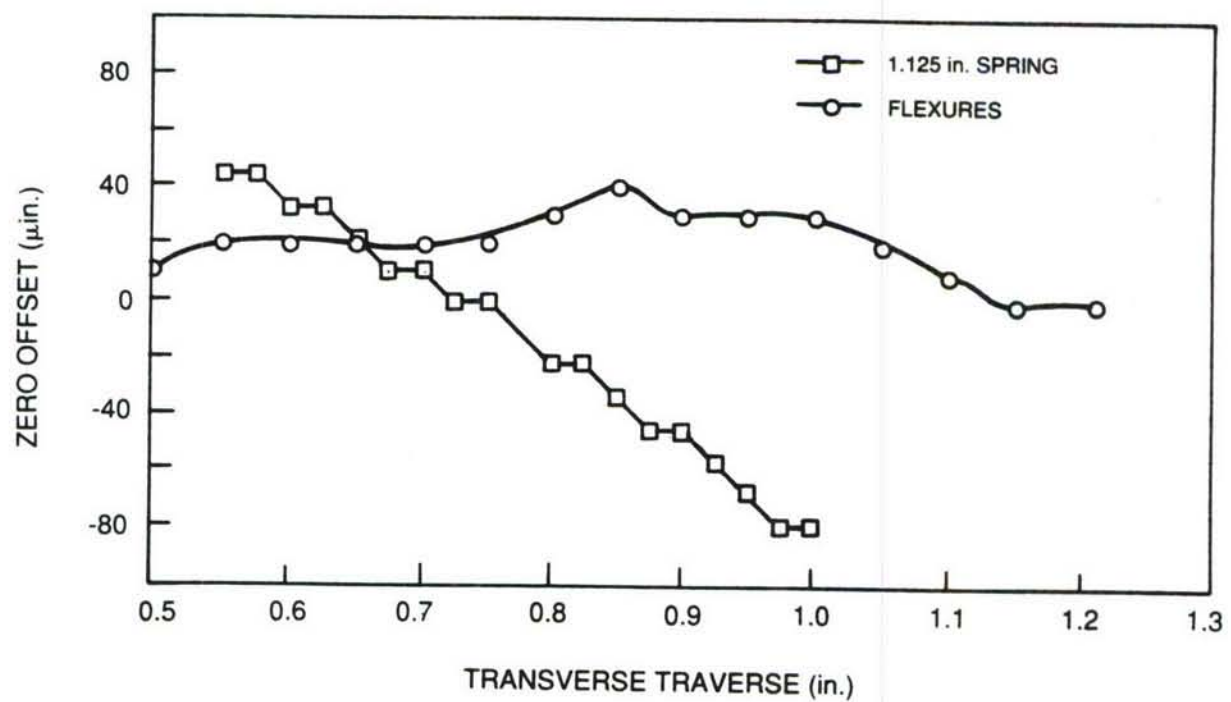
Figure 5 Effect of Changes in Transverse Alignment of Extensometer with Measurement Surface

90-6-49-4

45
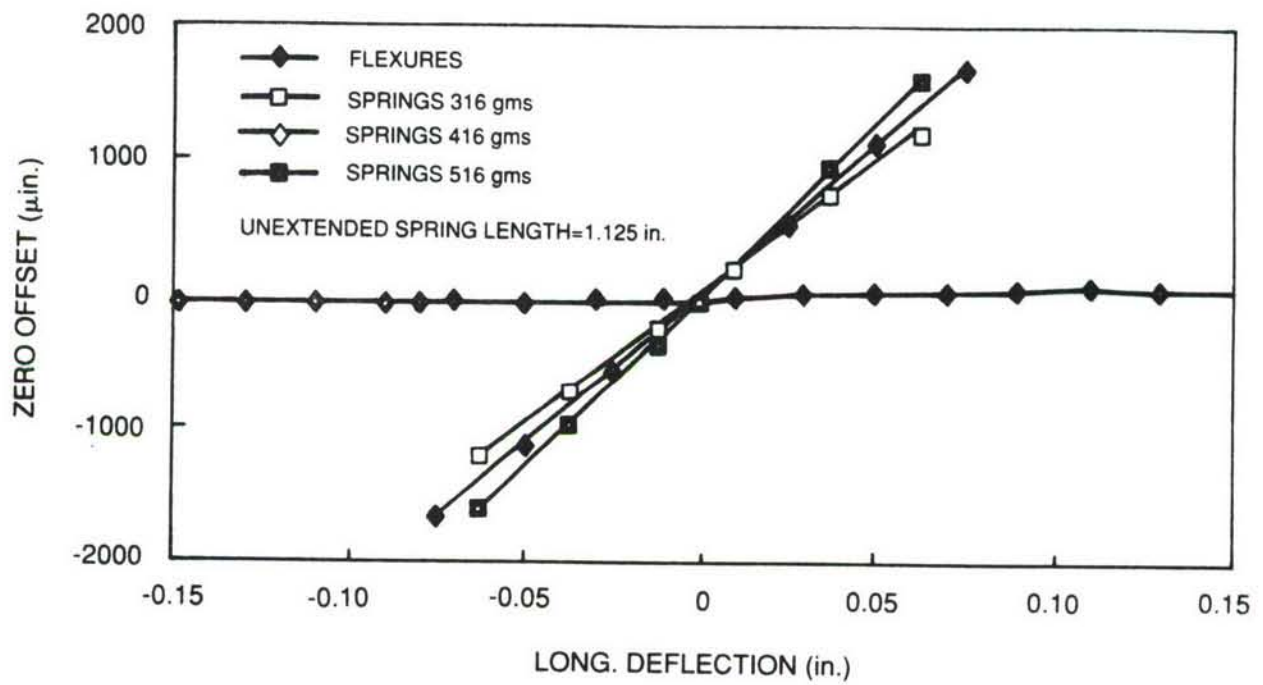
Figure 6 Effect of Changes in Longitudinal Alignment of Extensometer with Measurement Surface

90-6-49-2

46

SIDE VIEW

LEAD STRAP

TEST SURFACE

|← GAGE LENGTH →|

TOP VIEW

SPOT WELDS

× ×

× ×

CAPACITANCE GAP
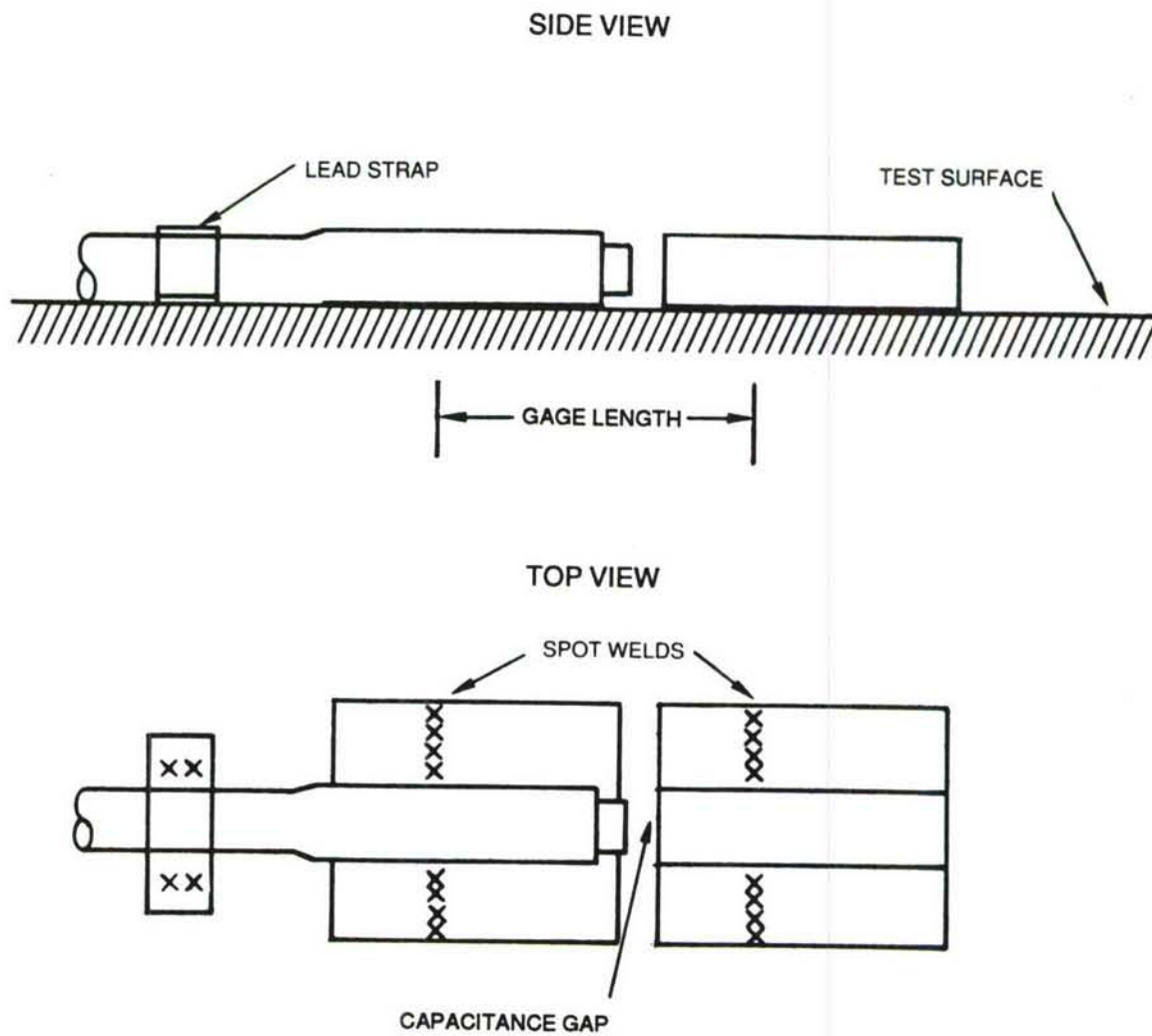
Figure 7 Capacitive Strain Sensor Installed on Test Surface

90-6-49-31

47
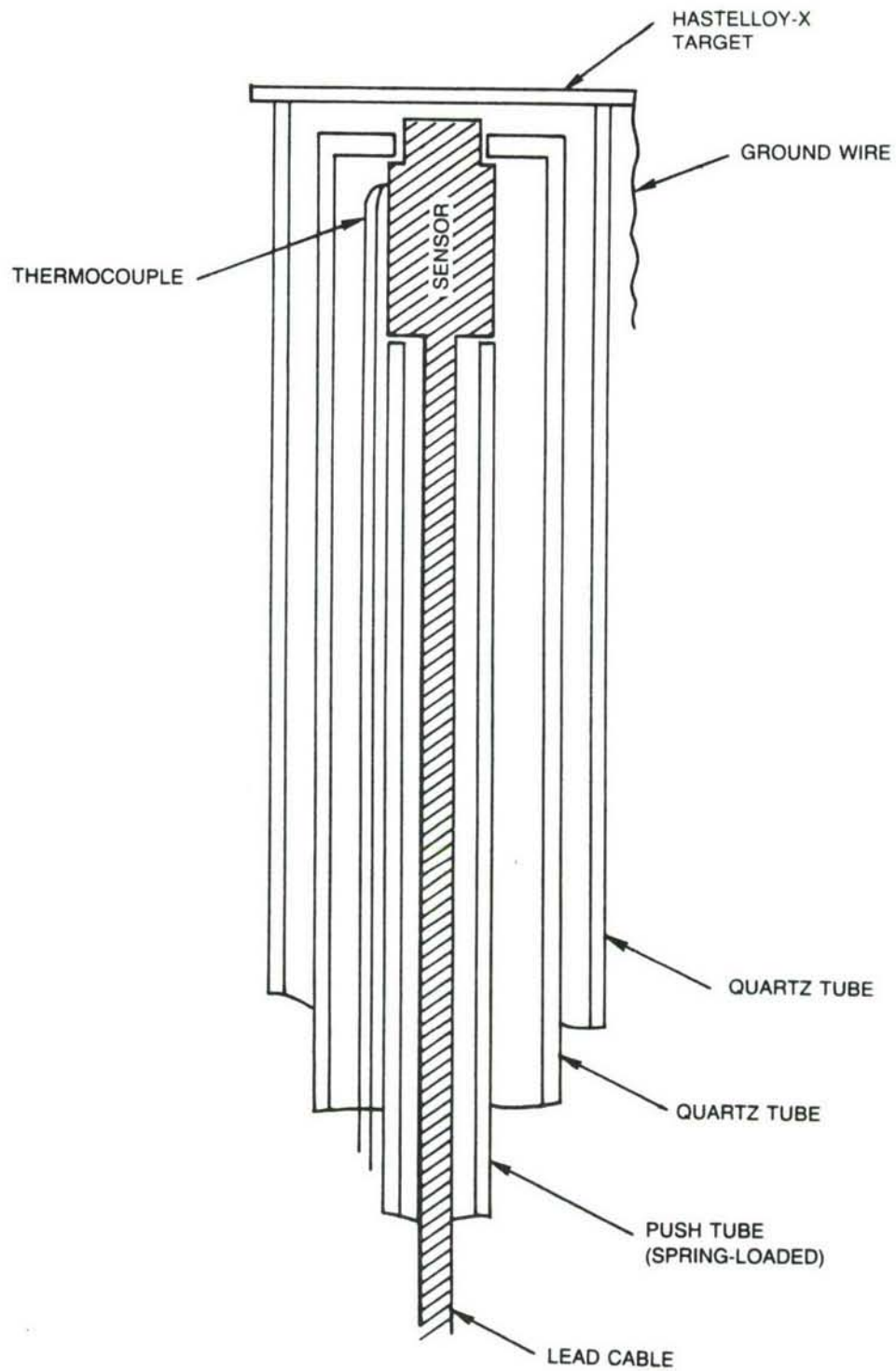
Figure 8 Elevated Temperature Calibration Fixture for Capacitive Sensor

87—12—31—4
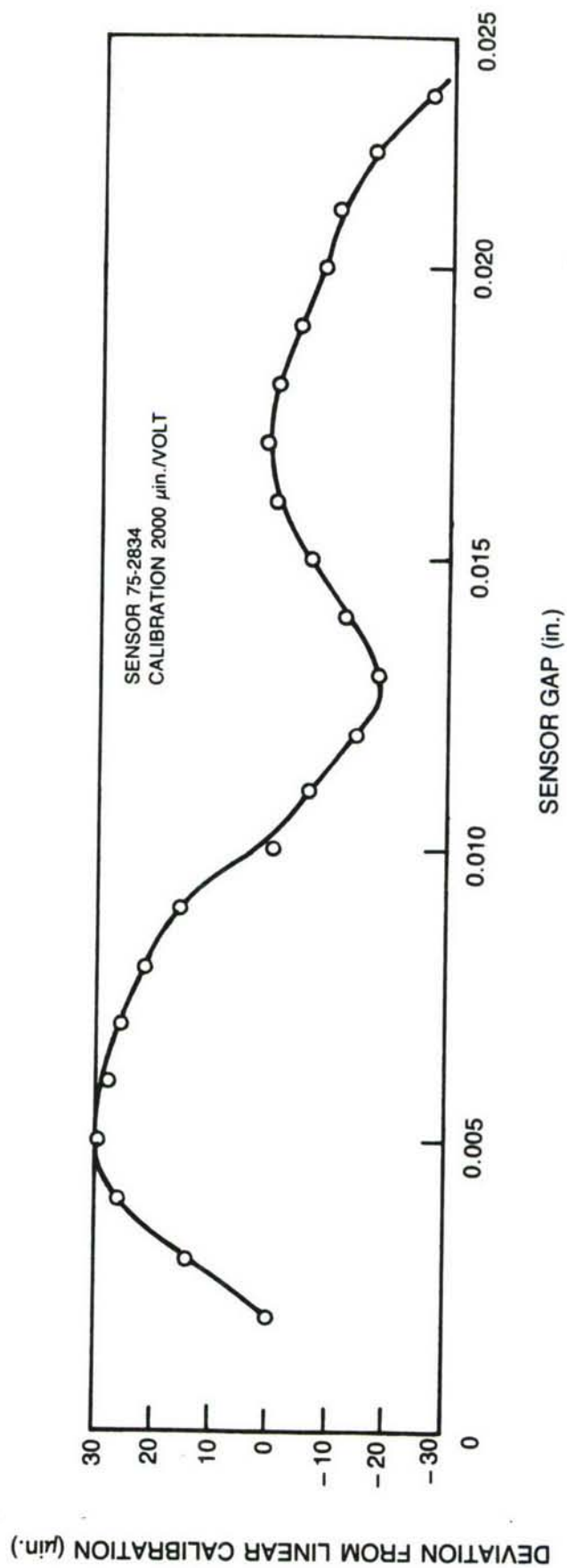
Figure 9 Deviation from Linear Calibration for Capacitive Strain Sensor

49
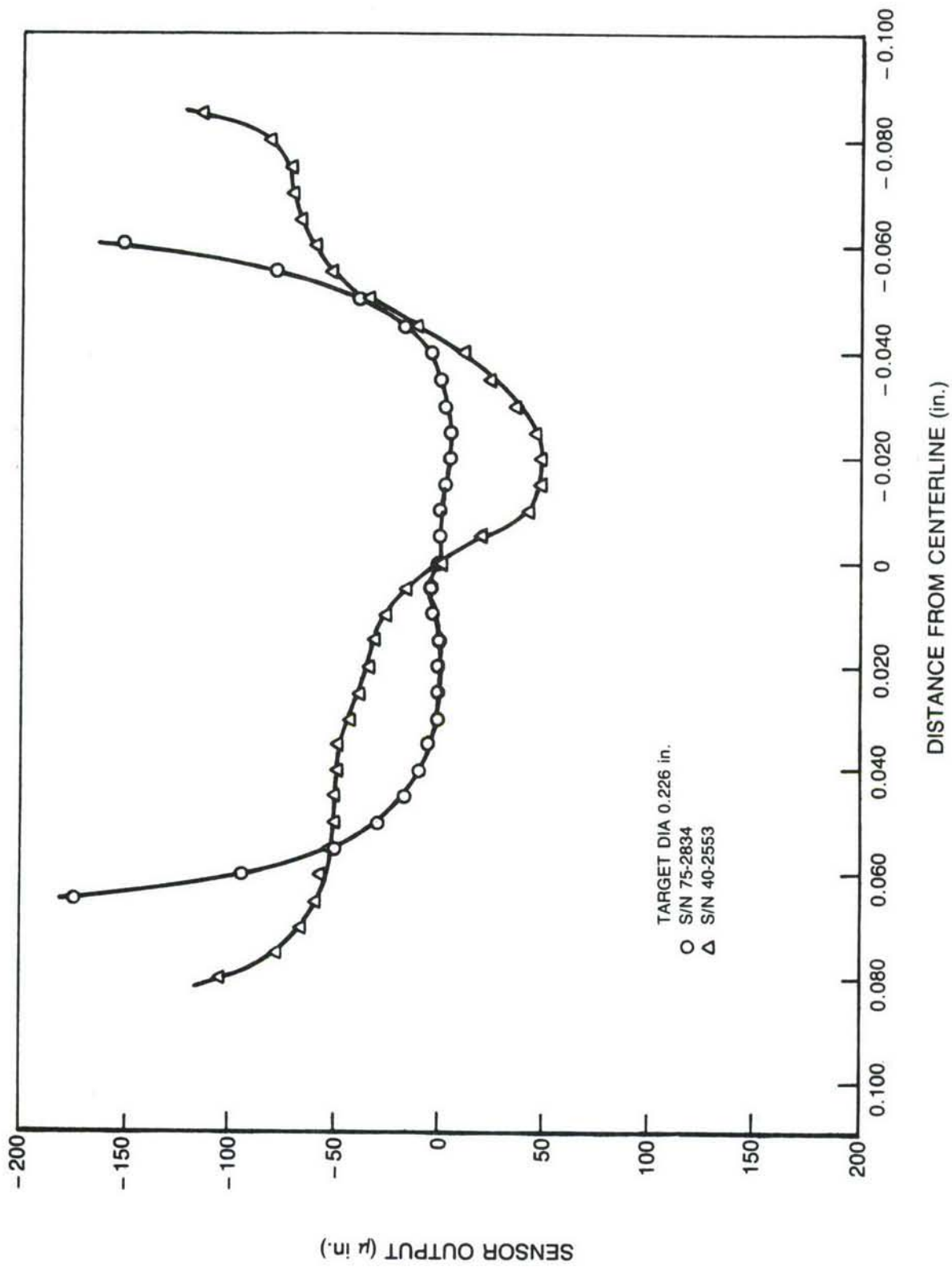
Figure 10 Output of Capacitive Strain Sensors Traversed Parallel to Target Face

DISTANCE FROM CENTERLINE (in.)

SENSOR OUTPUT (μ in.)

TARGET DIA 0.226 in.
O S/N 75-2834
△ S/N 40-2553

50
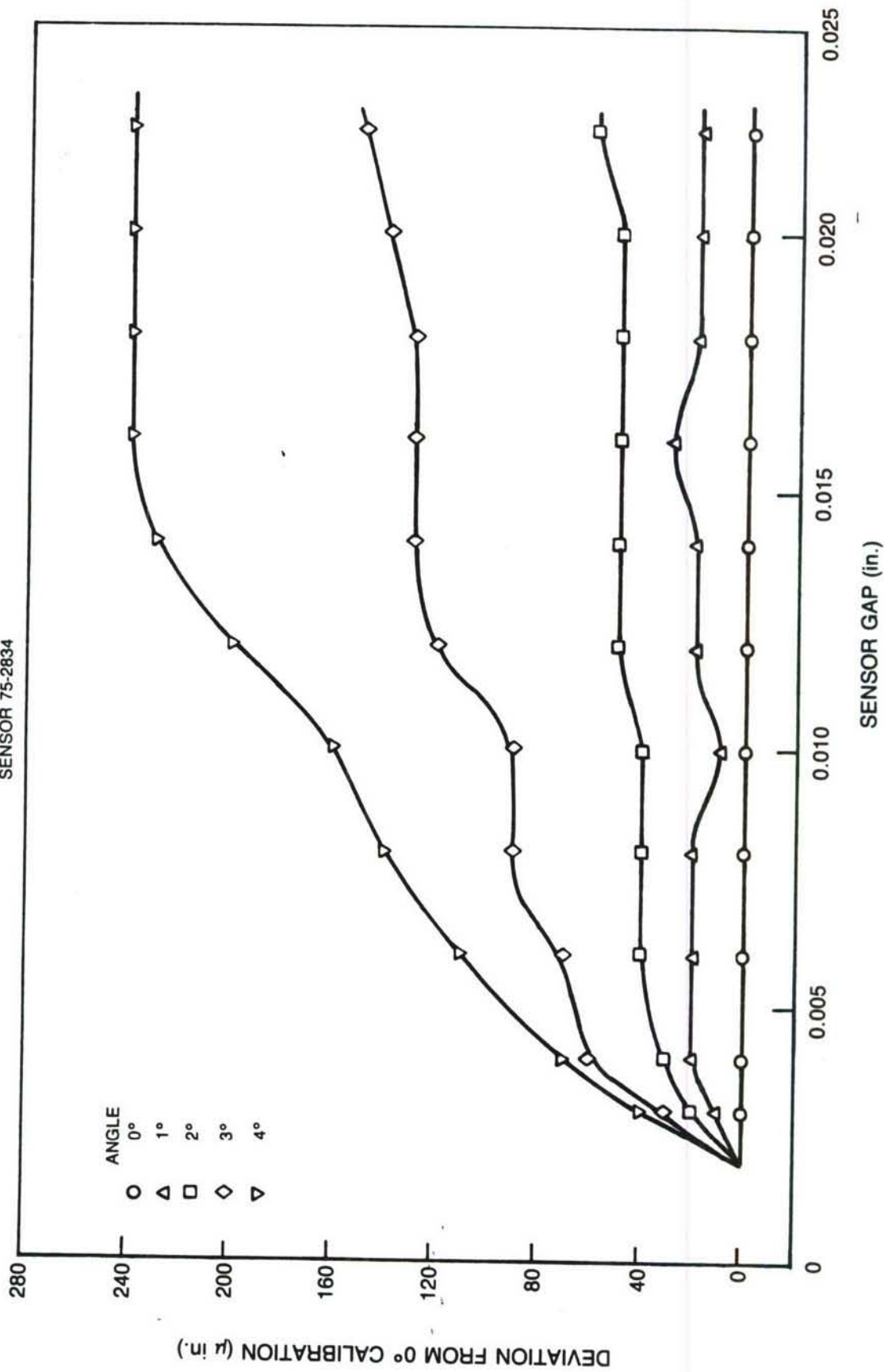
Figure 11 Change in Capacitive Sensor Calibration Due to Nonparallelism of Target and Sensor

SENSOR 75-2834

DEVIATION FROM 0° CALIBRATION (μ in.)

SENSOR GAP (in.)

ANGLE
○ 0°
△ 1°
□ 2°
◇ 3°
▷ 4°

87—12—31—2
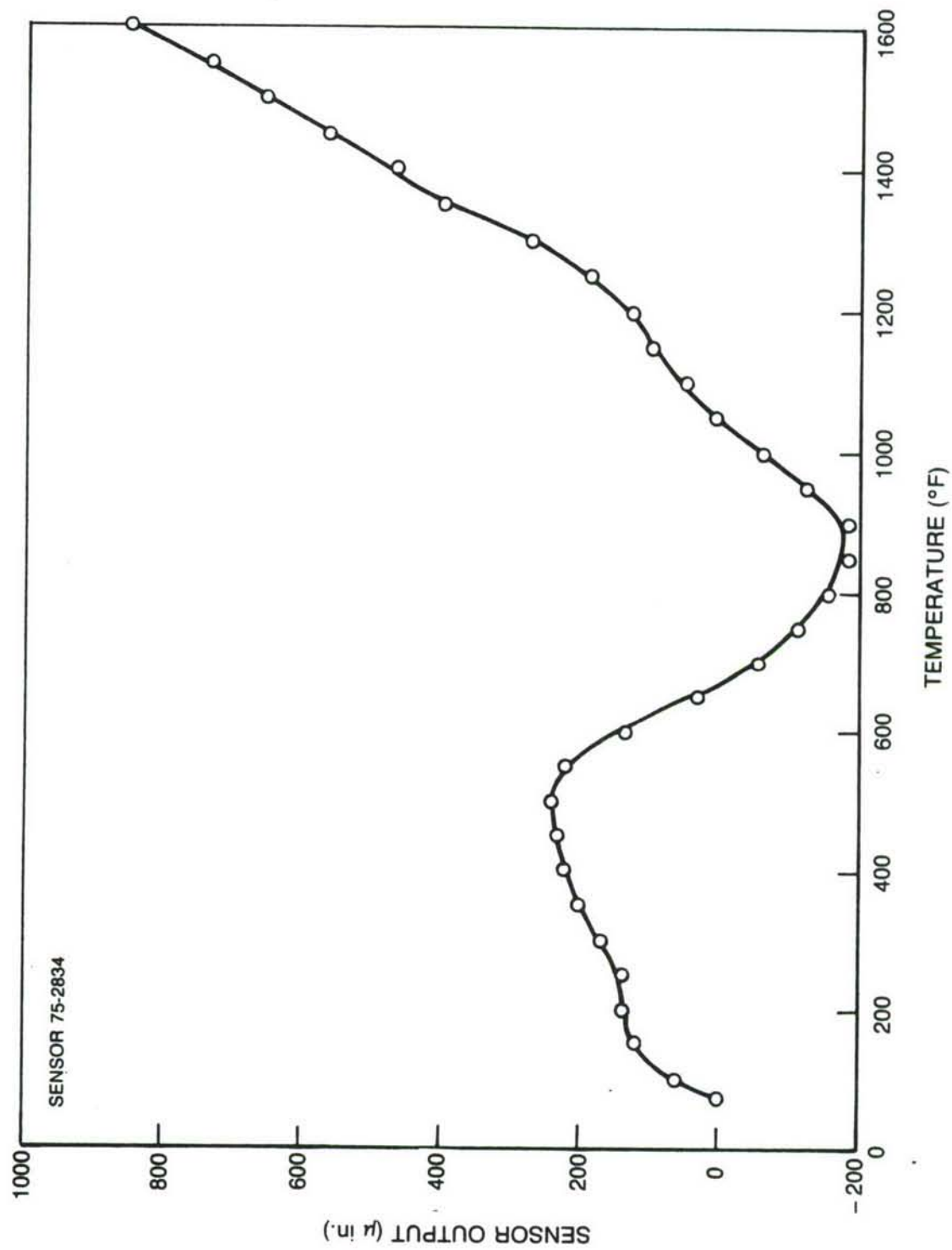
Figure 12 Change in Output of Capacitive Strain Sensor Heated to 1600°F at 15°F/min

SENSOR 75-2834

TEMPERATURE (°F)

SENSOR OUTPUT (μ in.)

52
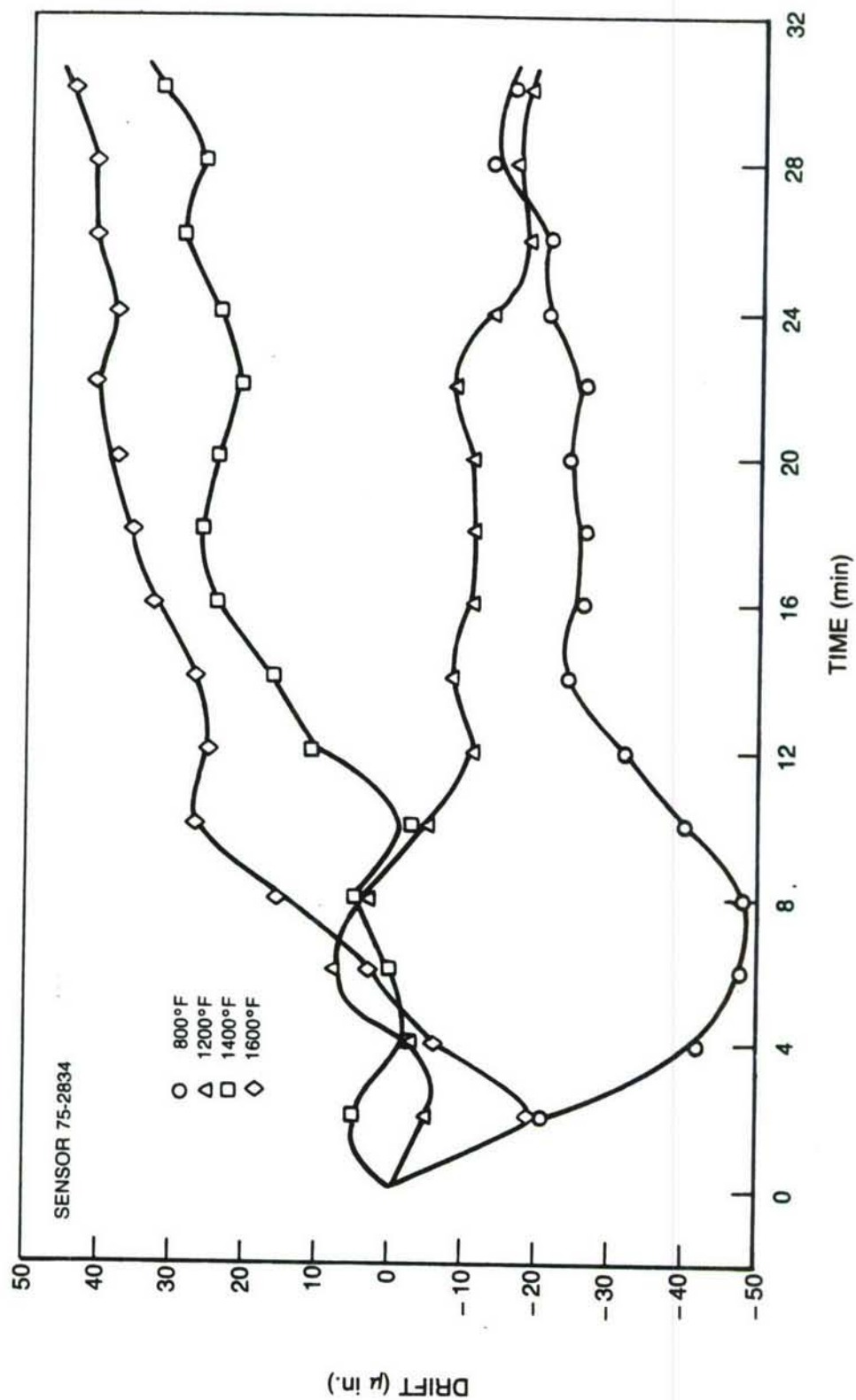
Figure 13 Capacitive Strain Sensor Drift at Elevated Temperatures

87—12—31—6
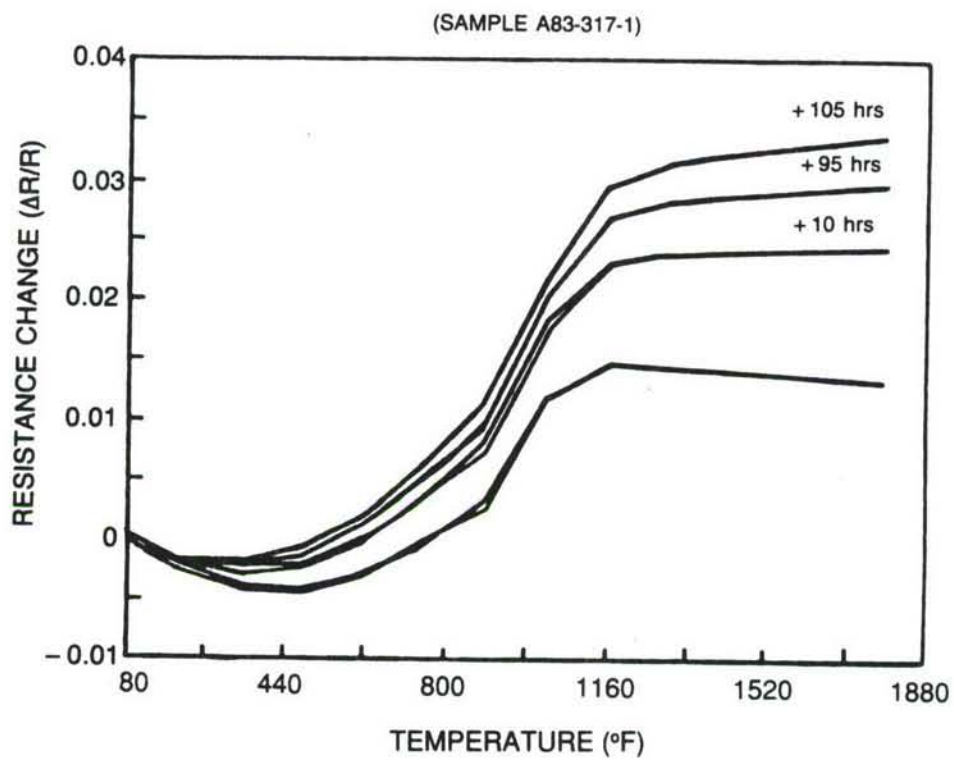
Figure 14 Change in Resistance vs Temperature of FeCrAl Mod #3 After Different Soak Times at 1790°F
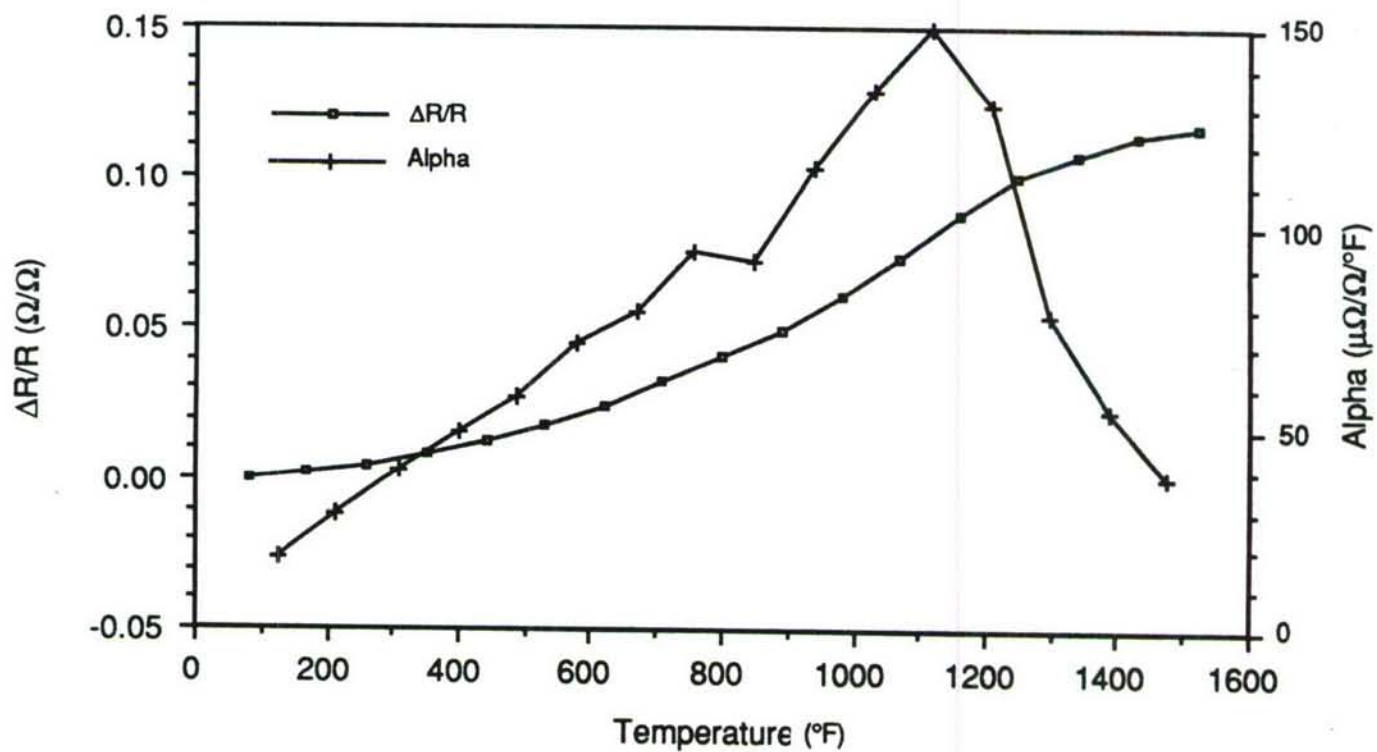
**Figure 15   Change in Resistance and Thermal Coefficient of
Resistance with Temperature for Sputtered FeCrAl**
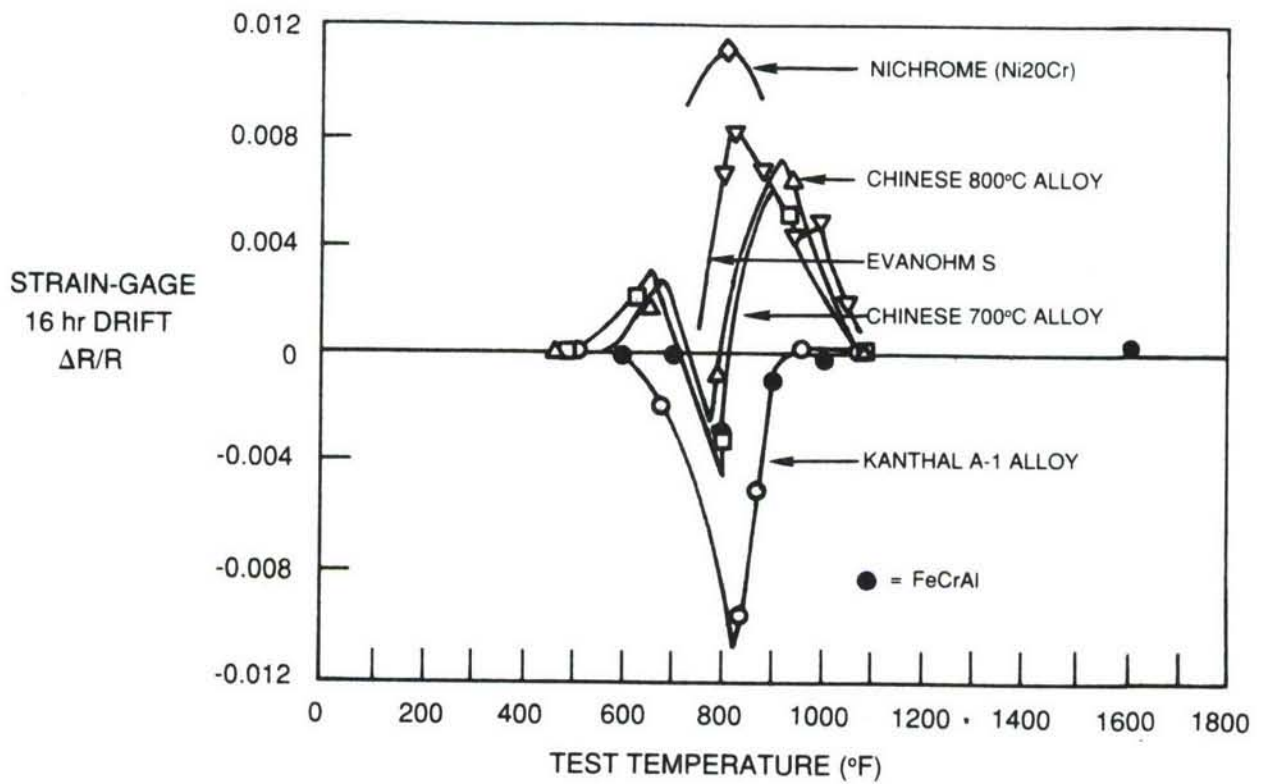
Figure 16 Stability of Thin Film FeCrAl Compared with Five Other Strain Gage Alloy Wires

90-6-49-6

56
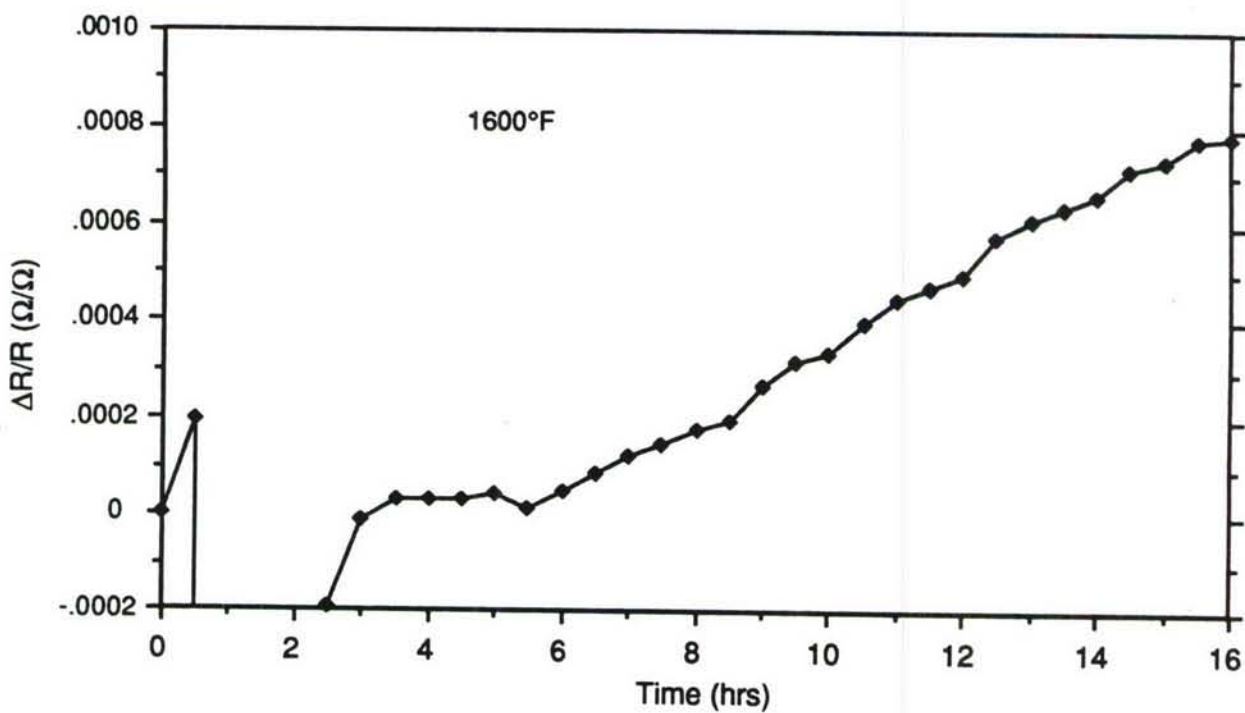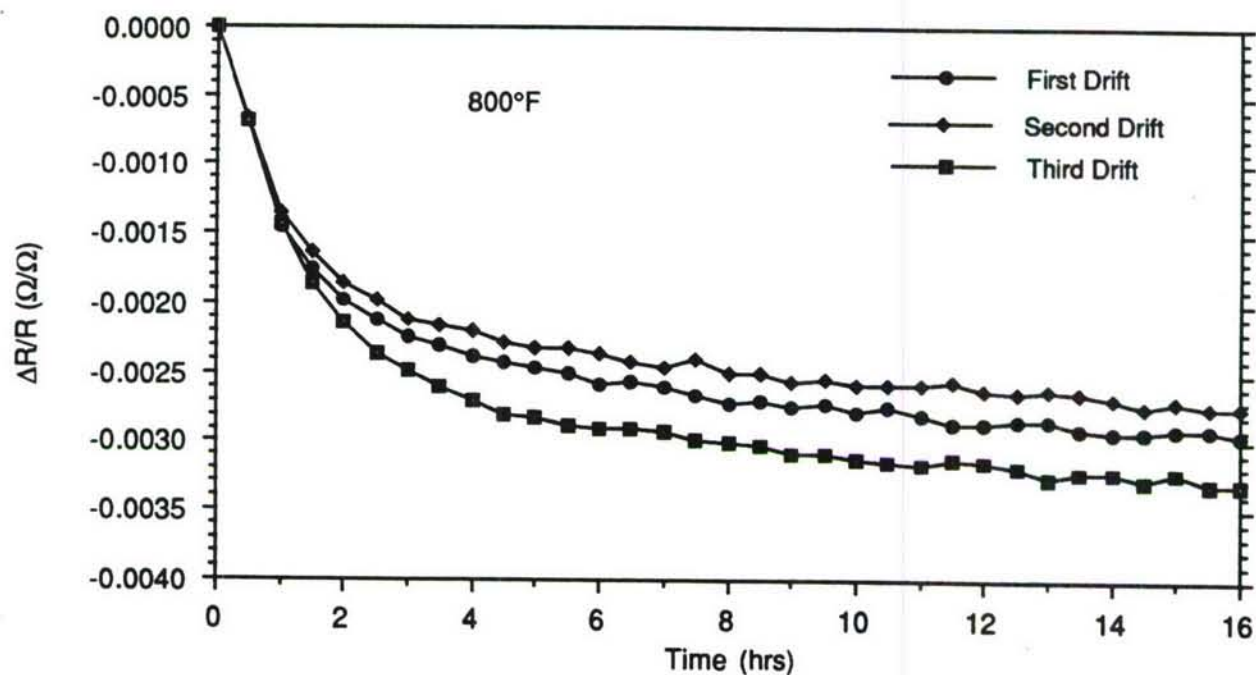
Figure 17 Change in Resistance vs. Time at 800°F and 1600°F for Sputtered FeCrAl

90-6-49-7
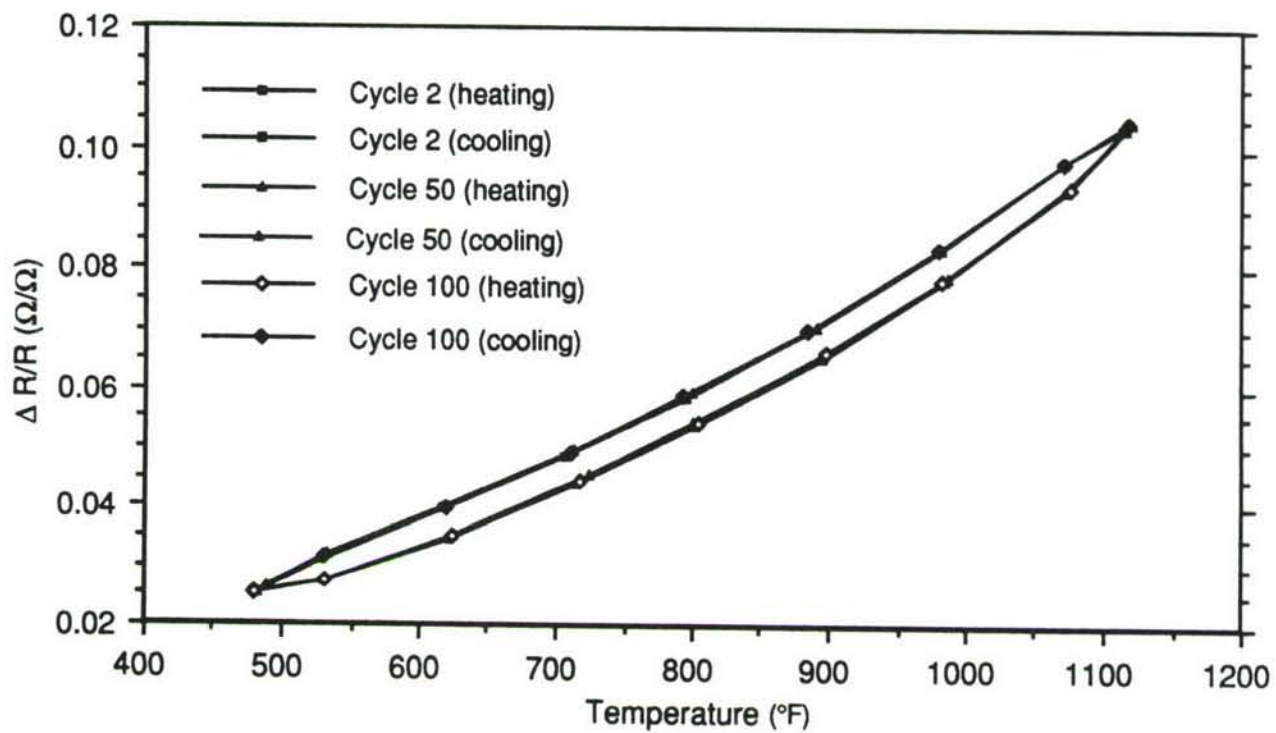
Figure 18   Cycles to 1150°F at 100°F/min for Sputtered FeCrAl

90-6-49-8

58
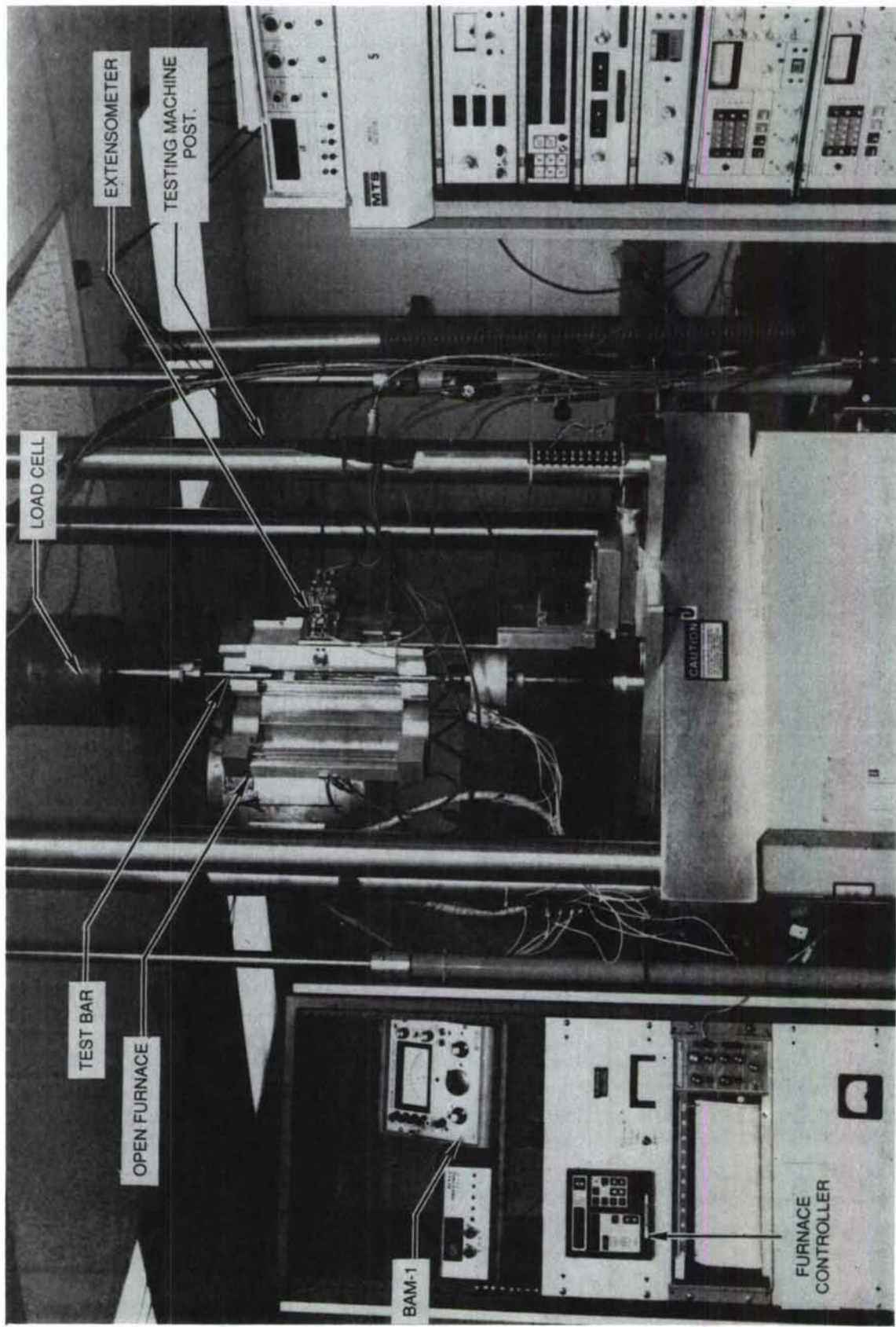
Figure 19 General View of Test Facility
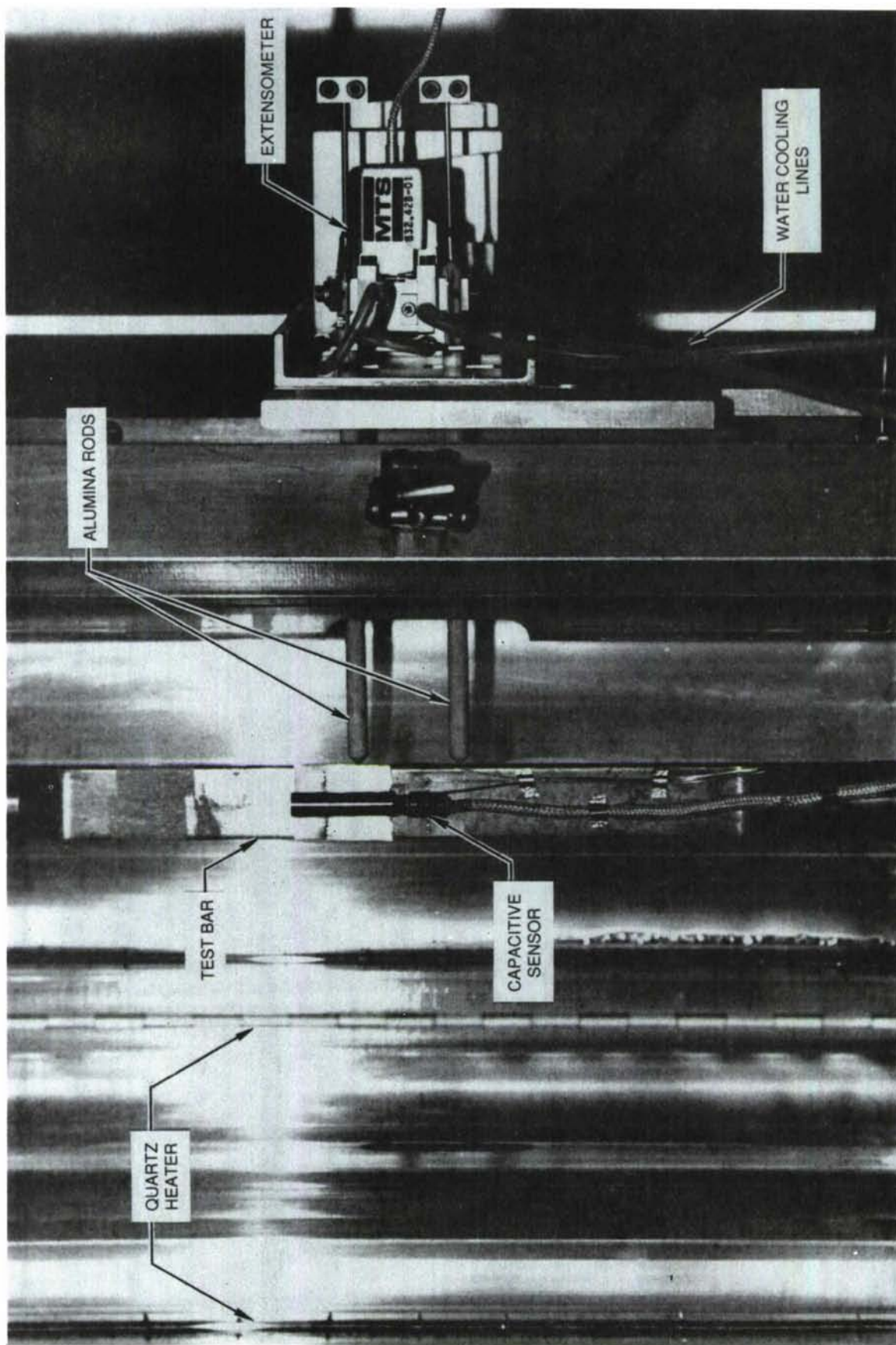
Figure 20 Closer View of Sample and Sensors in Test Facility

EXTENSOMETER

WATER COOLING LINES

ALUMINA RODS

TEST BAR

CAPACITIVE SENSOR

QUARTZ HEATER

MTS

Sputtered FeCrAl Gage
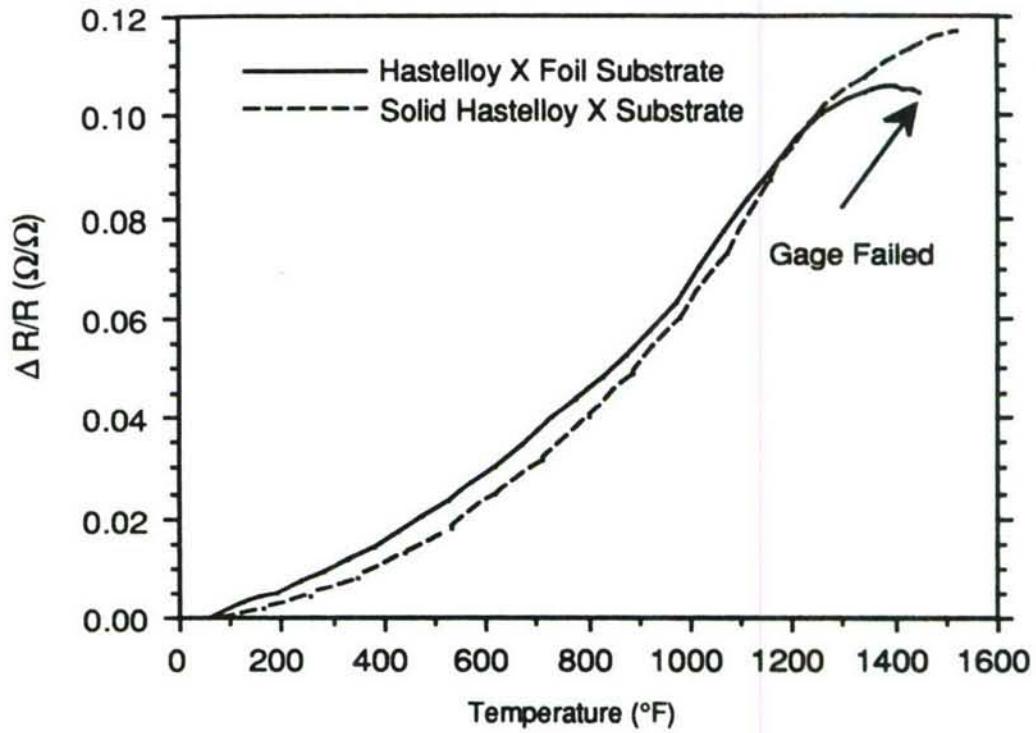
MTS Extensometer
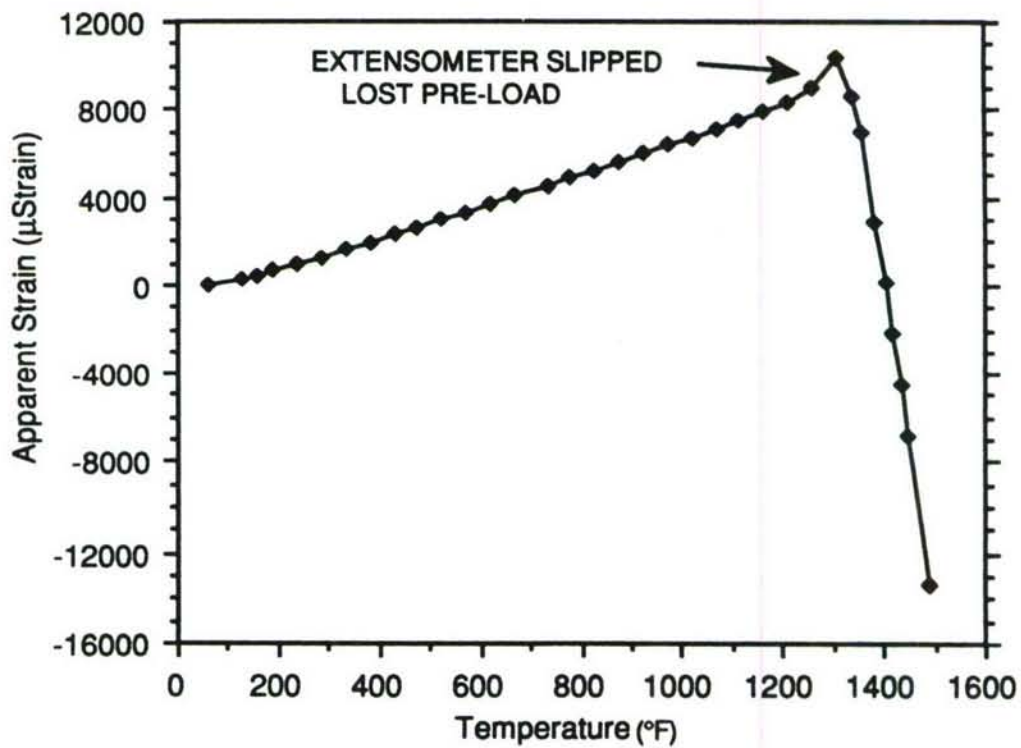
Figure 21   Apparent Strain of Sputtered Foil Gage and
Extensometer

90-6-49-11
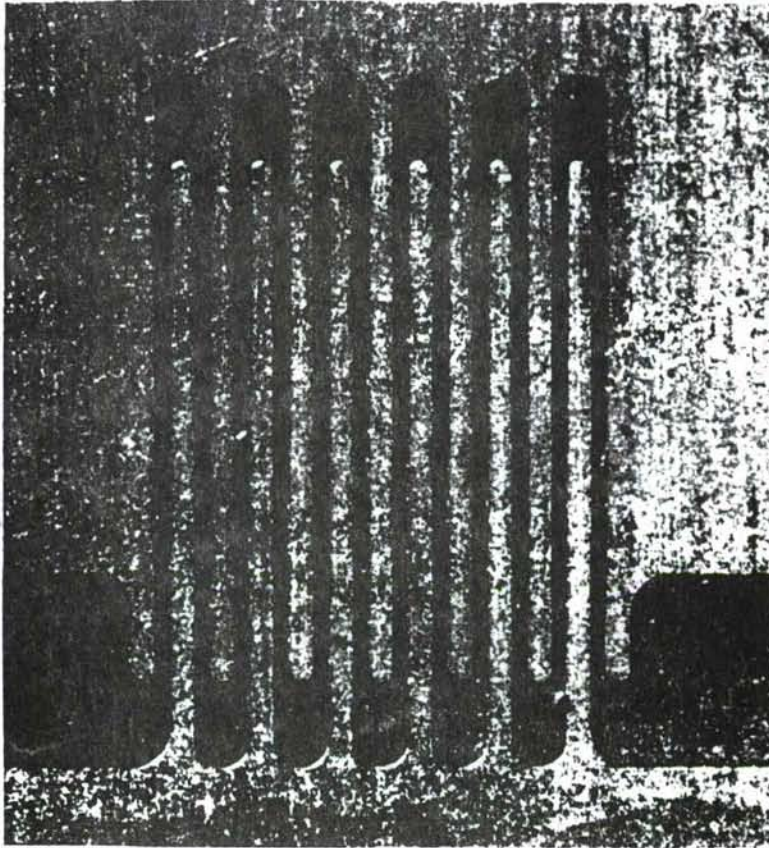
Figure 22 Photograph of Sputtered Strain Gage on Thin Foil After all Testing was Completed

Extensometer
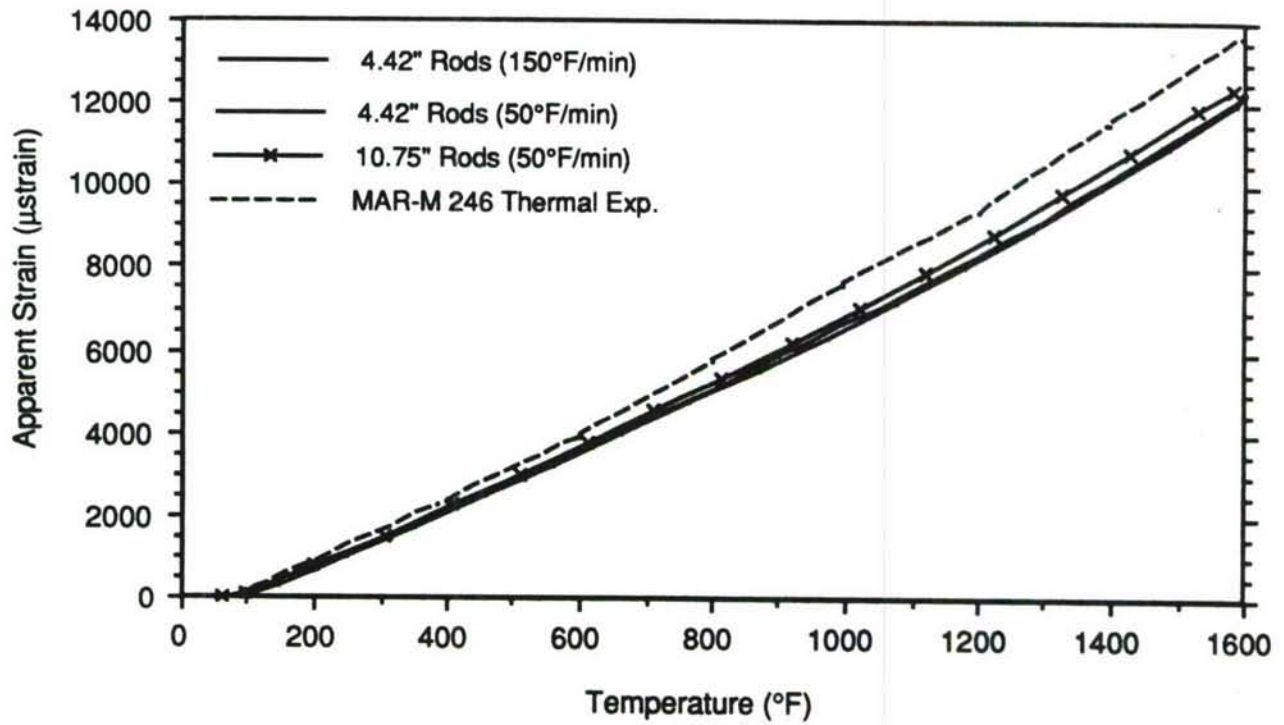
Capacitive Sensors
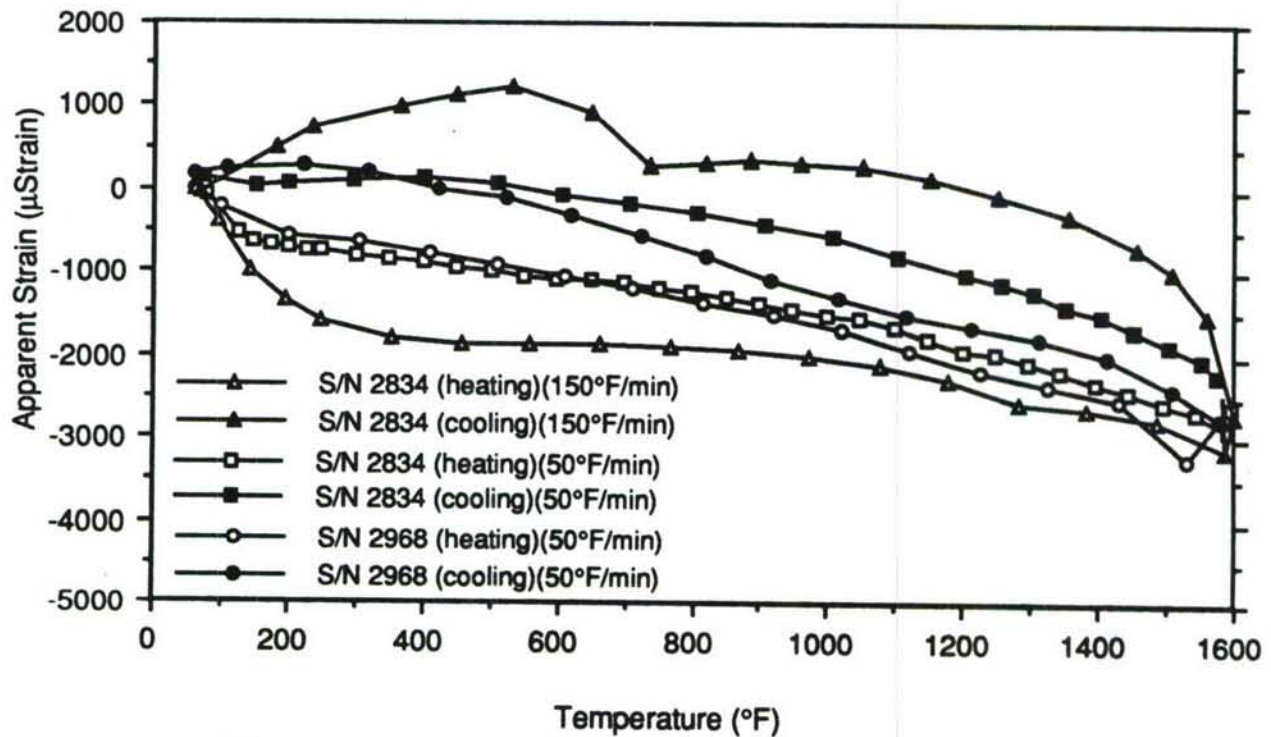
**Figure 23 Apparent Strain of Extensometer and Two
Capacitive Sensors to 1600°F**

90-6-49-13

63
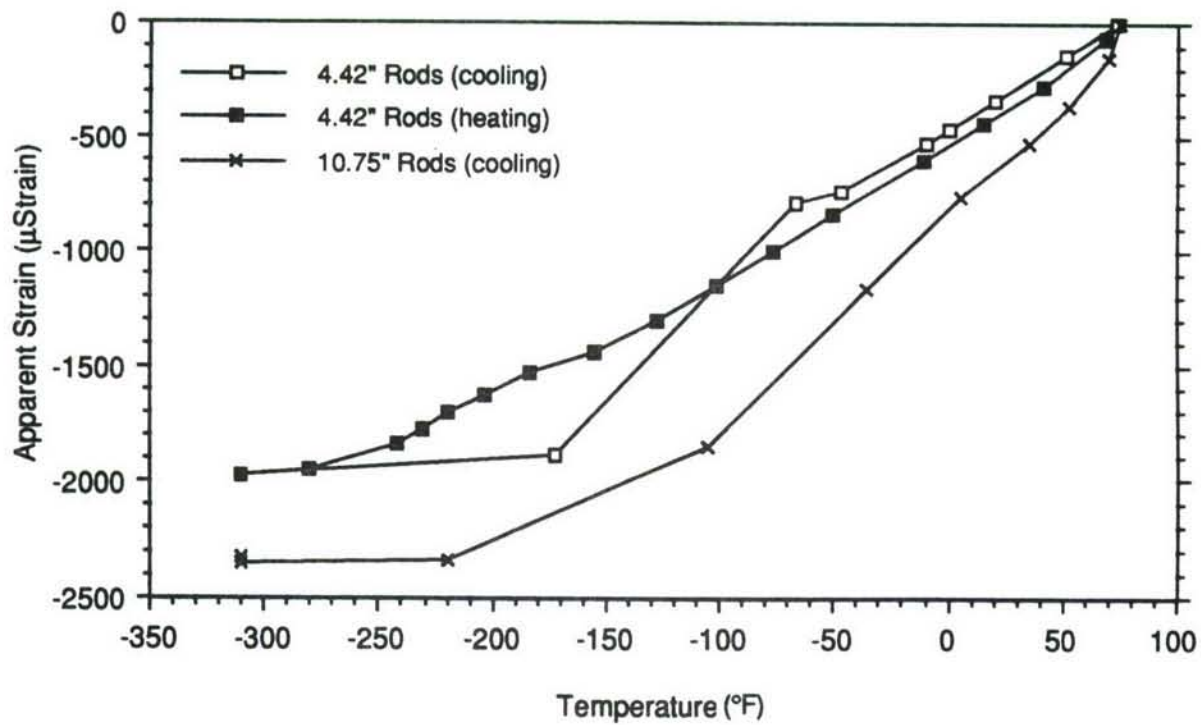
Extensometer

Capacitive Sensors
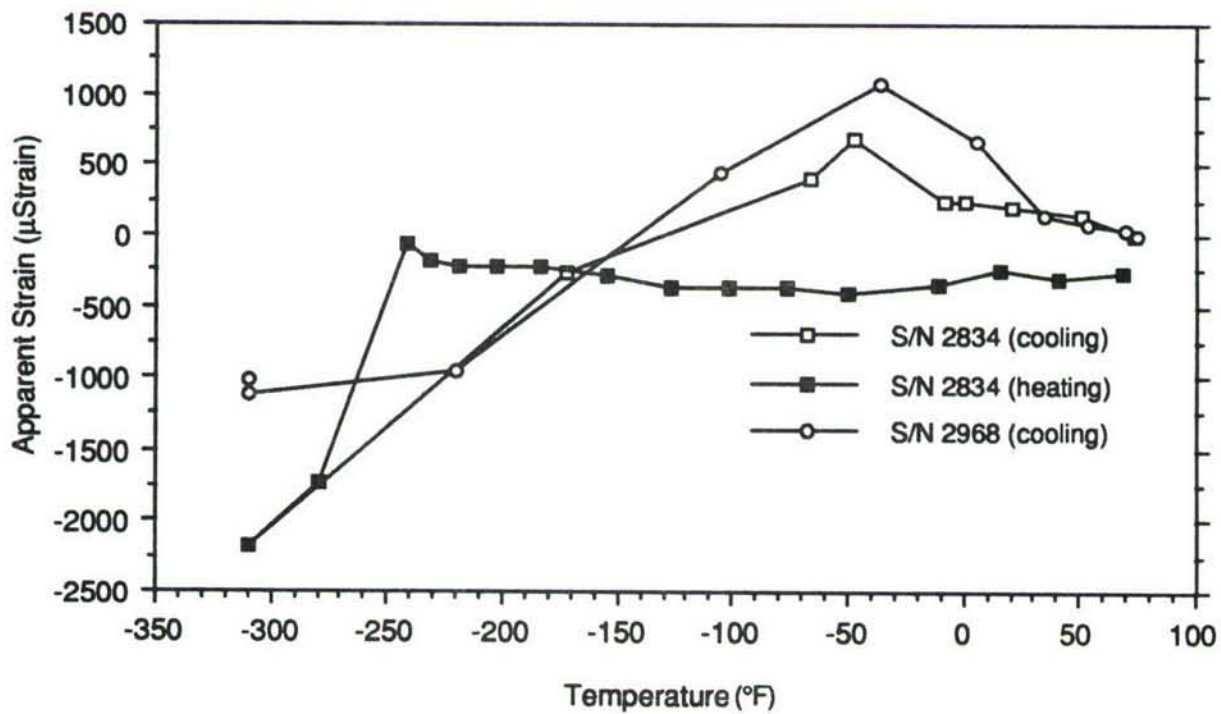
**Figure 24   Apparent Strain of Extensometer and Two
Capacitive Sensors to -310°F**

90-6-49-14

64

Extensometer
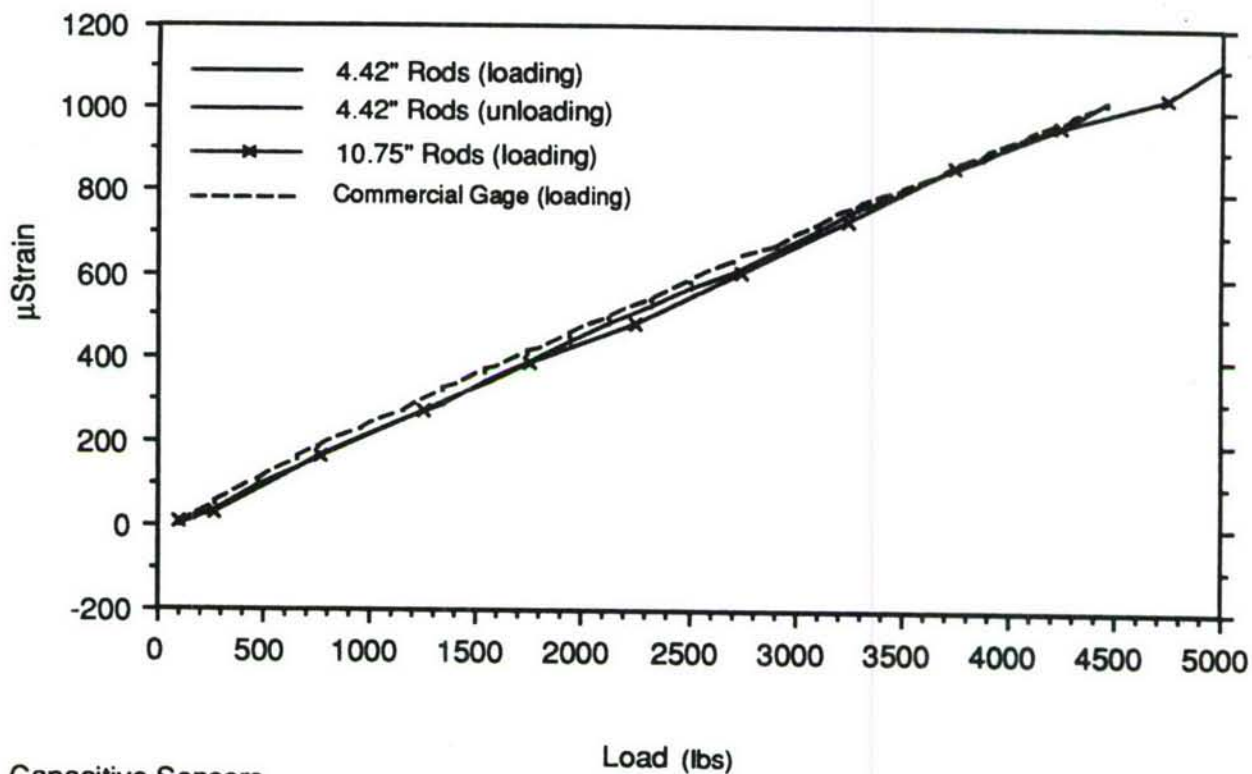
Capacitive Sensors

Load (lbs)
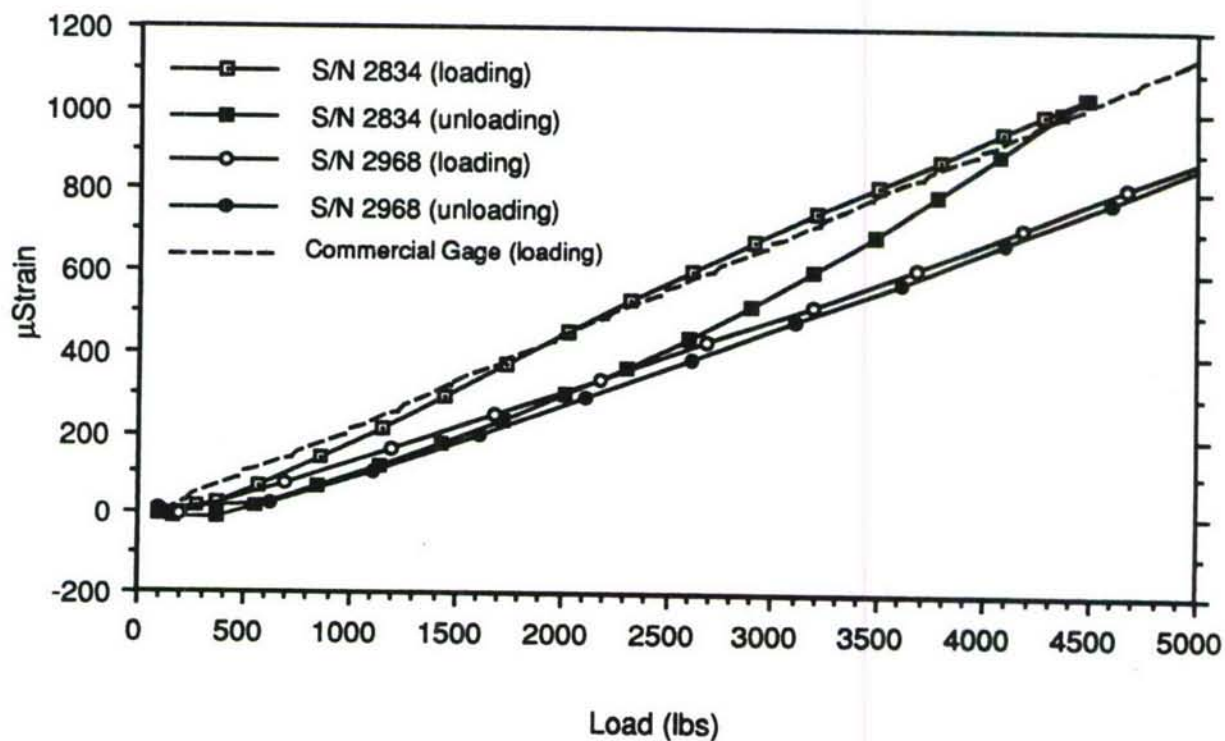
**Figure 25 Strain vs. Load for the Extensometer
and Capacitive Sensors at 75°F**

Extensometer
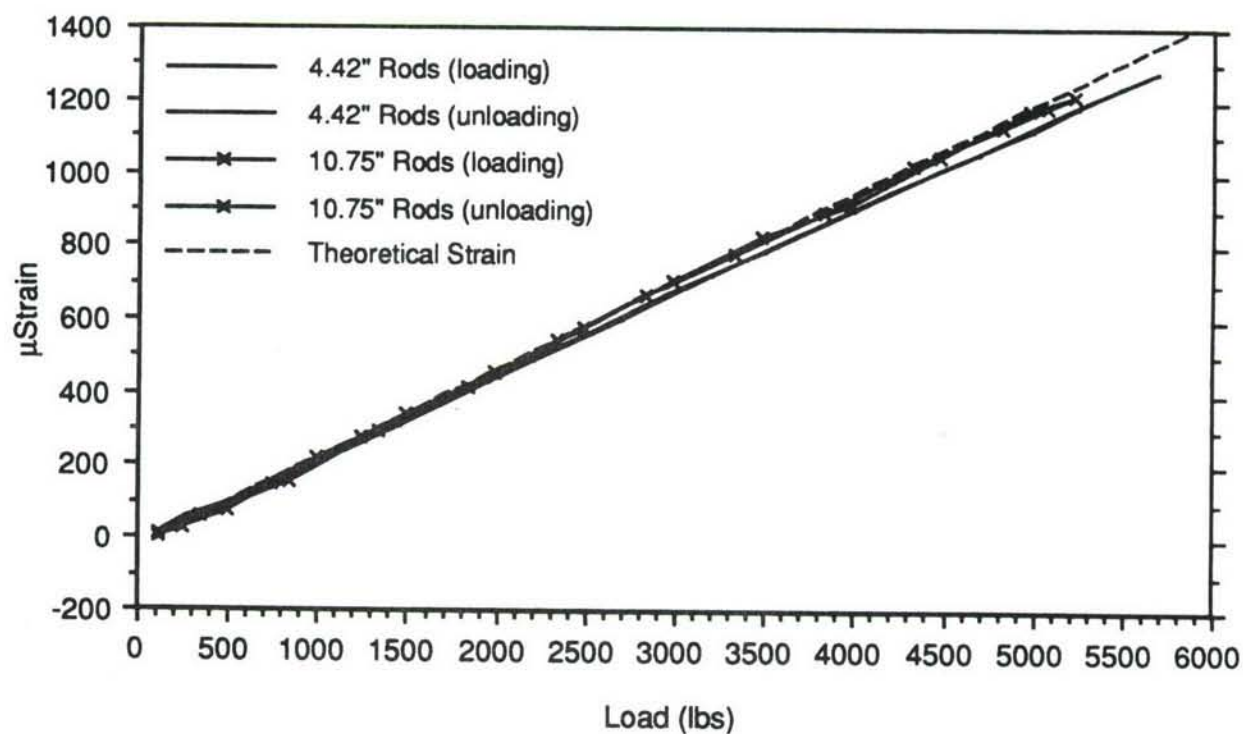
Capacitive Sensors
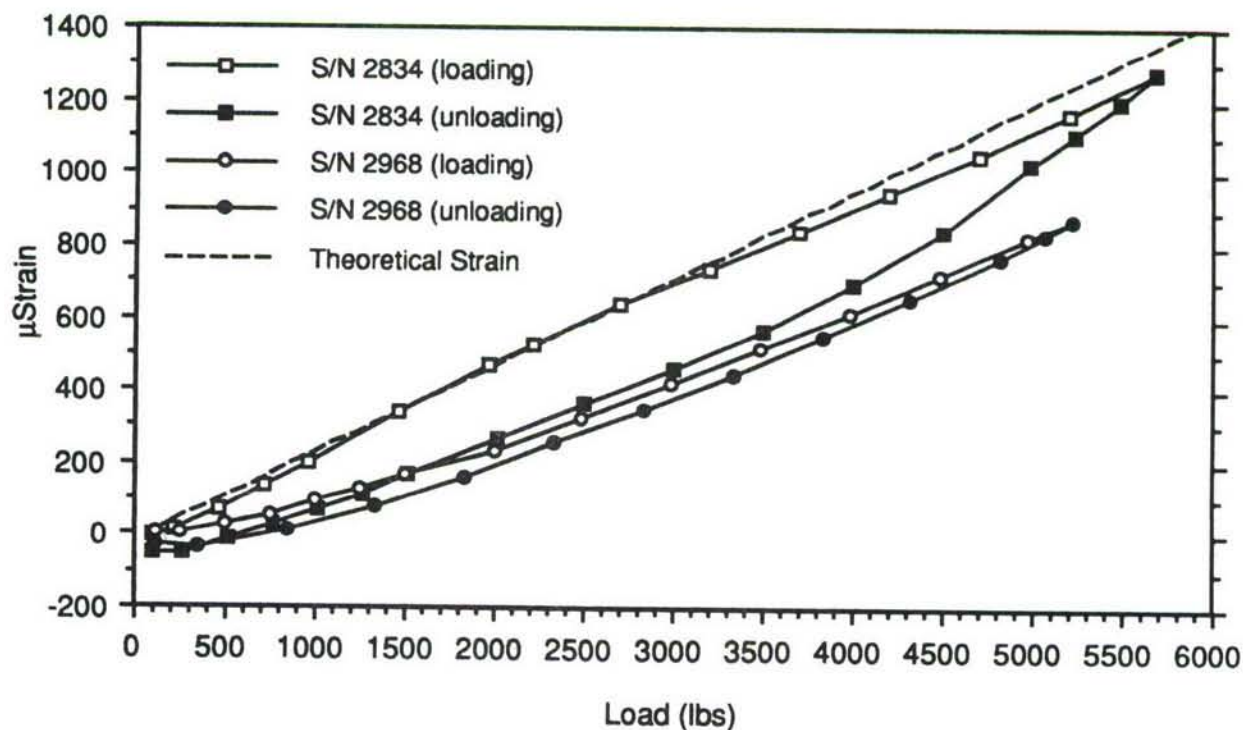
**Figure 26   Strain vs. Load for the Extensometer
and Capacitive Sensors at 400°F**

90-6-49-16

Extensometer

Capacitive Sensors

Figure 27 Strain vs. Load for the Extensometer and
Capacitive Sensors at 800°F

90-6-49-17

67
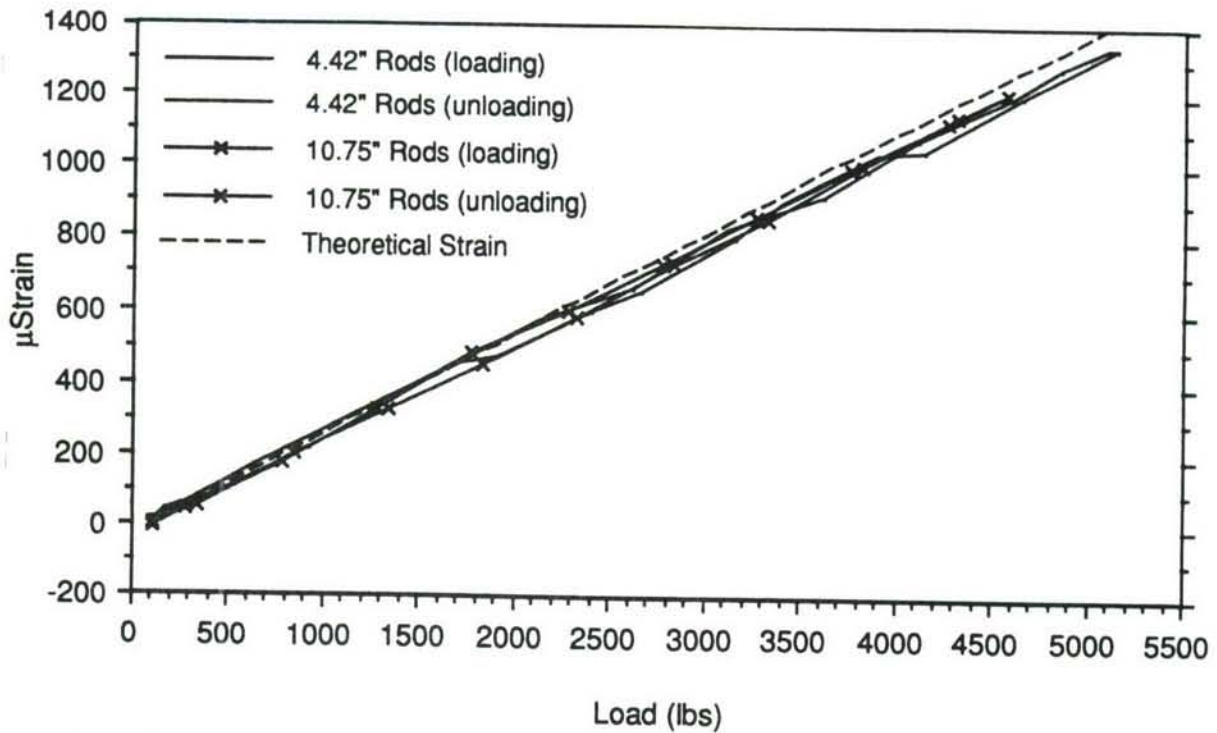
Extensometer

Capacitive Sensors
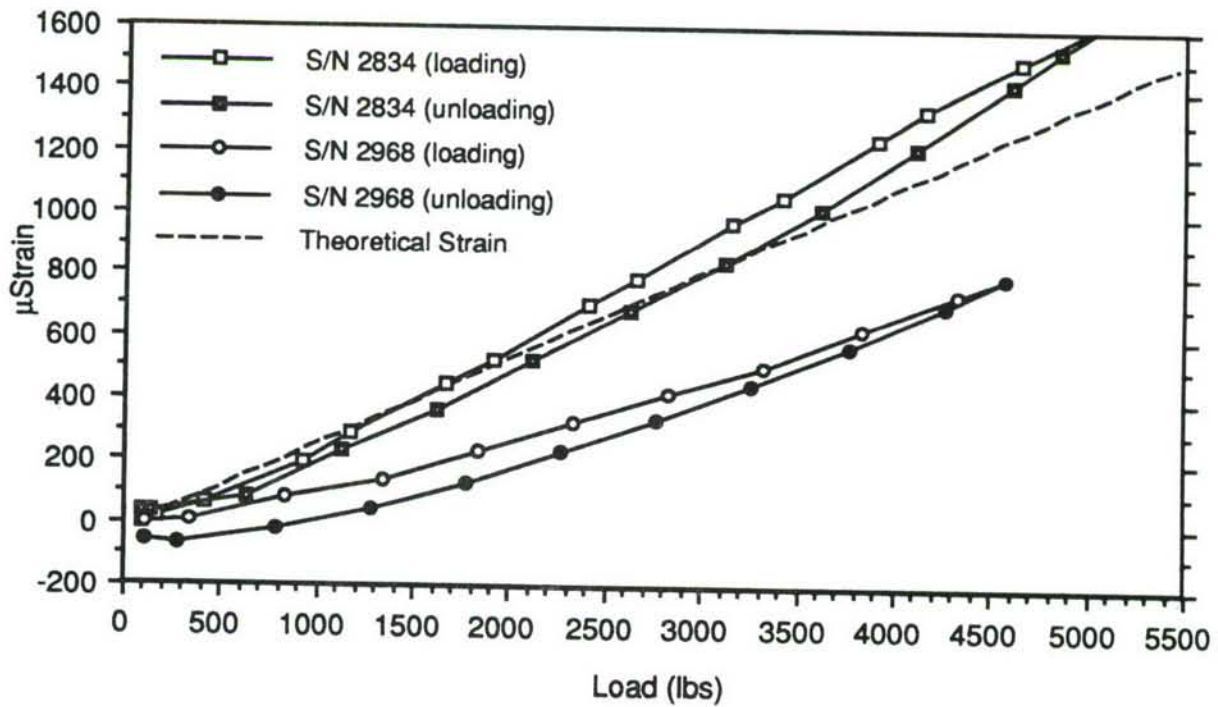
Figure 28   Strain vs. Load for the Extensometer and Capacitive Sensors at 1200°F

90-6-49-18

68
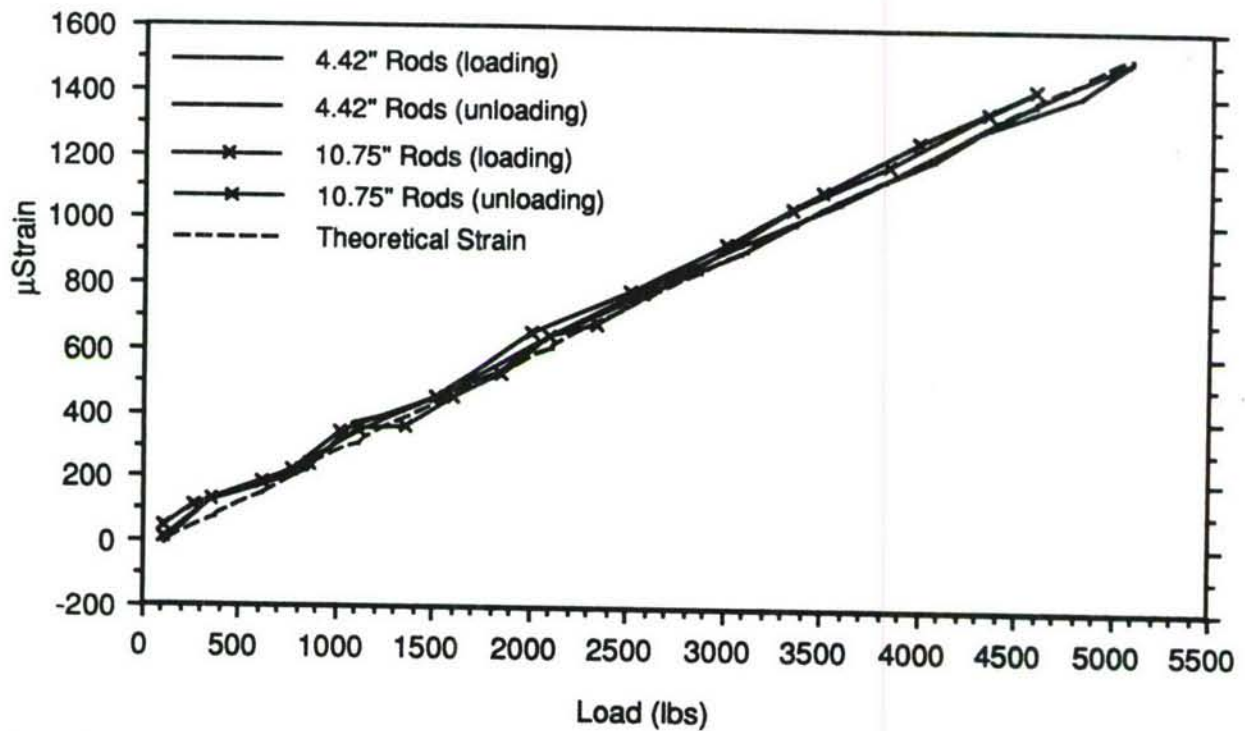
Extensometer

Capacitive Sensors
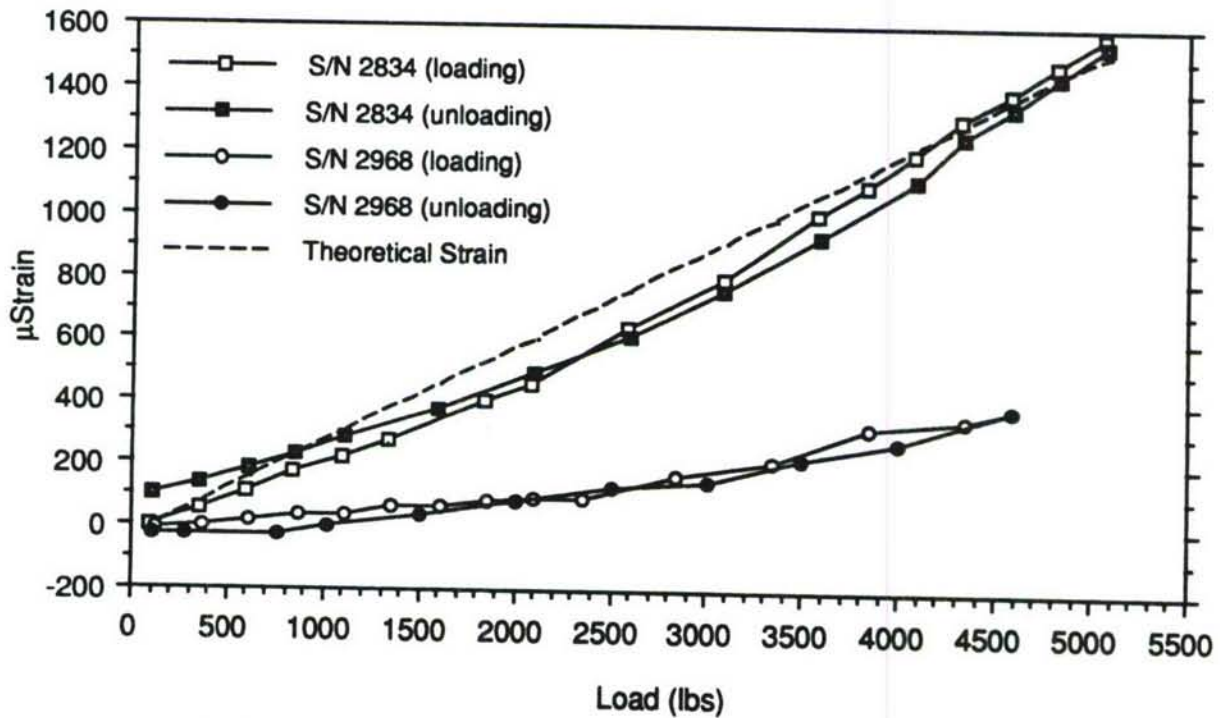
**Figure 29 Strain vs. Load for the Extensometer
and Capacitive Sensors at 1600°F**

Extensometer
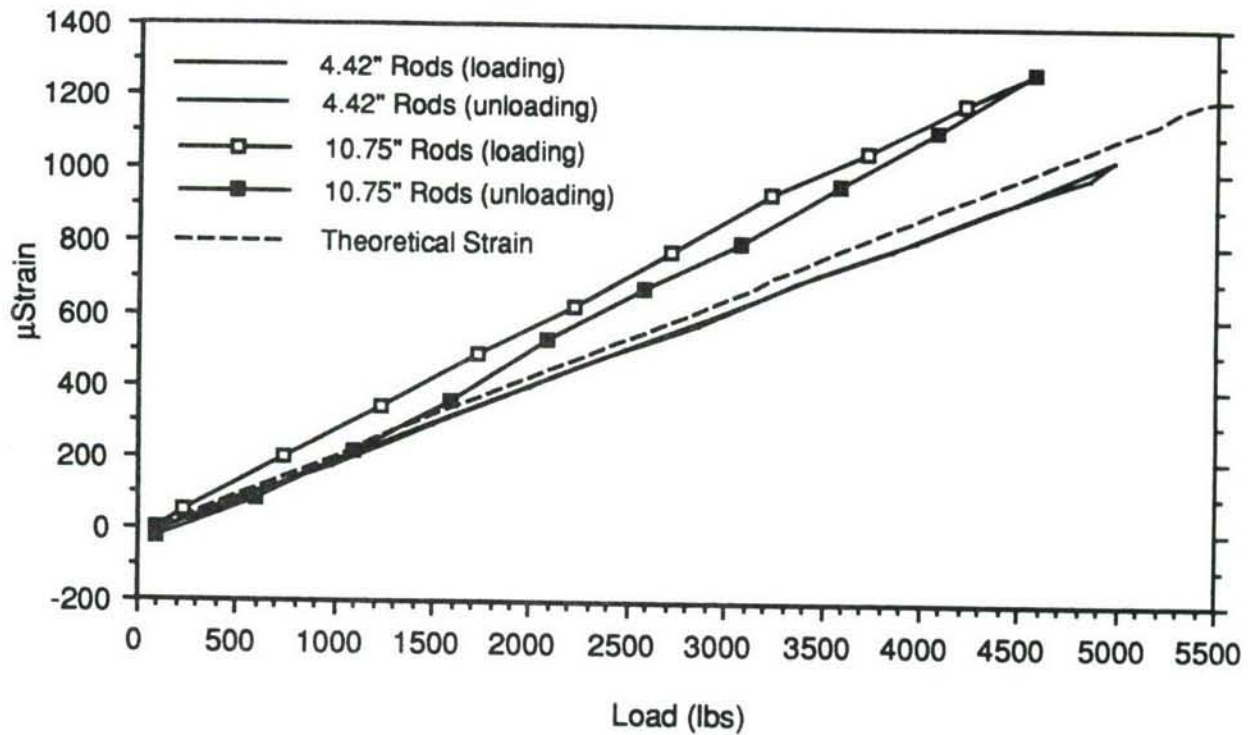
Capacitive Sensors
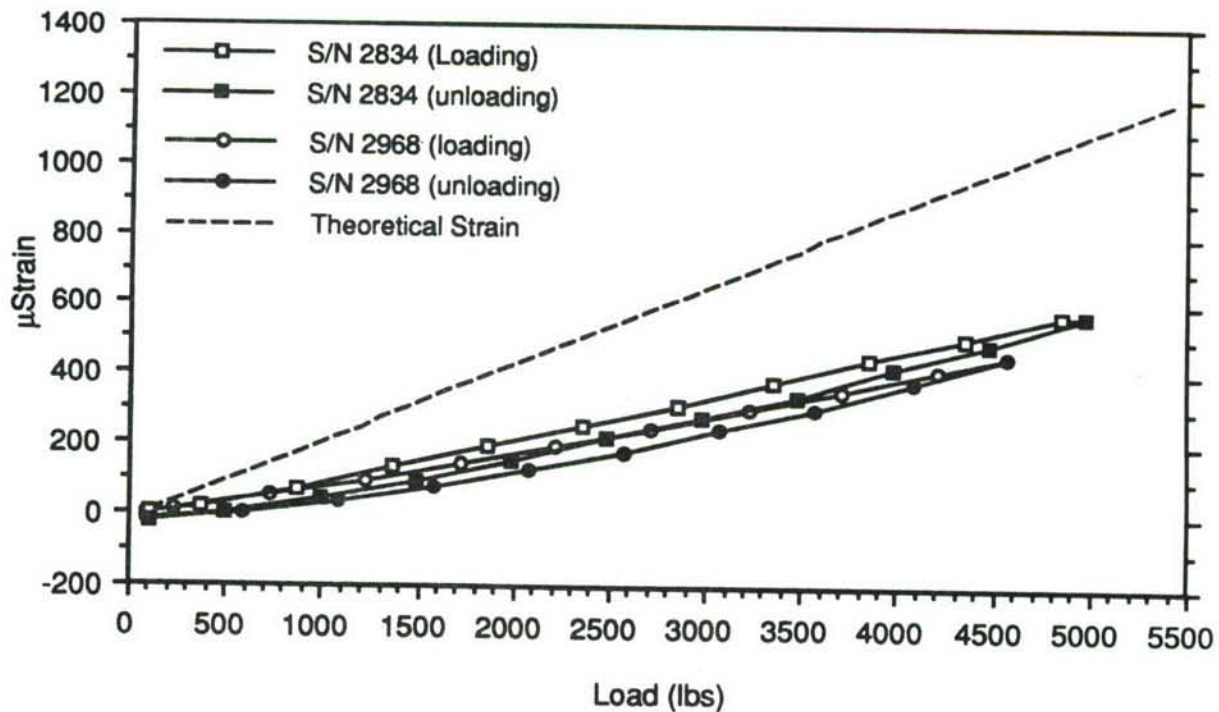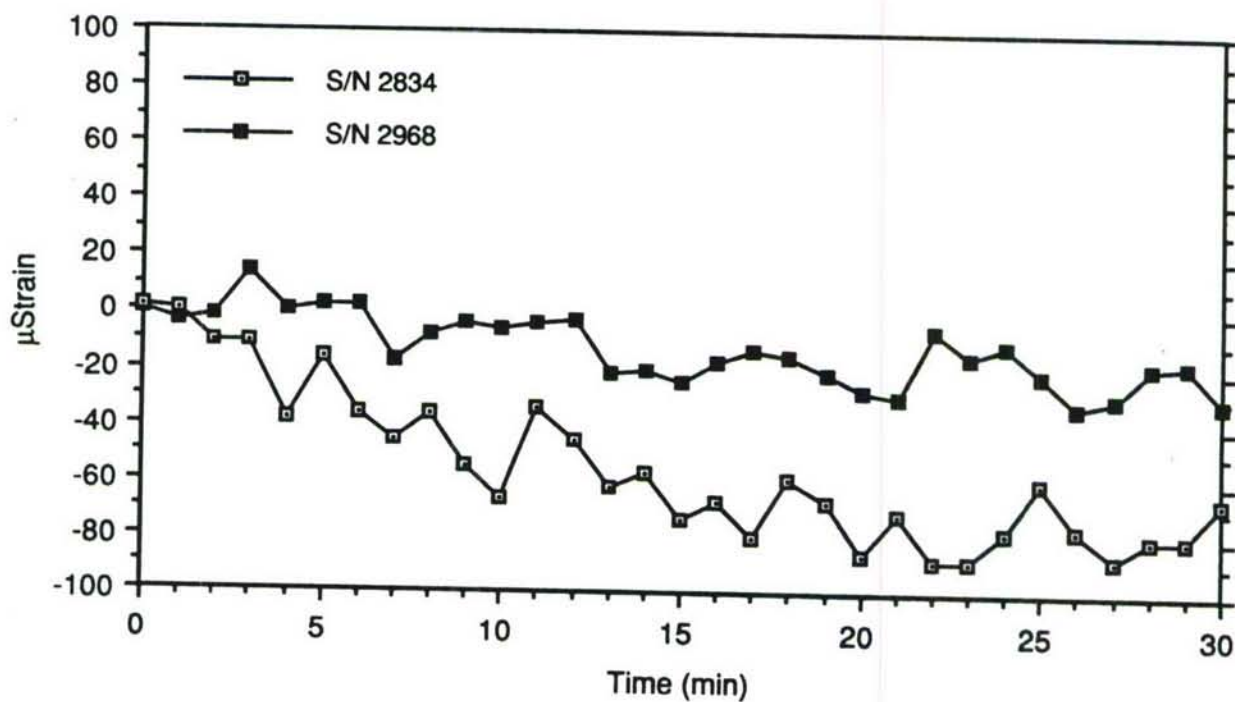

Figure 30 Strain for the Extensometer and
Capacitive Sensors at -310°F

90-6-49-20

70
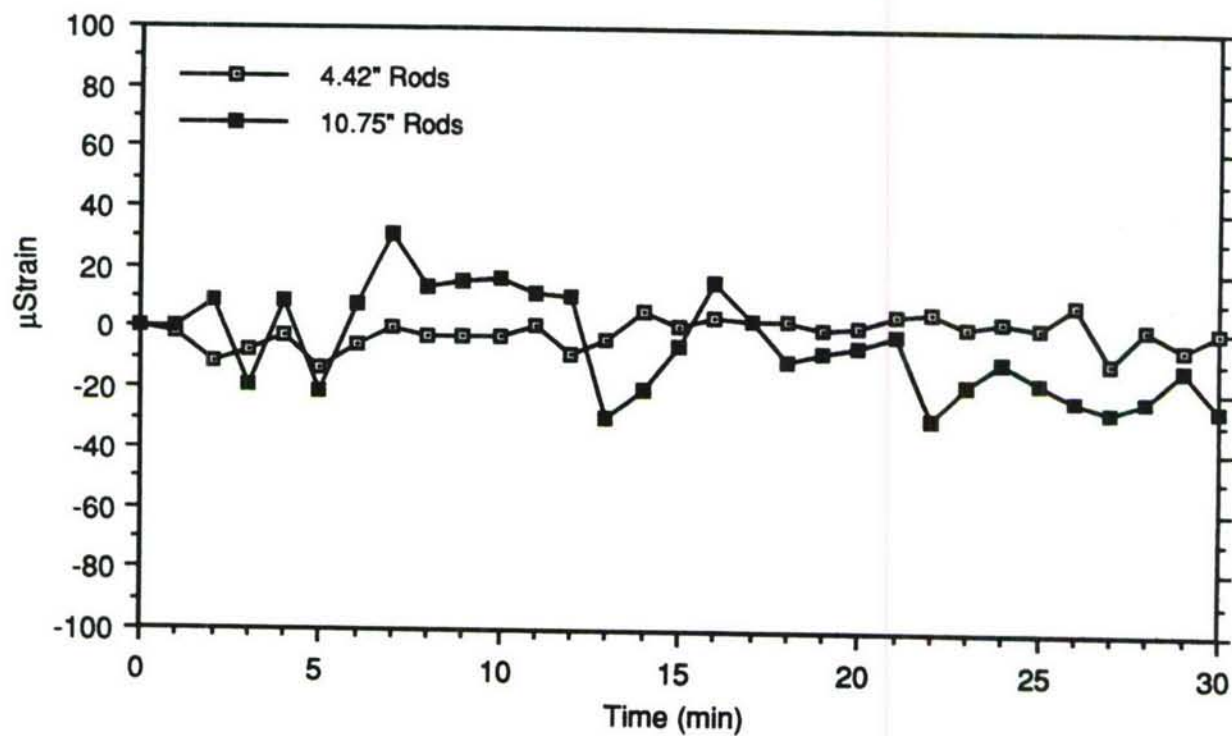
Extensometer
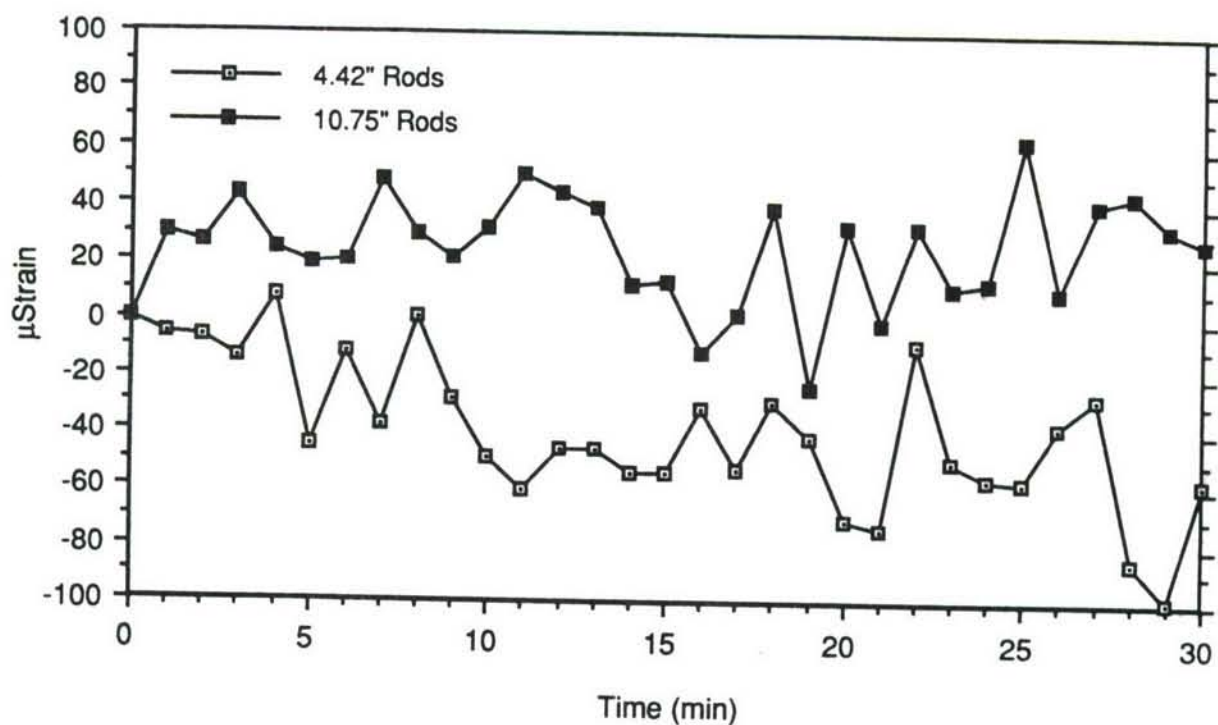

Capacitive Sensors
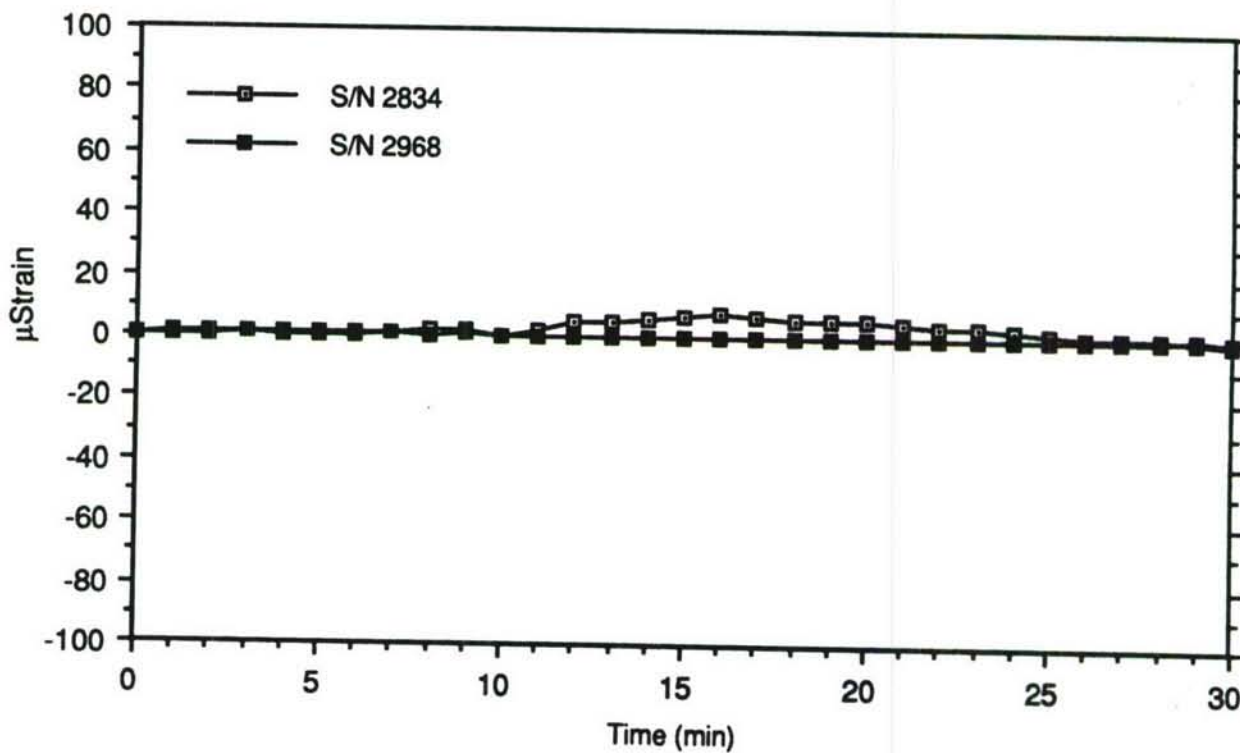
**Figure 31 Drift in Apparent Strain of the Extensometer
and Capacitive Sensors at 75°F**

90-6-49-21

71
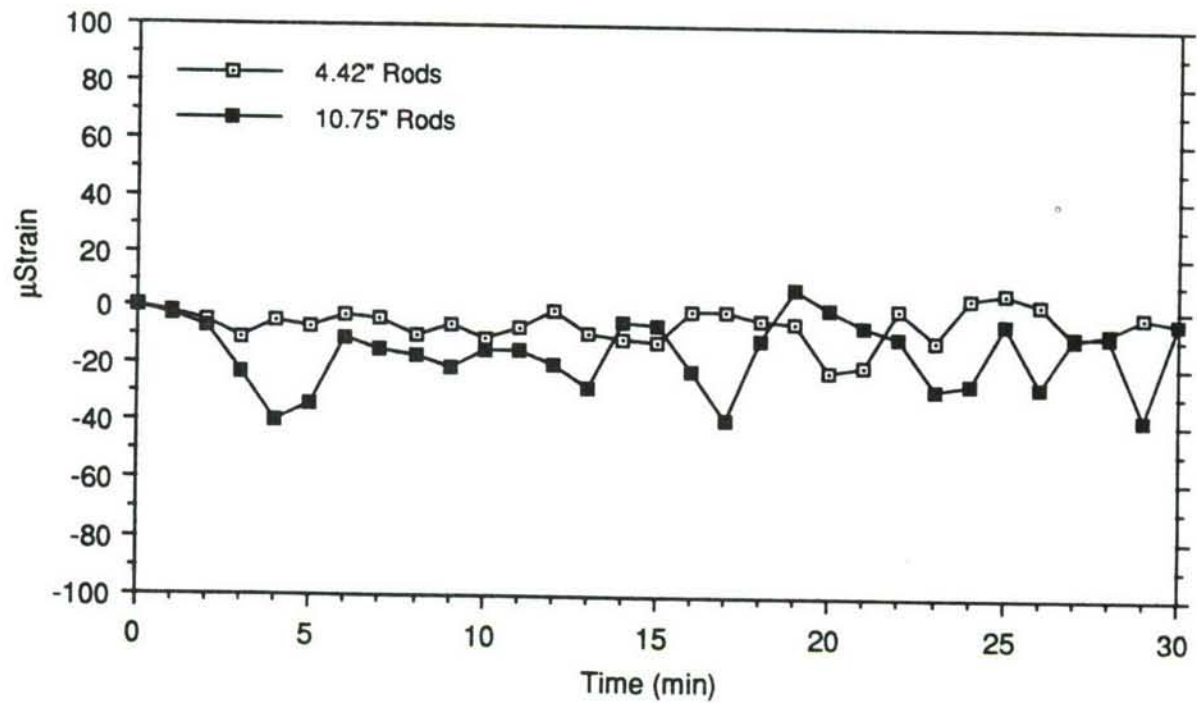
Extensometer

Capacitive Sensors
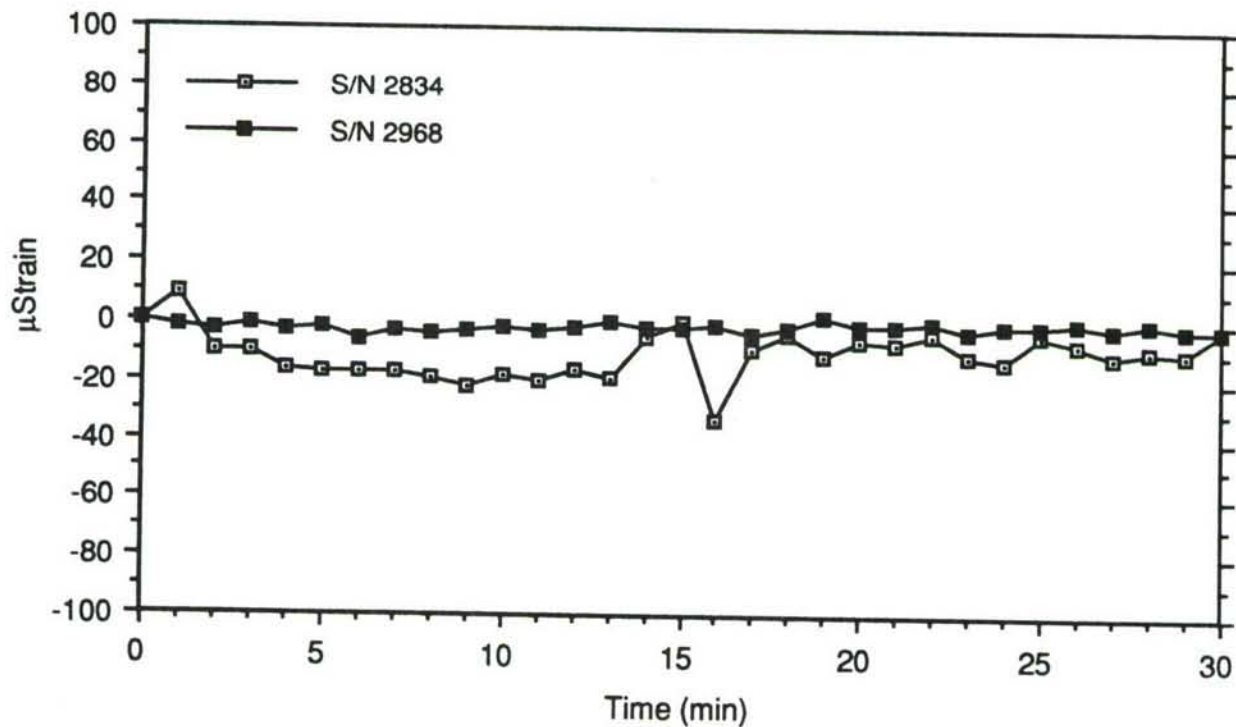
**Figure 32   Drift in Apparent Strain of the Extensometer
and Capacitive Sensors at 200°F**

Extensometer
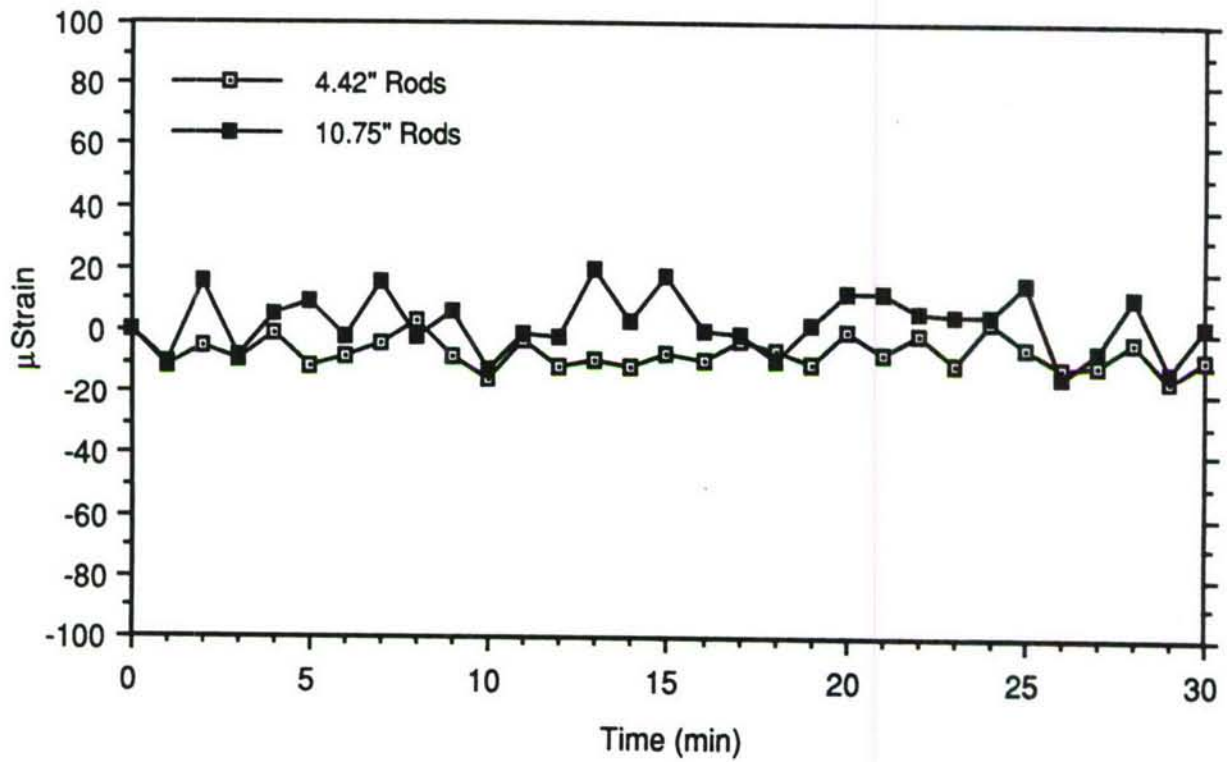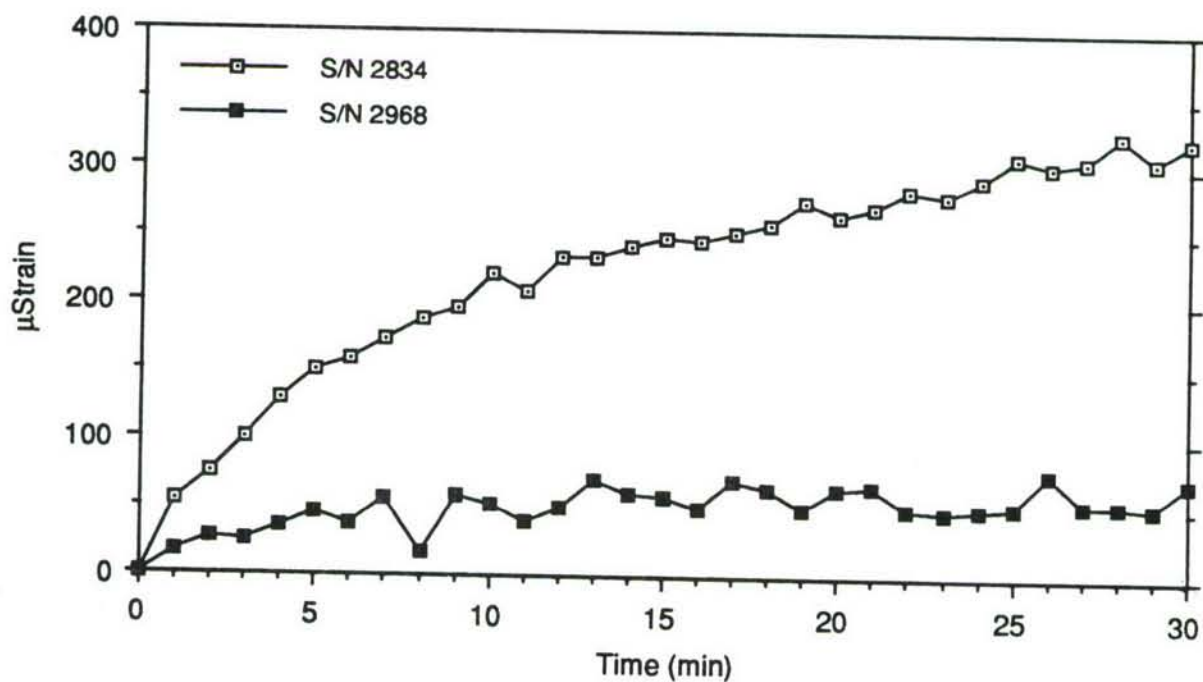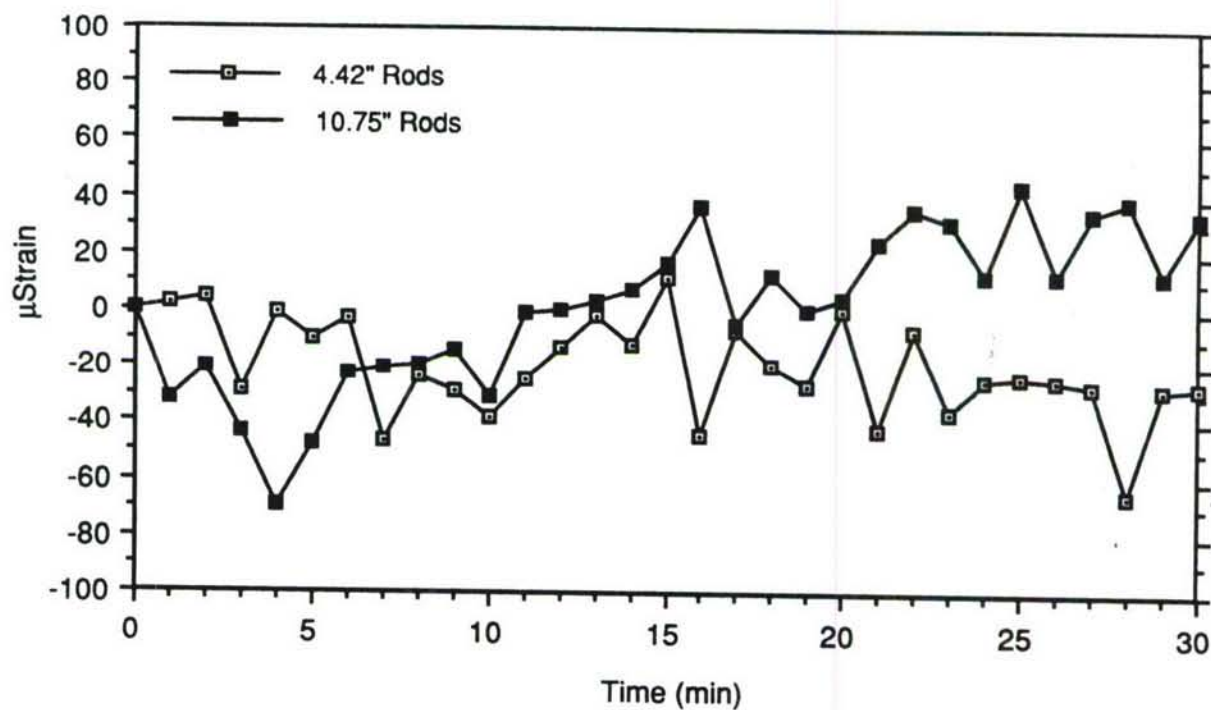

Capacitive Sensors
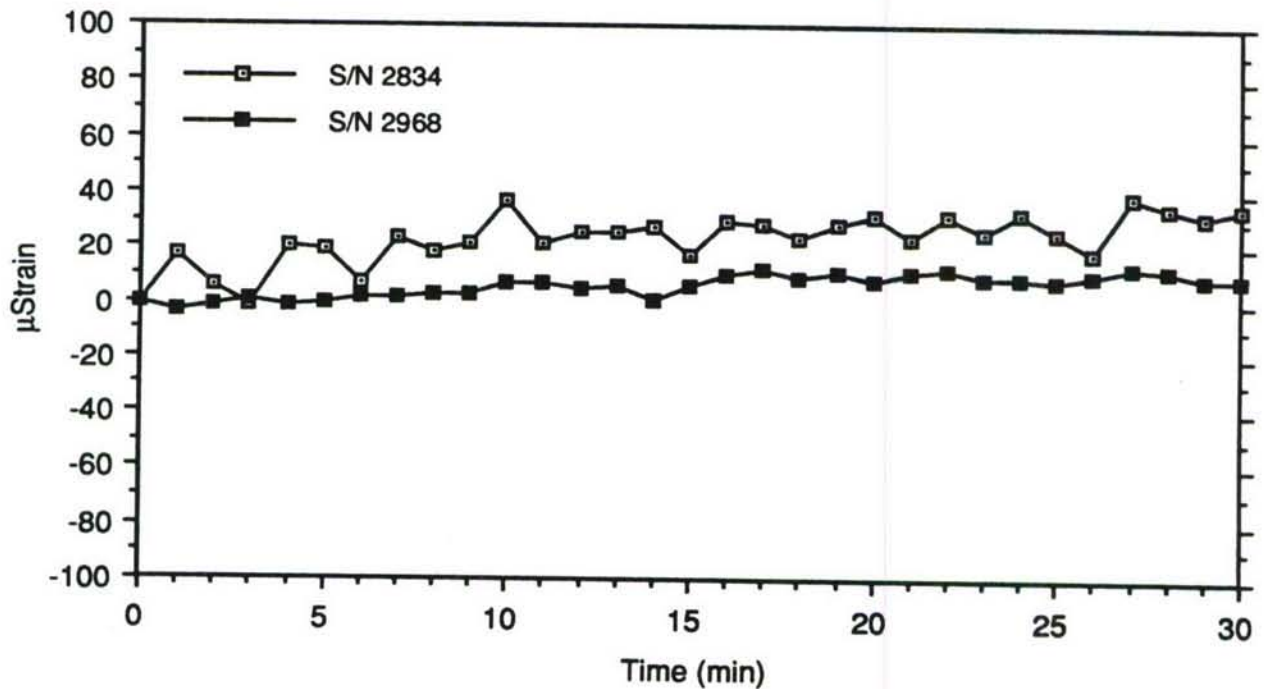
**Figure 33   Drift in Apparent Strain of the Extensometer
and Capacitive Sensors at 400°F**
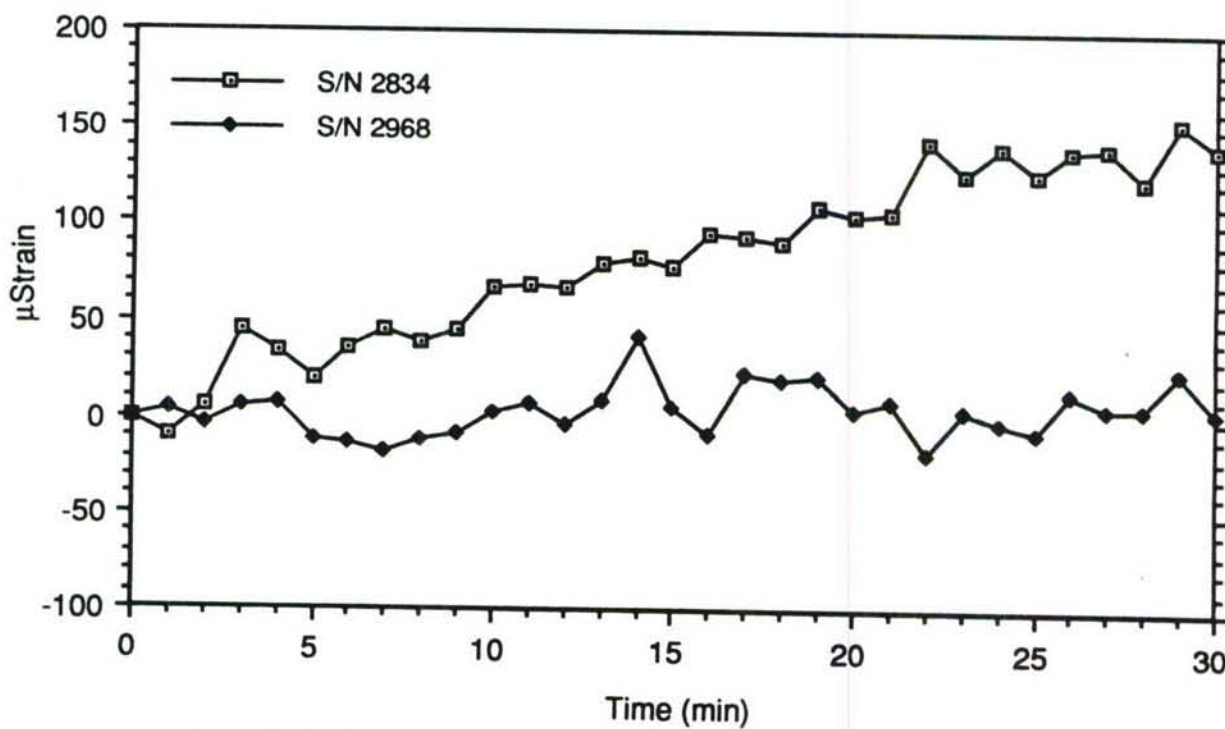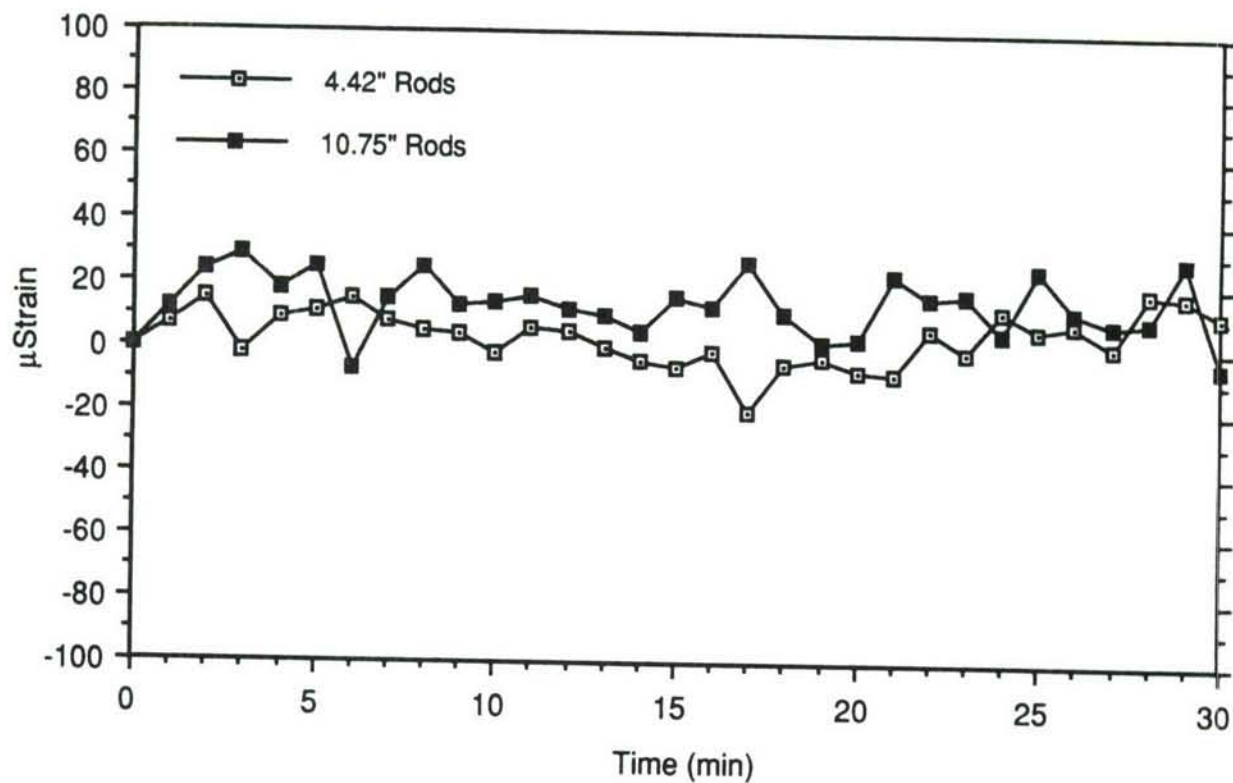
Extensometer
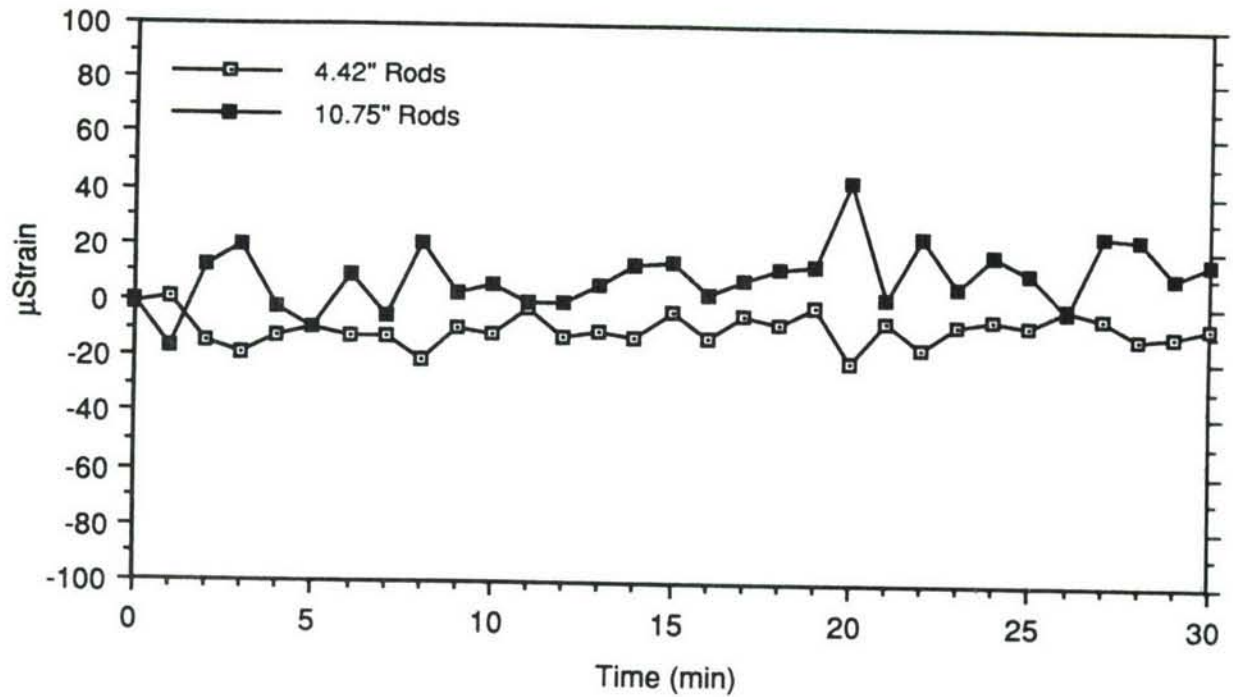
Capacitive Sensors
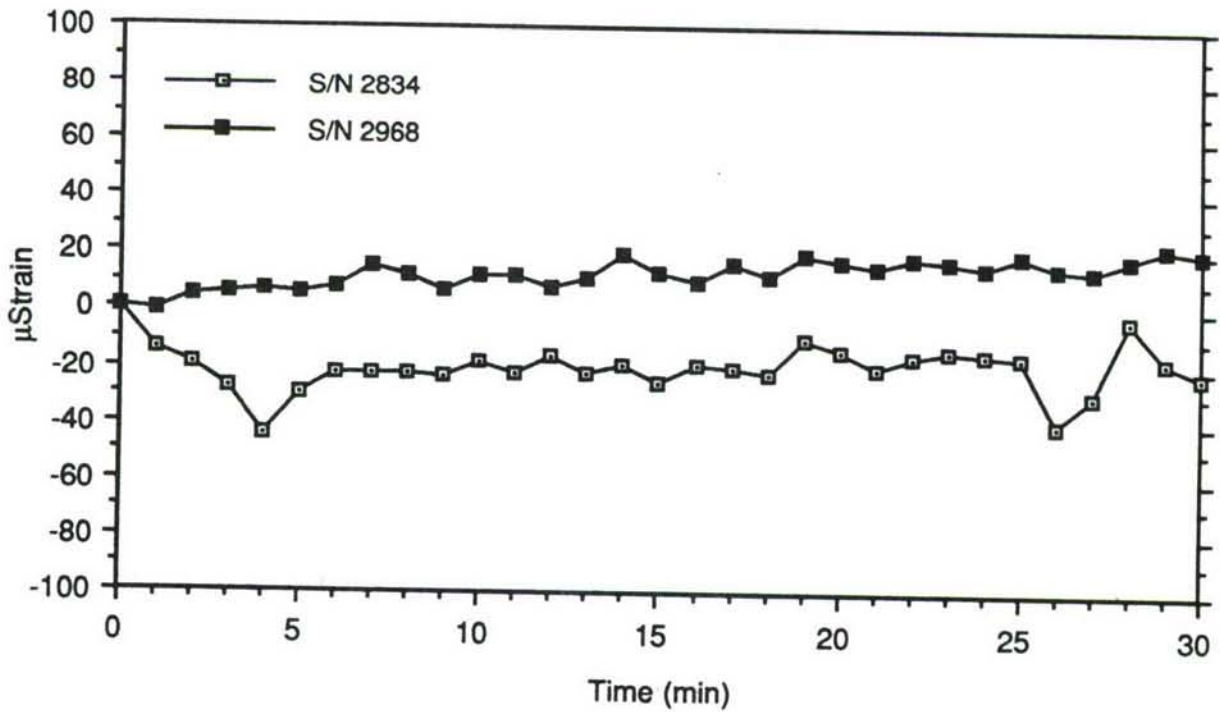
**Figure 34 Drift in Apparent Strain of the Extensometer
and Capacitive Sensors at 600°F**

Extensometer
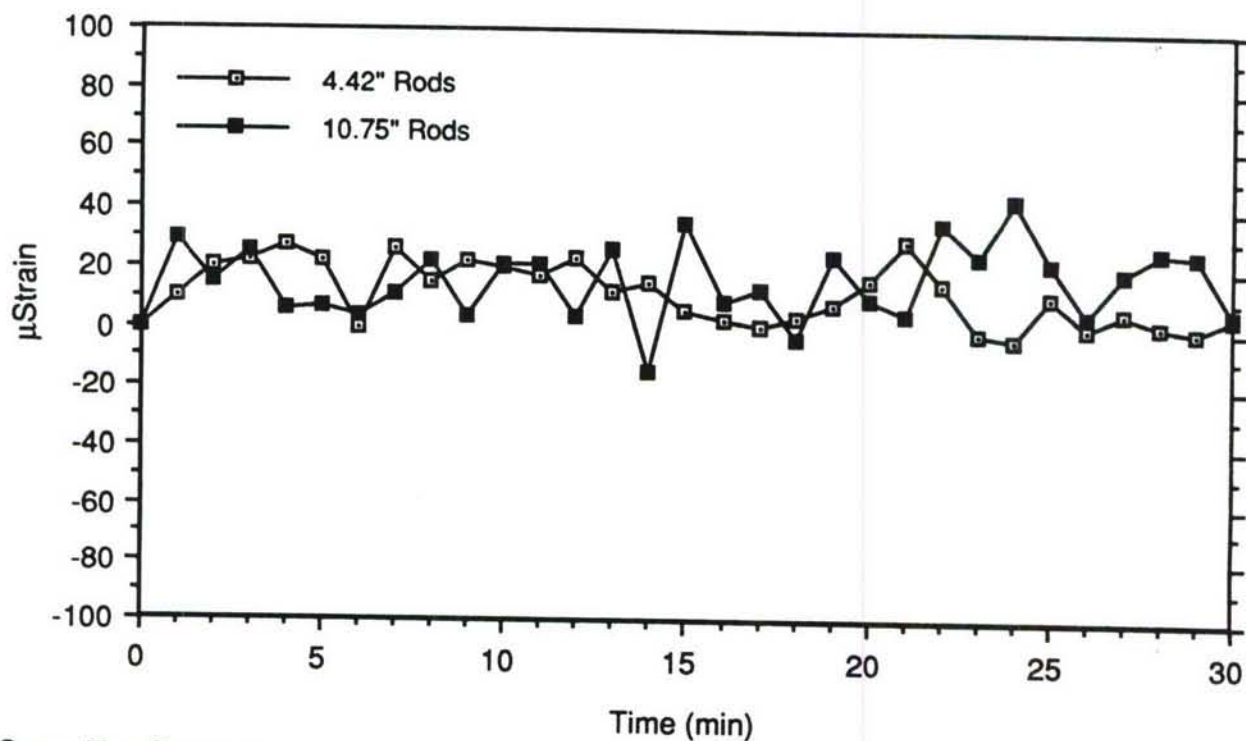
Capacitive Sensors
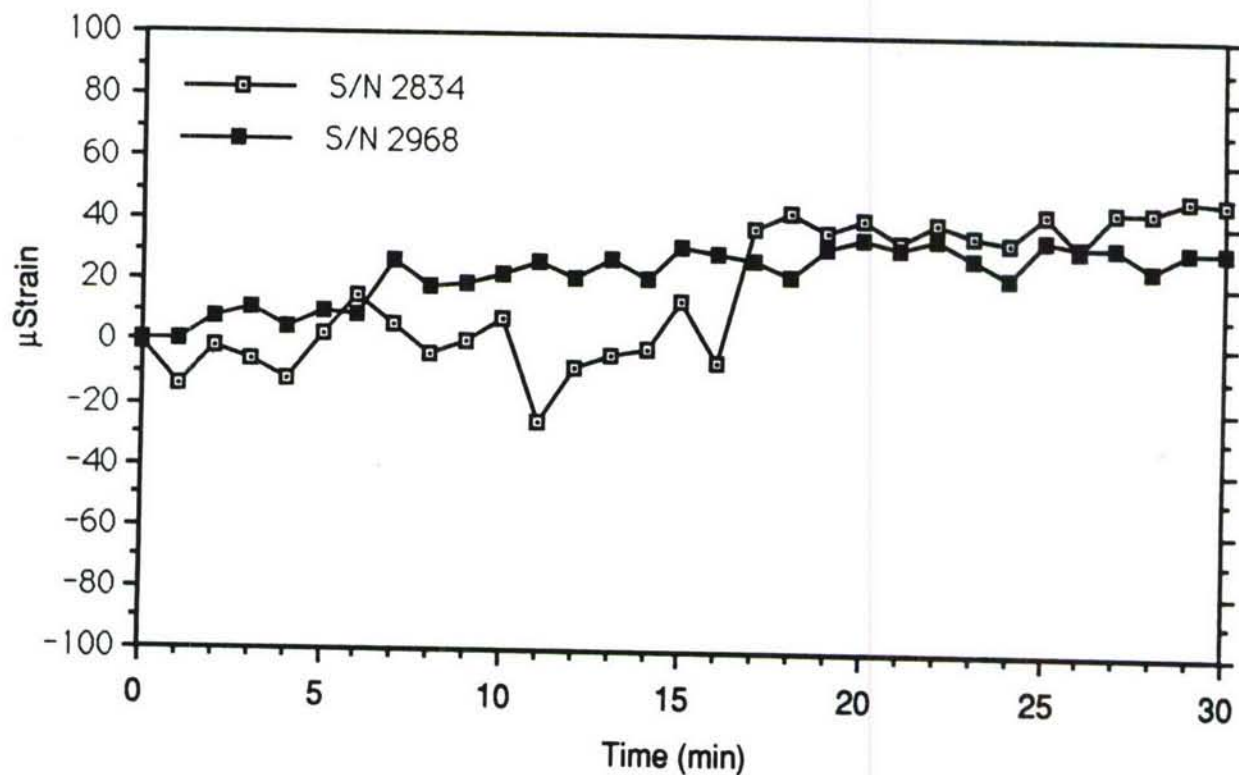
Figure 35   Drift in Apparent Strain of the Extensometer and Capacitive Sensors at 800°F

90-6-49-25

75
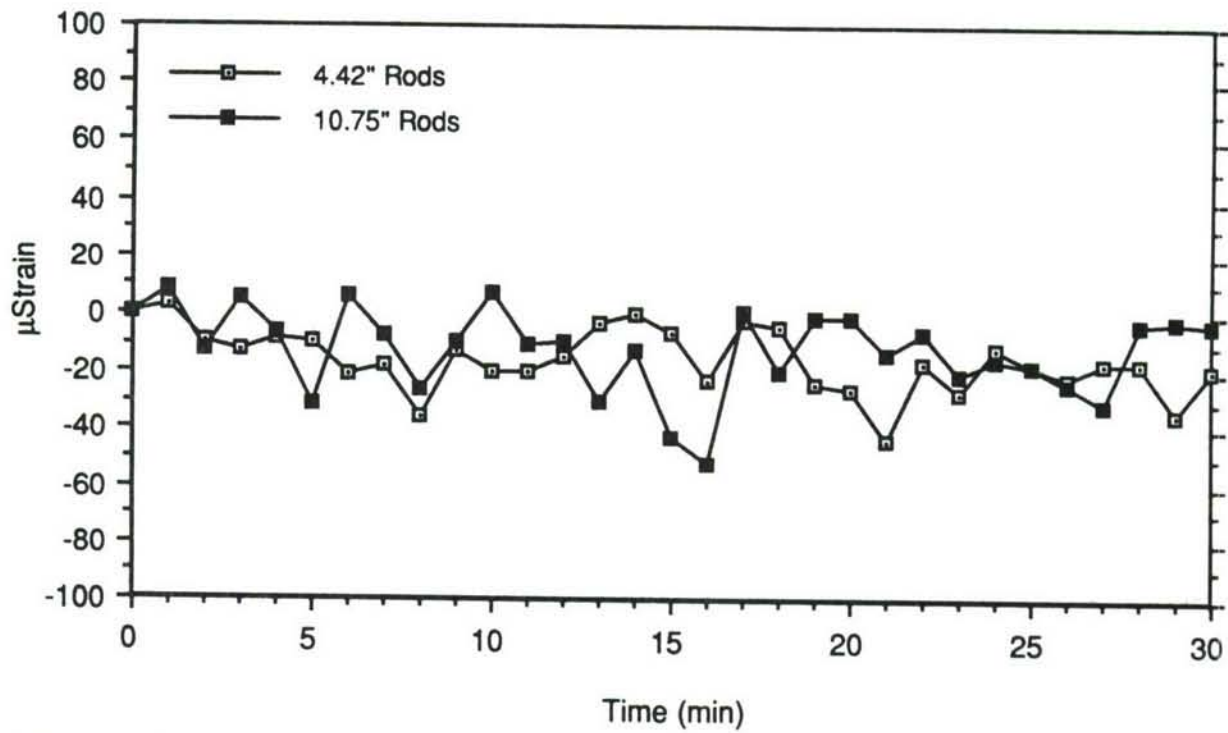
Extensometer

Capacitive Sensors
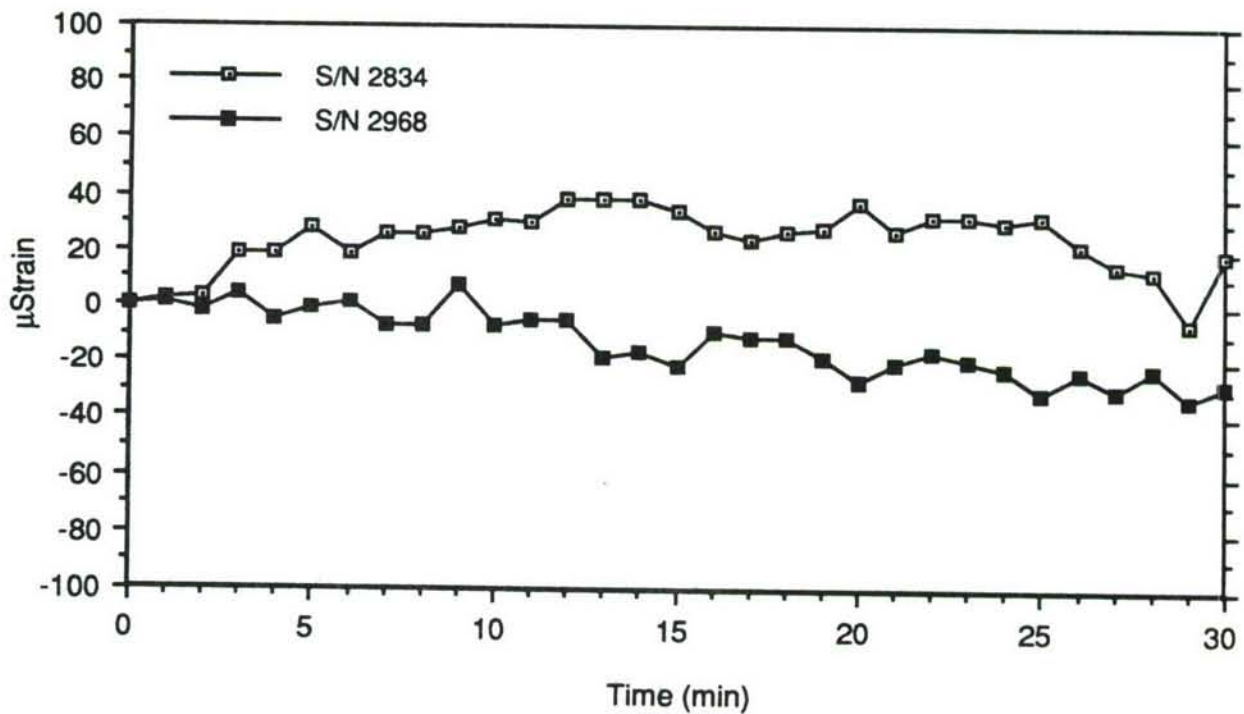
**Figure 36   Drift in Apparent Strain of the Extensometer
and Capacitive Sensors at 1000°F**

90-6-49-26
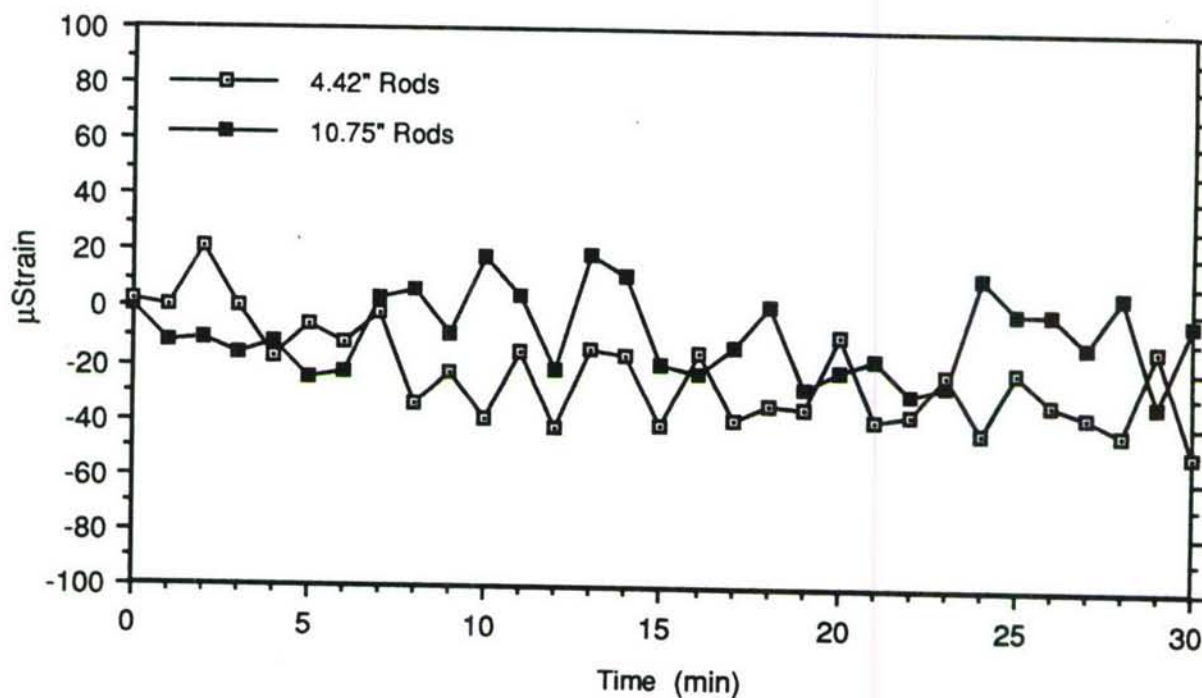
Extensometer

Capacitive Sensors

Figure 37 Drift in Apparent Strain of the Extensometer
and Capacitive Sensors at 1200°F

90-6-49-27

77

Extensometer

Capacitive Sensors

**Figure 38 Drift in Apparent Strain of the Extensometer
and Capacitive Sensors at 1400°F**
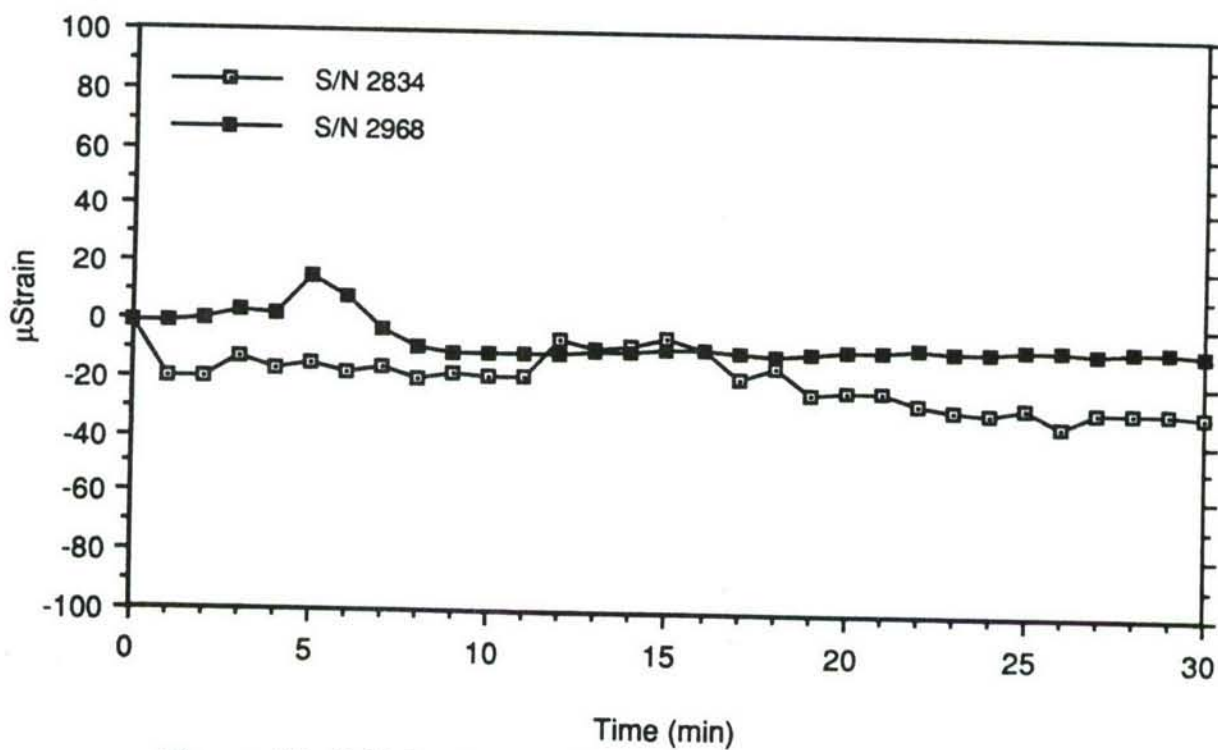
78

Extensometer

Capacitive Sensors

Figure 39   Drift in Apparent Strain of the Extensometer and
the Capacitive Sensors at 1600°F

90-6-49-29

79

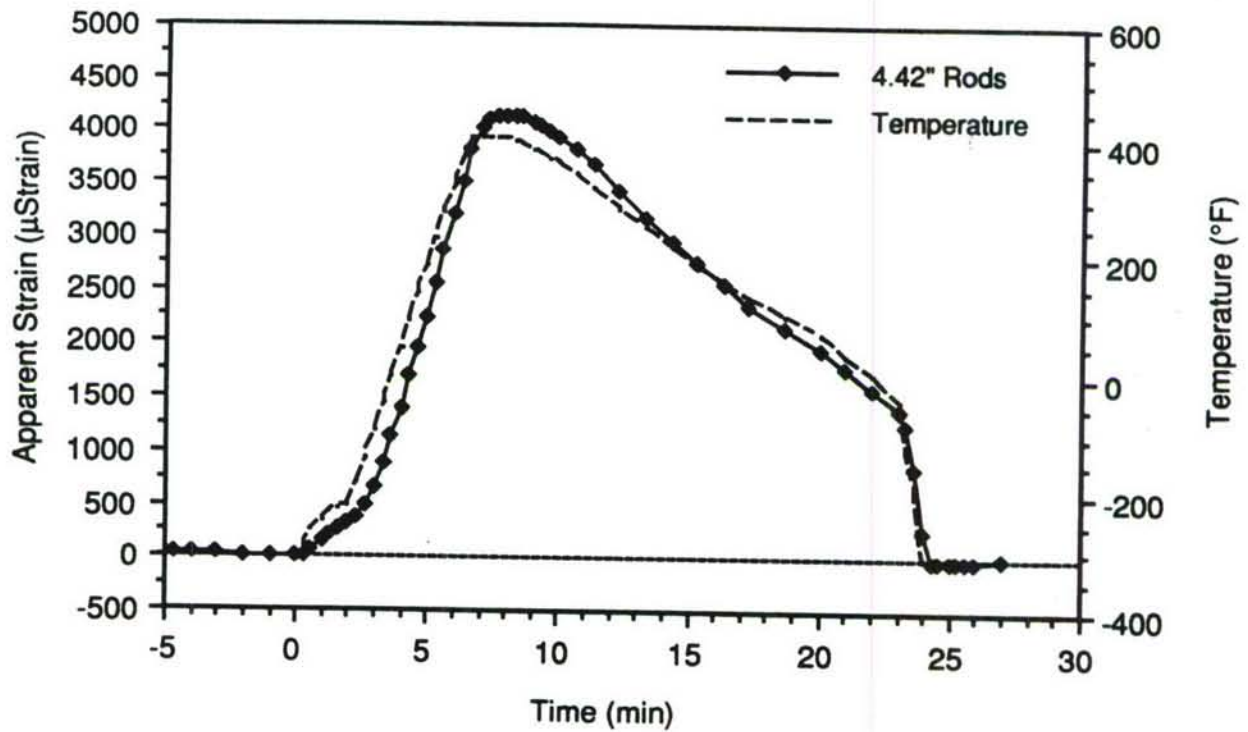Extensometer

Capacitive Sensors

Figure 40   Drift In Apparent Strain of the Extensometer and Capacitive Sensors at -310°F

90-6-49-30

Extensometer (4.42" Rods)

Extensometer (10.75" Rods)

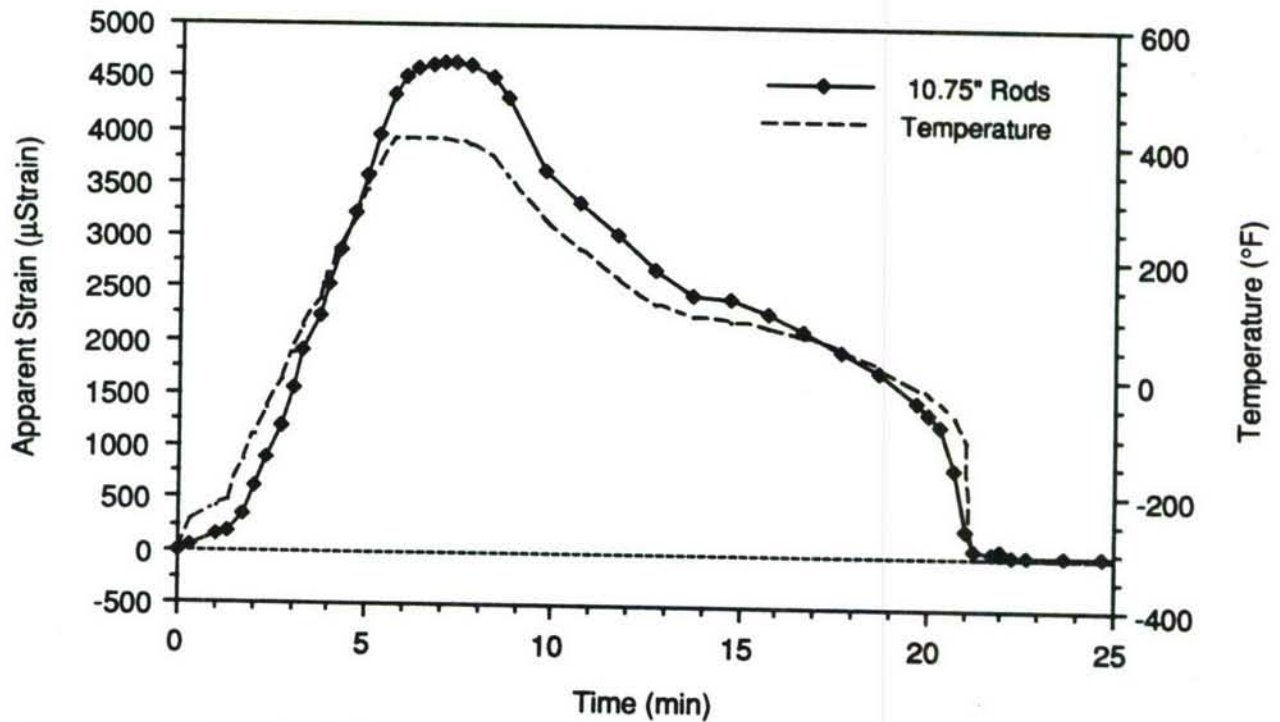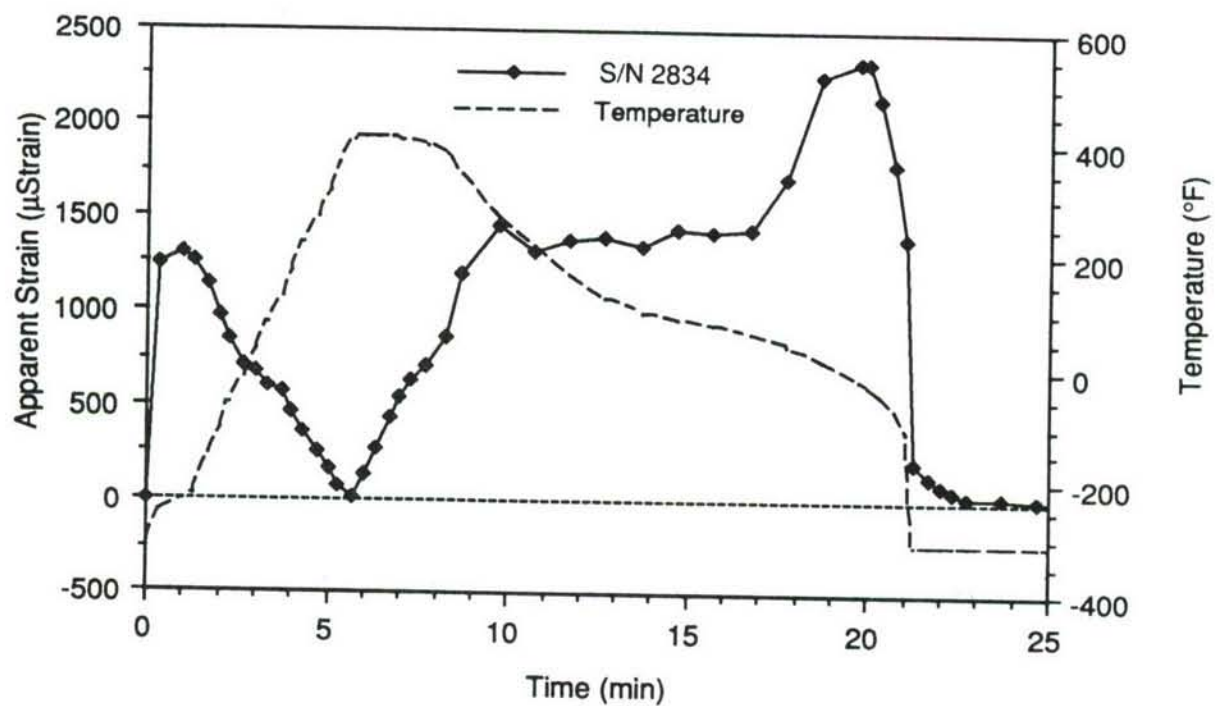**Figure 41   Response of Extensometer with Different
Size Rods to the Simulated Ascent Cycle**
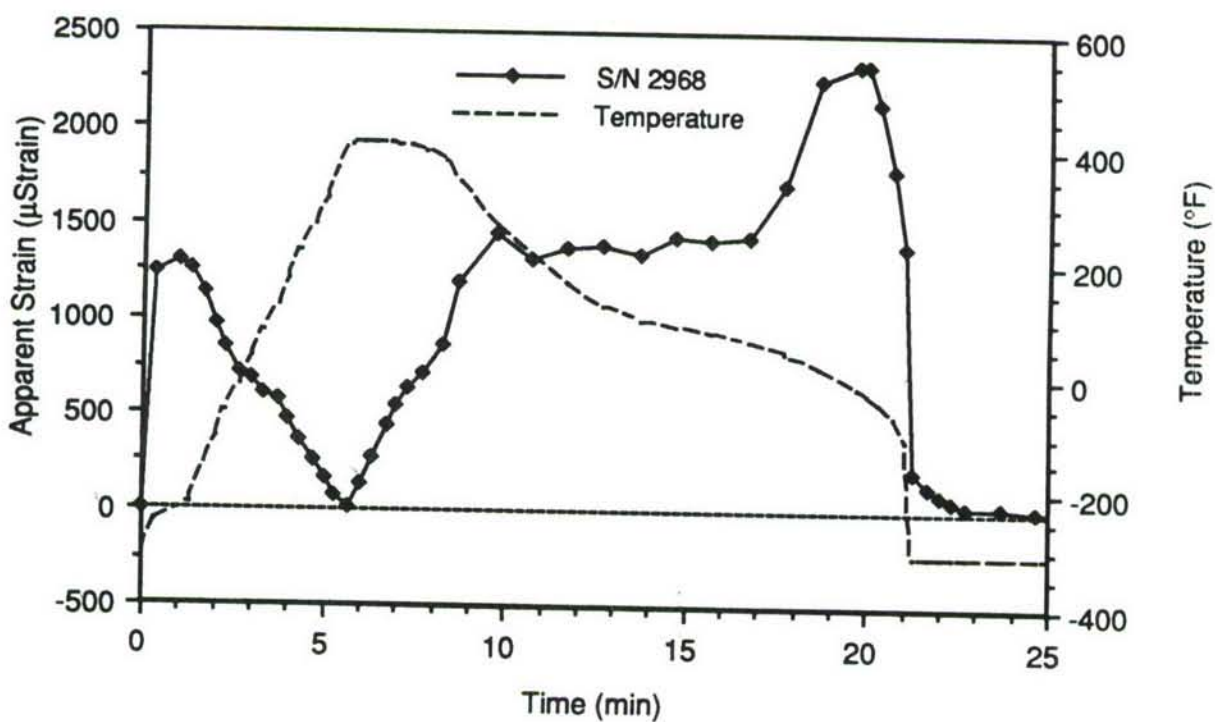
Capacitive Sensor S/N 2834

Capacitive Sensor S/N 2968

Figure 42   Response of Two Different Capacitive Sensors to the Ascent Cycle

90-6-49-32

**Figure 43   Response of Extensometer with Different
Size Rods to the Reentry Cycle**

90-6-49-33

Capacitive Sensor S/N 2834

Capacitive Senor S/N 2968

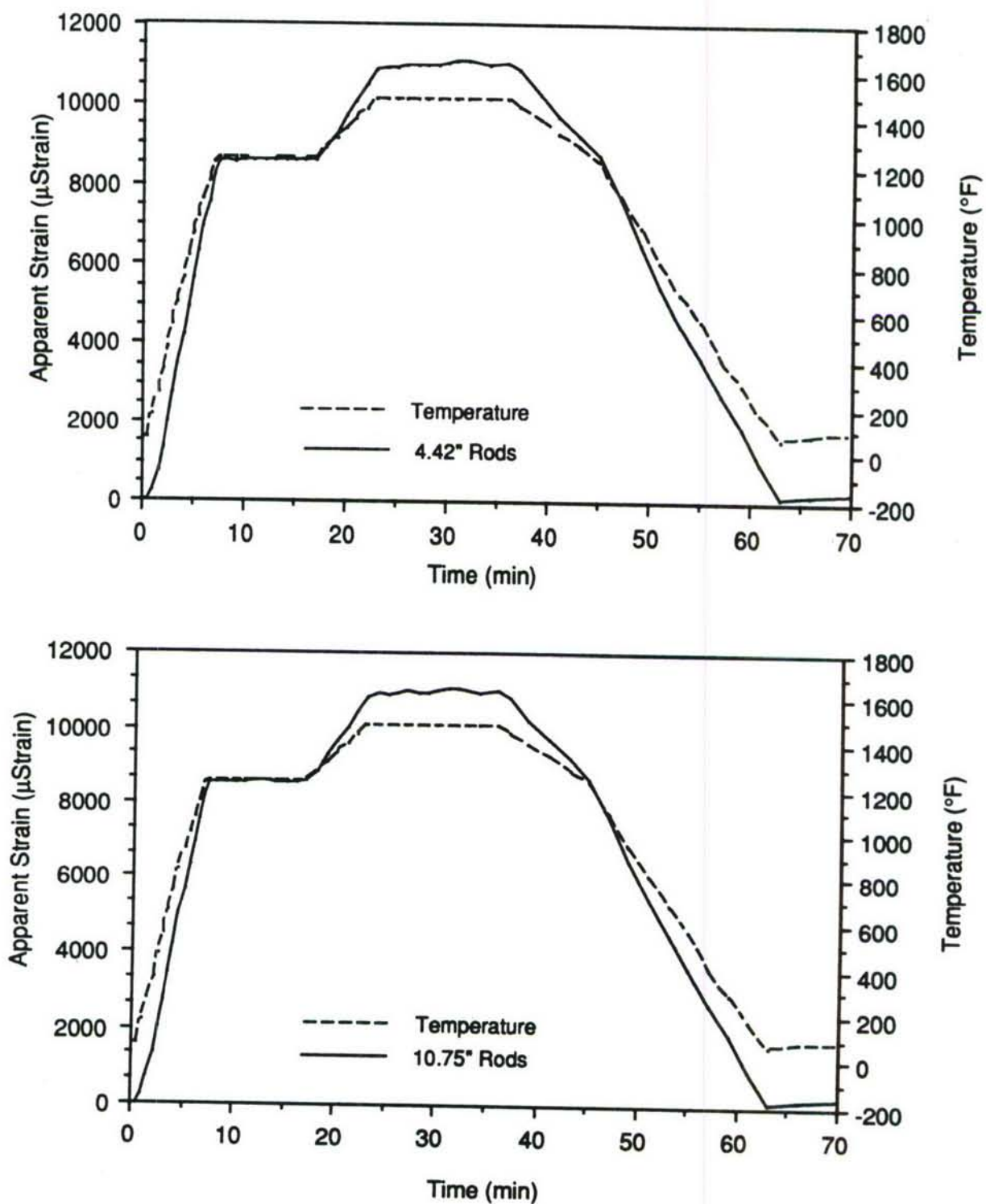**Figure 44 Response of Two Different Capacitive
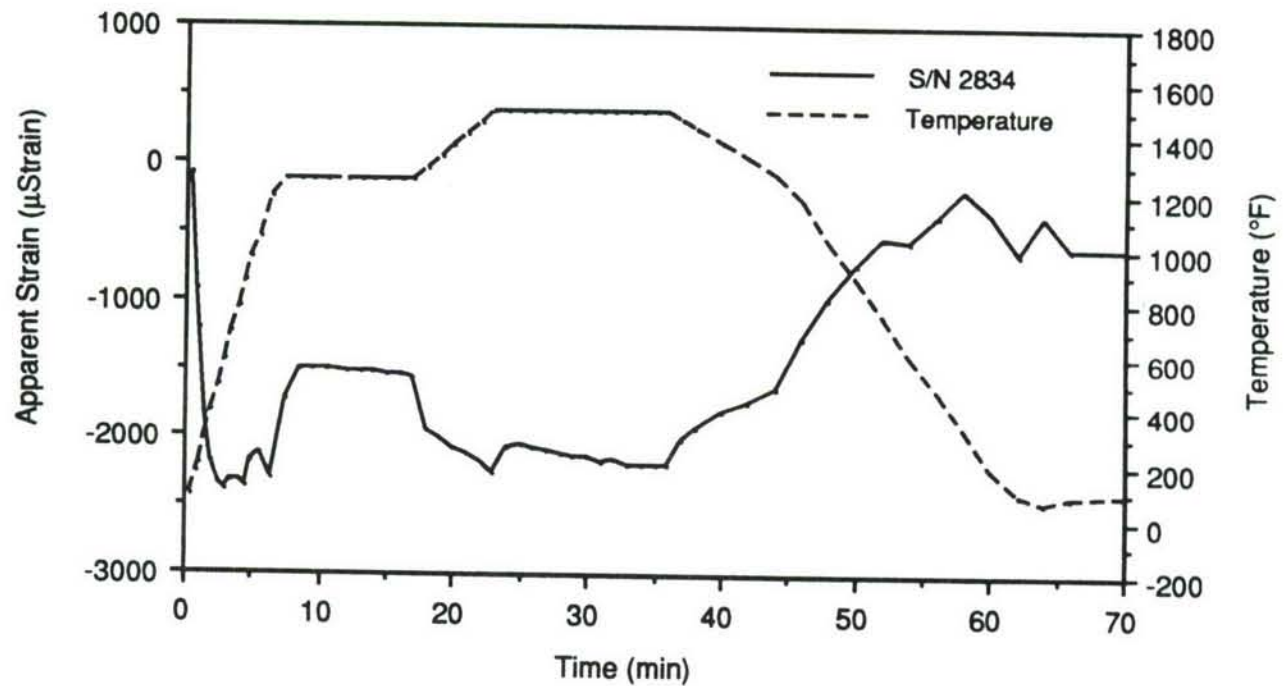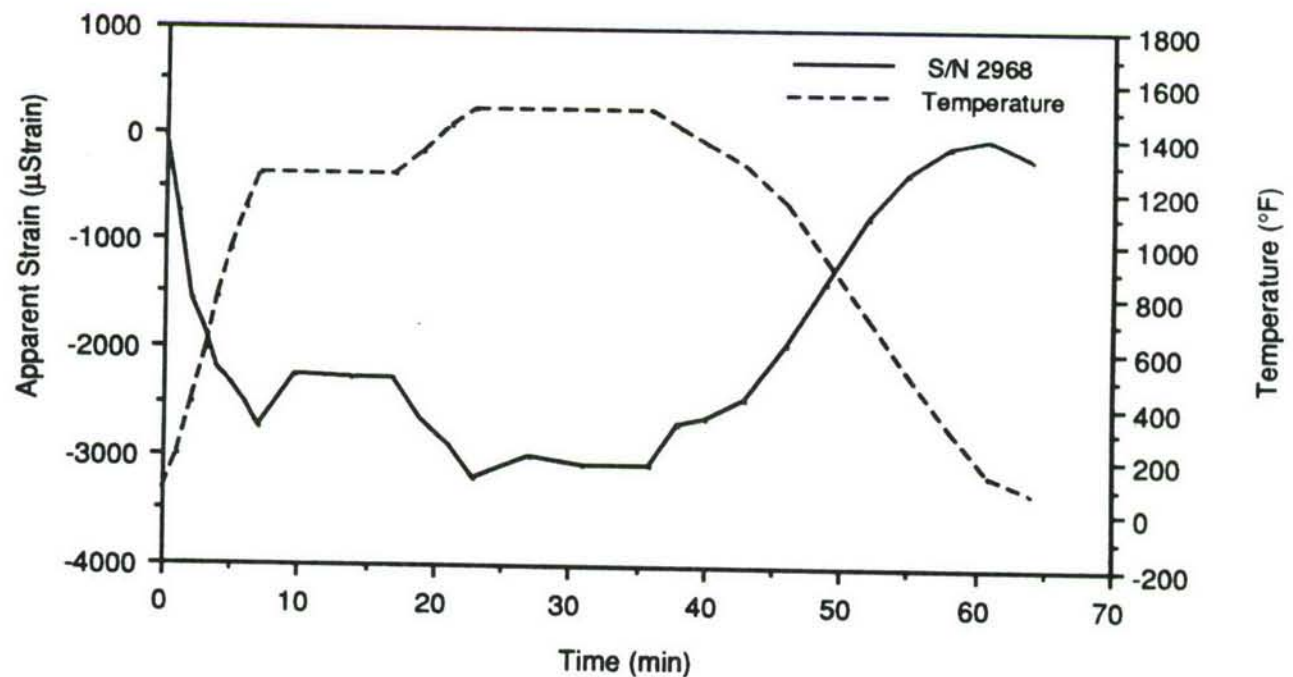Sensors to the Reentry Cycle**

90-6-49-34

TABLE 1

EVALUATION FACTORS FOR STRAIN GAGE SYSTEMS

Property	Symbol	Importance Factor
Accuracy	(A)	0.9
Repeatibility and chemical stability	(R)	0.7
Measurement stability (drift)	(S)	0.5
Strain Range	(SR)	0.5
Judgement (Experience, potential, ease of use)	(J)	0.2
Thermal sensitivity	(TS)	0.4
Cost/unit	(C)	0.2

Goodness Factor = 0.9(A)+0.7(R)+0.2(C)+0.5(J)+0.2(TC)+0.2(SR)

TABLE 2

RESULTS OF COMPARISONS OF VARIOUS STRAIN
MEASUREMENT TECHNIQUES FOR USE TO 1600°F

Technique	Goodness Factor
Ceramic Rod Extensometer	35.1
Capacitance Gage (Hitec)	31.0
Sputtered Strain Gage	27.0
Capacitance (CERL - Planer)	26.8
Eddy Current Transducers	26.4
Wire strain Gage	25.9
Capacitive (Boeing)	25.0
Optical Flags	24.8
Telescope, Photography	24.7
Laser (Spinning Mirror)	24.2
Laser Speckle	22.2
Microwave Resonance	22.0
Dual Core Optical Fibers	21.3
Fiber Bundles	20.6
Morie Fringes	19.9
Gas Pressure	18.6
Surface Acoustic Wave	14.9

Goodness Factor = 0.9(A)+0.7(R)+0.2(C)+0.5(J)+0.2(TC)+0.2(SR)

TABLE 3

CHANGE OF CAPACITIVE STRAIN SENSOR
CALIBRATION WITH TEMPERATURE

Temperature (°F)	Calibration (μin/volt)	Change (%)
72	2000	0
800	2010	0.5
1200	2092	4.6
1400	2125	6.3
1600	2198	9.9

TABLE 4

SIMULATED REENTRY
EXTENSOMETER STRAIN MEASUREMENTS
CORRECTED FOR APPARENT STRAIN

4.42-in. Alumina Rods

Hold Temperature (°F)	Measured Strain (in/in)	Apparent Strain from R.T.* (in/in)	Strain Difference (in/in)
1237	0.00857	0.00863	-0.00006
1484	0.01098	0.01104	-0.00006

10.75 in. Alumina Rods

Hold Temperature (°F)	Measured Strain (in/in)	Apparent Strain from R.T.* (in/in)	Strain Difference (in/in)
1247	0.00892	0.00875	-0.00017
1491	0.01136	0.01110	-0.00026

* From Fig. 25

88